PNNL-24476, Rev 0
WTP-RPT-241, Rev 0

Pacific Northwest
NATIONAL LABORATORY

Proudly Operated by Battelle Since 1965

Simulant Basis for the Standard High Solids Vessel Design

September 2016

RA Peterson
SK Fiskum
SR Suffield
RA Daniel
PA Gauglitz
BE Wells

Prepared for the U.S. Department of Energy
under Contract DE-AC05-76RL01830

PACIFIC NORTHWEST NATIONAL LABORATORY
operated by
BATTELLE
for the
UNITED STATES DEPARTMENT OF ENERGY
under Contract DE-AC05-76RL01830

Printed in the United States of America

Available to DOE and DOE contractors from the
Office of Scientific and Technical Information,
P.O. Box 62, Oak Ridge, TN 37831-0062;
ph: (865) 576-8401
fax: (865) 576-5728
email: reports@adonis.osti.gov

Available to the public from the National Technical Information Service
5301 Shawnee Rd., Alexandria, VA 22312
ph: (800) 553-NTIS (6847)
email: orders@ntis.gov <http://www.ntis.gov/about/form.aspx>
Online ordering: http://www.ntis.gov

This document was printed on recycled paper.
(8/2010)

Simulant Basis for the Standard High Solids Vessel Design

RA Peterson
SK Fiskum
SR Suffield
RA Daniel
PA Gauglitz
BE Wells

September 2016

Test Specification:	N/A
Work Authorization:	WA# 048
Test Plan:	TP-WTPSP-132, Rev 1.0
Test Exceptions:	N/A
Focus Area:	Pretreatment
Test Scoping Statement(s):	NA
QA Technology Level:	Applied Research
Project Number:	66560

Prepared for the U.S. Department of Energy
under Contract DE-AC05-76RL01830

Pacific Northwest National Laboratory
Richland, Washington 99352

Executive Summary

The Waste Treatment and Immobilization Plant (WTP) is working to develop a Standard High Solids Vessel Design (SHSVD) process vessel. To support testing of this new design, WTP engineering staff requested that a Newtonian simulant and a non-Newtonian simulant be developed that would represent the Most Adverse Design Conditions (in development)[1] with respect to mixing performance as specified by WTP. The majority of the simulant requirements are specified in 24590-PTF-RPT-PE-16-001, Rev. 0.[2] The first step in this process is to develop the basis for these simulants. This document describes the basis for the properties of these two simulant types. The simulant recipes that meet this basis will be provided in a subsequent document.

Newtonian Simulant Basis

The intent of this process is to develop the requirements for the Newtonian simulant properties from the design basis and the Most Adverse Design Condition. The key elements of the WTP design basis are as follows:

1. Matches the design basis 95% Upper Limit PSD provided in Jewett et al. 2002[3] plus a maximum particle size of 700 microns. Tolerances are provided in this report.
2. Has an average solid phase density of 2.9 g/mL +/- 0.1 g/mL.
3. All particles greater than or equal to 310 microns have a density 2.9 +/- 0.1 g/mL.

Additional constraints to address the "Most" Adverse criteria include:

4. Has a maximum particle density of 6 g/mL +/- 1 g/mL.
5. Is constrained so that the high-density solids have the largest possible particle size consistent with requirement 1.

The ranges of viscosities and densities for Newtonian fluids were identified based on design basis fluid properties specified for the SHSVD, where a series of assumptions for a modified flow sheet was assumed to have been implemented. In the modified flowsheet, the density range is 1.0 to 1.50 g/mL and the viscosity range is 1 to 10 cP. A density of 1.137 g/mL and a viscosity of approximately 1.53 ±0.1 cP were chosen for the carrier fluid to represent an adverse process condition.

[1] Specified in the Standard High Solids Vessel Design (SHSVD) Test Specification 24590-WTP-ES-ENG-14-012 Rev 1 (in development).

[2] Slaathaug, E. 2016. *Basis for Simulant Properties for Standard High Solids Vessel Mixing Testing*. 24590-PTF-RPT-PE-16-001, Rev. 0, Bechtel National, Inc., Richland, Washington.

[3] Jewett, JR, SD Estey, L Jensen, NW Kirch, DA Reynolds, and Y Onishi. 2002. *Values of Particle Size, Particle Density, and Slurry Viscosity to Use in Waste Feed Delivery Transfer System Analysis*. RPP-9805, Numatec Hanford Corporation, Richland, Washington.

Non-Newtonian Simulant Basis

Non-Newtonian simulant rheological properties were chosen based on the assumption that higher yield strength and viscosity would yield conservative results. Bingham parameters of 33.0 Pa (+3 Pa/-0 Pa)/32.0 cP (+ 3 cP/-0 cP) were identified as the appropriate targets for testing.

Acronyms and Abbreviations

BBI	Best Basis Inventory
HLW	high-level waste
ICP	inductively coupled plasma emission spectroscopy
MADC	Most Adverse Design Condition
PJM	pulse-jet mixer
PSD	particle size distribution
PSDD	particle size and density distribution
R&D	research and development
SEM	scanning electron microscopy
SHSVD	Standard High Solids Vessel Design
TEM	transmission electron microscopy
TOC	Tank Operations Contractor
WAC	Waste Acceptance Criteria
WFD	waste feed delivery
WTP	Waste Treatment Plant
WTPSP	Waste Treatment Plant Support Program
XRD	X-ray diffraction

Contents

Figures

Tables

1.0 Introduction

This document provides the requirements for test simulants to meet the specification provided by the Waste Treatment and Immobilization Plant (WTP) in Slaathaug 2016 and provides the basis for development of simulants that will be required for Standard High Solids Vessel Design (SHSVD) testing. The scope of the mixing tests to be performed with this simulant will be defined in the Subsystems Requirements Report (SSRR) and the Test Specification 24590-WTP-ES-ENG-14-012 Revision 1 (in development).[1] A subsequent document will provide the components selected to match these conditions. Both Newtonian and non-Newtonian simulants may be used to demonstrate the full range of design basis conditions.

Quality Requirements

Pacific Northwest National Laboratory complies with the requirements found in the following standards and implements them in their Waste Treatment Plant Support Program (WTPSP) Quality Assurance Program:

- ASME NQA-1-2000, *Quality Assurance Requirements for Nuclear Facility Applications*, Part I, Requirements for Quality Assurance Programs for Nuclear Facilities
- ASME NQA-1-2000, Part II, Subpart 2.7, Quality Assurance Requirements for Computer Software for Nuclear Facility Applications
- ASME NQA-1-2000, Part IV, Subpart 4.2, Guidance on Graded Application of Quality Assurance (QA) Requirements for Nuclear-Related Research and Development

Records will be stored as hardcopy records in a 2-hour fire-rated container.

This project recognizes that quality assurance applies in varying degrees to a broad spectrum of research and development (R&D) in the technology life cycle. The WTPSP uses a graded approach for the application of the quality assurance controls such that the level of analysis, extent of documentation, and degree of rigor of process control are applied commensurate with their significance, importance to safety, life cycle state of work, or programmatic mission. The technology life cycle is characterized by flexible and informal quality assurance activities in basic research, which becomes more structured and formalized through the applied R&D stages. The processes and work used as input to this report were conducted at the "Applied Research" level. Applied research consists of research tasks that acquire data and documentation necessary to assure satisfactory reproducibility of results. The emphasis during this stage of a research task is on achieving adequate documentation and controls necessary to be able to reproduce results.

[1] Slaathaug, E. 2016. *Basis for Simulant Properties for Standard High Solids Vessel Mixing Testing*. 24590-PTF-RPT-PE-16-001, Rev. 0, Bechtel National, Inc., Richland, Washington.

2.0 Simulant Requirements

This section documents the simulant development requirements and the physical and chemical constraints for planned testing as specified by WTP.

2.1 Simulant Development Requirements

Simulant development was required to follow the *Simulant Development, Approval, Validation, and Documentation* guide (24590-WTP-GPG-RTD-004, Rev. 3A). Applicable elements from the guide include the following:

- Define scope for simulant use (found in the SHSVD Test Specification 24590-WTP-ES-ENG-14-012 Rev 1 (in development).
- Specify simulant requirements (described herein).
- Design simulant (the subject of a subsequent qualification report).

The simulant constraints are defined in Section 2.2. The simulant design requirements are detailed in Section 3.0. Section 4.0 provides a summary of this report, and Section 5.0 provides references. Appendix A provides an assessment of the maximum prevalent particle density expected in adverse feed to the WTP.

2.2 Simulant Constraints

For the defined testing in the test SHSVD vessel, the WTP placed several constraints on the solid simulant components for operational efficacy:

1. The simulant components must be commercially available at the quantities needed for testing (in some cases up to several tons).
2. The simulant components should be non-hazardous with respect to handling and disposal to the extent practical. It is noted, however, that the dust hazard likely cannot be eliminated should the WTP decide to prepare the simulant from the dry solid components.
3. Batch-to-batch particle size distribution (PSD) variability should be minimal to support the preparation of multiple batches.
4. Simulant components must be compatible with one another, the vessel components and instrumentation, and solids phase components must be compatible with the carrier fluid.
5. Simulant components must not be prohibitively expensive, as defined by the client upon evaluation of the cost of the projected component.
6. To the extent practical, non-separable components (with the exception of clays) should be uniquely identifiable by quantitative analytical methods such as; inductively coupled plasma emission spectroscopy analysis (ICP) and X-ray fluorescence, or other quantitative analytical method.

3.0 Simulant Properties

The SHSVD test campaign is designed to qualify this vessel design for use in the WTP Pretreatment Facility (PTF) through several demonstrations under most adverse design conditions (MADC). These evaluations of the WTP design bases (WTP contract, Interface Control Documents, WTP Basis of Design, etc.) were performed by WTP Engineering and are described by Slaathaug in 24590-PTF-RPT-PE-16-001[1]. This evaluation identified requirements for both Newtonian and non-Newtonian simulants, specific physical characteristics of which are described in Section 3.1 and Section 3.2 below, and it is specified to include the largest Newtonian simulant particles in the non-Newtonian simulant as provided in Section 3.2.1.[2]

An additional, information only, test has been proposed to evaluate the performance of the SHSVD in a 'de-inventory' operating mode. This test is described in *De-Inventory Testing for the Standard High Solids Vessel* 24590-WTP-ES-ENG-16-021 (Johnson 2016)[3] and requires a simulant replicating the viscosity and density of a proposed 10M NaOH vessel flush solution. This is discussed in Section 3.3.

MADC for the simulants is specified in the SHSVD Test Specification 24590-WTP-ES-ENG-14-012 Rev 1 (July 20, 2016 Draft) relative to the mixing qualification test requirements, methodology, and data needs as summarized therein. Four requirements are listed for verification:

- Mix to Support Transfer
- Mix to Support De-Inventory of Vessel Contents
- Mix to Support Sampling
- PJM and Sparger Control.

Comparison of the specified Newtonian simulant characteristics to a representatively adverse process stream is qualitatively made relative to general metrics for particle mobilization, suspension, settling, and pipeline transfer (e.g., Appendix A), and discussion of both the Newtonian and non-Newtonian simulant specifications to a selection of the listed requirements for verification is provided.

[1] Slaathaug, E. 2016. *Basis for Simulant Properties for Standard High Solids Vessel Mixing Testing*. 24590-PTF-RPT-PE-16-001, Rev. 0, Bechtel National, Inc., Richland, Washington.

[2] Defined by BNI (2011). Newtonian describes a waste's rheology characterized by a single viscosity, whereas non-Newtonian describes a waste whose rheology is characterized by both a Bingham yield stress and consistency, so the apparent viscosity is a function of the strain rate.

[3] Johnson, P. 2016. *De-Inventory Testing for the Standard High Solids Vessel* 24590-WTP-ES-ENG-16-021, Bechtel National, Inc., Richland, Washington.

3.1 Newtonian Simulant

3.1.1 Solids Phase Criteria

SHSVD Newtonian simulant development requires a blend of non-hazardous solids for SHSVD testing that meet the following criteria from the *Basis for Simulant Properties for Standard High Solids Vessel Mixing Testing*, 24590-PTF-RPT-PE-16-001 (Slaathaug 2016):

1. Matches the design basis 95% Upper Limit PSD provided in Jewett 2002 plus a maximum particle size of 700 microns. Tolerances are provided in **Table 3.1**.
2. Has an average solid phase density of 2.9 g/mL +/- 0.1 g/mL.
3. All particles greater than or equal to 310 microns have a density 2.9 +/- 0.1 g/mL.
4. Has a maximum particle density of 6 g/mL +/- 1 g/mL.
5. Is constrained so that the high-density solids have the largest possible particle size consistent with requirement 1.

Requirements 1 through 3 are provided by the design basis for the WTP. Since these parameters reflect the design basis of the facility, they should be reflected in the proposed simulant that is to be used to test this design basis. Requirement 4 was selected by Slaathaug (2016) as it represents the highest density prevalent minerology in Tank Farm waste. The fifth requirement from Slaathaug (2016) is associated with a need to make the simulant adverse to mixing with respect to its particle size and density distribution by maximizing its propensity to settle within the constraints of the design basis. This characteristic is the final piece of defining the Most Adverse Design Condition (MADC)[1] for the Newtonian simulant for testing, which also includes solids concentration, liquid density and viscosity, and bulk average solids density. **Table 3.1** provides a summary of the required light scattering PSD for the Newtonian simulant given in Slaathaug (2016)[2].

Table 3.1. Required particle size distribution for Newtonian simulant (Slaathaug 2016)**.**

Volume Percent Particles less than Design Basis Target	Design Basis Particle Size (micron)	SHSVD Simulant Particle Size Tolerance (micron)
1%	1	NA
5%	1.6	NA
25%	5	NA
50%	11	NA
75%	58 +/- 29	29-87
95%	210 +/- 21	189-231
99%	310 +/- 31	239-341
100%	700+/- 70	630-770
NA – No tolerance defined for the smaller particles, the Design Basis values are to be used simply as targets		

[1] Specified in section 4.6 of the Standard High Solids Vessel Design (SHSVD) Test Specification 24590-WTP-ES-ENG-14-012 Rev 1 (July 20, 2016 Draft)

[2] The method of measurement for the particle size distribution, which is light scattering, is discussed by Jewett et al. (2002).

3.1.2 Most Adverse Design Condition, Newtonian

Requirements 1 through 3 in Section 3.1.1 define a PSD and an average density, but they do not define a particle size and density distribution (PSDD). A useful assessment is to propose theoretical PSDDs and evaluate them using metrics for particle mobilization, suspension, settling, and pipeline transfer (see Appendix A).

One theoretical formulation is the WTP high-level waste feed vector, as described in the Tank Utilization Assessment report (Jenkins et al. 2013). This assessment is used in Appendix A to estimate the PSDDs of the waste to be vitrified. The PSDDs were then evaluated using general metrics for particle mobilization, suspension, settling, and pipeline transfer to select a representative most adverse waste batch for processing at the WTP. Batch 108 (out of 631 projected slurry deliveries to the WTP and 203 batches from the leached sludge feed batches) was identified as the most adverse. The average particle density of Batch 108 is 2.8 g/mL.

A second theoretical formulation (Basis of Design; BOD) is the design basis PSD and to assign all particles a density of 2.9 g/mL. A third formulation is to assume conditions consistent with the 5 requirements identified by Slaathaug (Representative Newtonian MADC). These three PSDD formulations are presented in Figure 3.1 as particle density as a function of particle size. While the BOD and Representative Newtonian MADC formulations consist of a single density at each respective particle size, the Batch 108 generally consists of 9 unique particles with densities ranging from 2.4 to 6.74 g/mL. The Batch 108 particle density for each particle size is therefore provided as the volume weighted average.

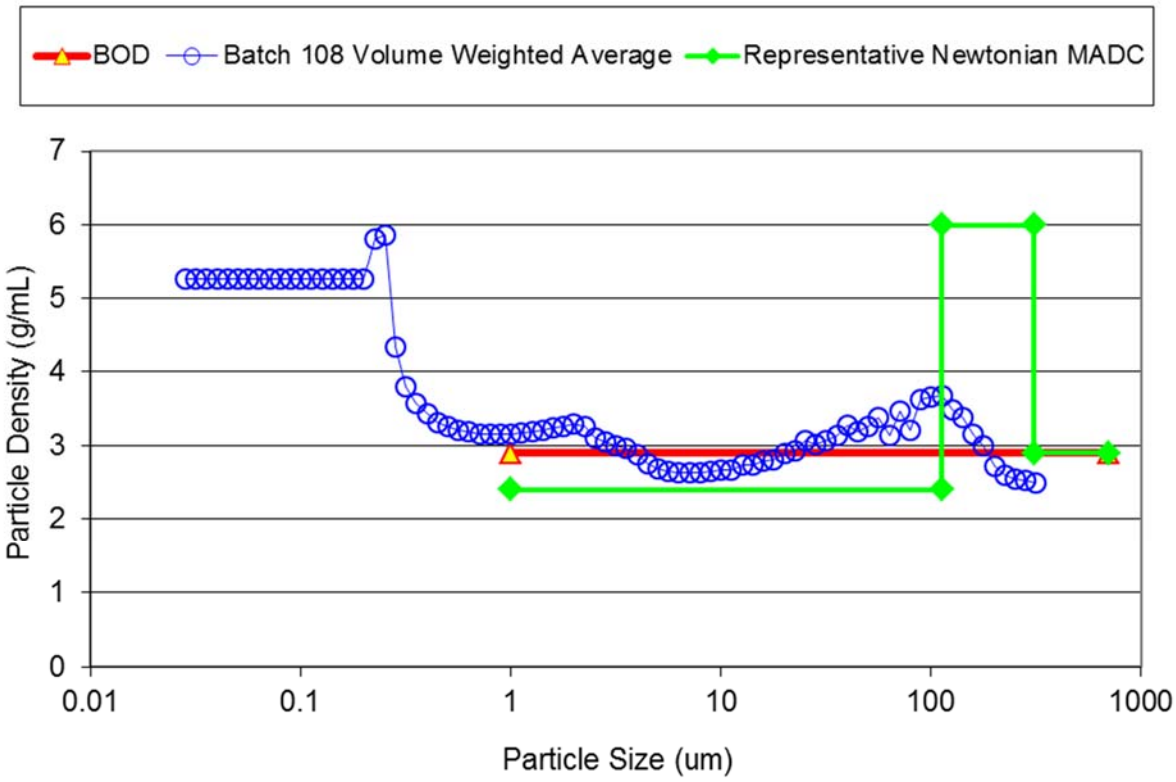

Figure 3.1. Particle Density as a function of Particle Size.

From the three PSDDs of Figure 3.1, it is possible to generate estimates of various metrics of mixing performance for each of the three theoretical formulations (i.e., Appendix A). Comparisons can thus be made of the relationship of particle size and density between the representative Newtonian MADC simulant and Batch 108, the most adverse process stream per the general metrics for particle mobilization, suspension, settling, and pipeline transfer. Since application of the metrics of Appendix A is dependent solely on density and particle size and a more adverse result is achieved with larger and denser solids, increasing the fraction of the densest particles at the larger sizes may be anticipated to result in a more adverse condition.

There is evidence to support that the presence of larger solids result in a more adverse condition. A comparison can be made using test data results for bottom motion from 24590-QL-HC1-M00Z-00003-09-00176. Two experiments were performed, one using the complete Herting (2012) simulant and a second test that had omitted largest particles (approximately 6% of the mass of the complete Herting 2012 simulant solids). The tests demonstrated that the complete simulant, i.e., including the large particles, required a significantly higher PJM nozzle velocity for equivalent bottom motion. Kuhn et al. (2013) describes a vessel performance assessment methodology for bottom clearing in a PJM mixed vessel that includes the critical shear stress for particle erosion (see Appendix A, A.6.5) and particle settling rate (see Appendix A, A.5). Again, larger and more dense particles have a higher critical shear stress for particle

erosion and particle settling rate, see Appendix A. Therefore, these metrics will be use to compare the representative Newtonian MADC simulant and Batch 108.

The calculated critical shear stress for particle erosion and particle settling rate for the individual particles of the representative Newtonian MADC simulant and Batch 108 are provided in Figure 3.2 and Figure 3.3 respectively. The BOD is also included. As anticipated, the representative Newtonian MADC simulant has the most adverse particles in comparison to Batch 108 and the BOD. As emphasized in Appendix A, each particle size and density of the PSDDs is evaluated separately with all other model input parameters (e.g., liquid phase properties, solids concentration, etc.) held constant. Therefore, it is the comparison of the model results for the particulates that is of significance, not the specific model results themselves.

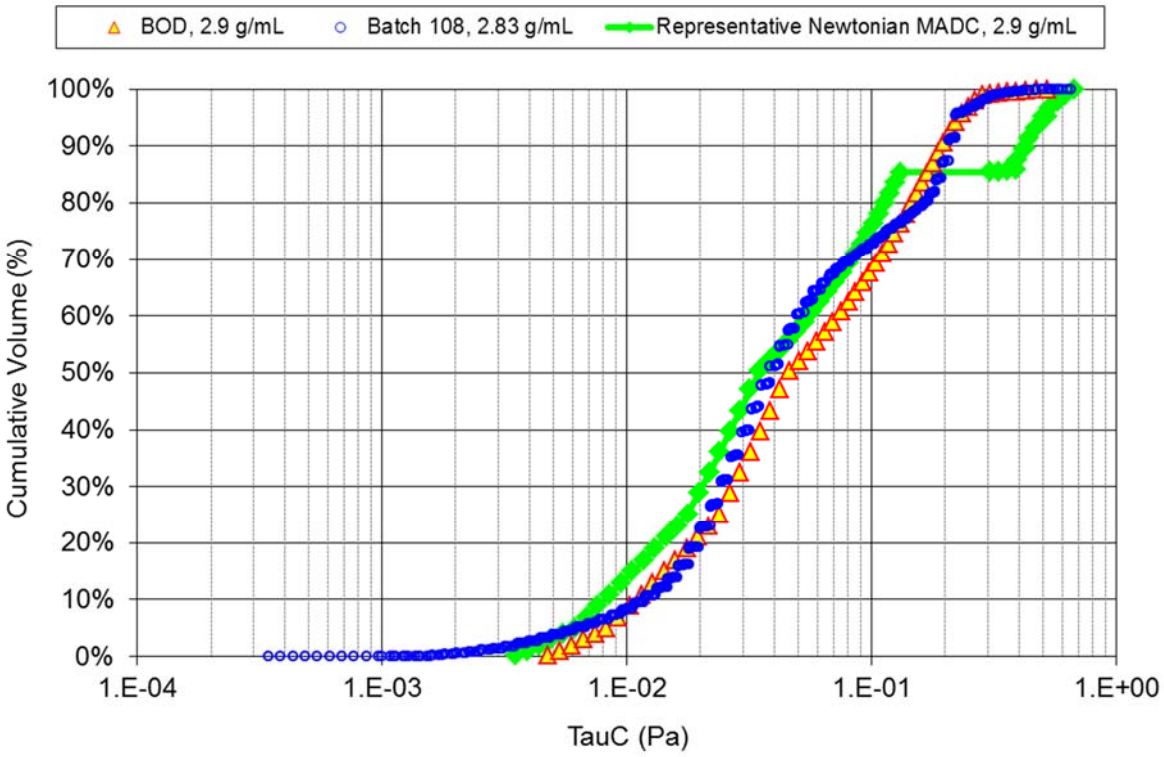

Figure 3.2. Calculated Critical Stress for Erosion (see Appendix A) for the Particles of the Representative Newtonian MADC Simulant, Batch 108, and the BOD

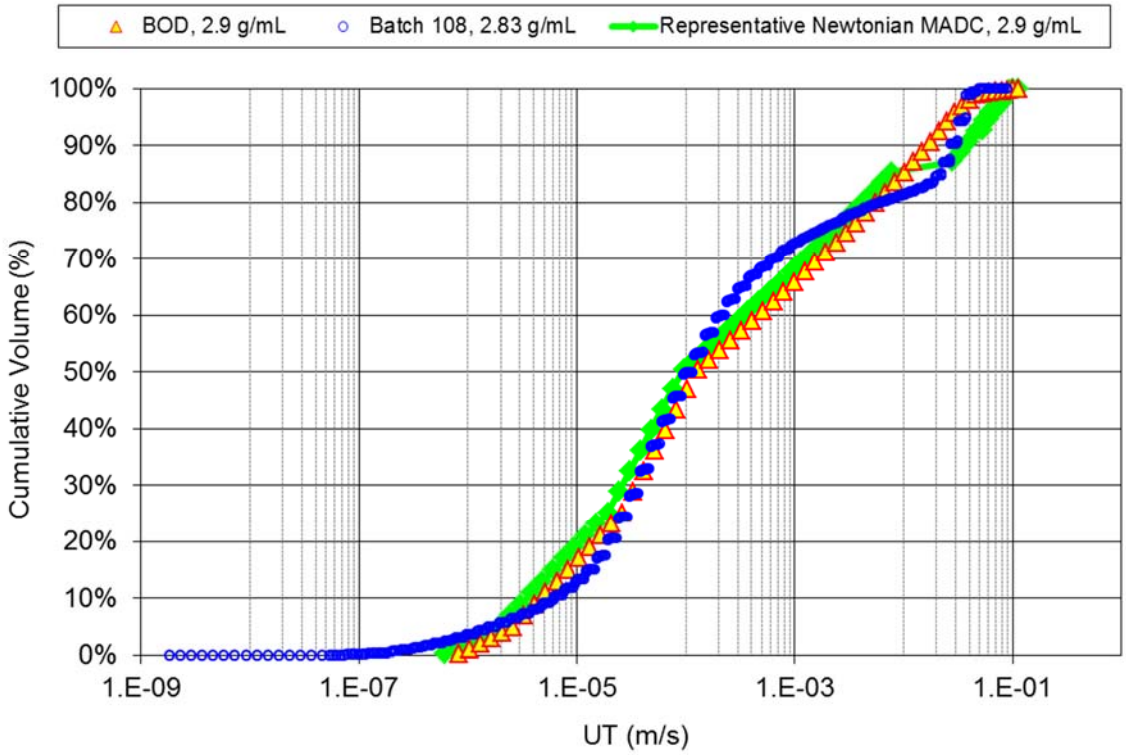

Figure 3.3. Calculated Settling Rate (see Appendix A) for the Particles of the Representative Newtonian MADC Simulant, Batch 108, and the BOD

The representative Newtonian MADC simulant has the most adverse particles for these two metrics. Thus, a demonstration of a more adverse result is provided, suggesting that the representative Newtonian MADC simulant is more adverse than Batch 108 for a bottom motion metric (all other test parameters equal). Note, however, that there are differences between the particles represented in Figures 3.2 and 3.3 and those employed in the tests described in 24590-QL-HC1-M00Z-00003-09-00176. Although it has not been definitively demonstrated that the representative Newtonian MADC simulant is more adverse than Batch 108 because of the marginal lower-result differences shown in Fig 3.2 and 3.3 below approximately the 85th percentile relative to the higher-result differences above the 85th percentile, the representative Newtonian MADC simulant is expected to be the more adverse for bottom motion.

As described, the impact of the differences in the less-adverse solids relative the increased probability of the larger, more dense, particles has not been evaluated, nor have metrics specified to address the requirements listed for verification in 24590-WTP-ES-ENG-14-012 Rev 1 (July 20, 2016 Draft). Slaathaug documented conditions for the representative Newtonian MADC simulant without assessment of whether these conditions would be more adverse relative to some of the specific requirements outlined in 24590-WTP-ES-ENG-14-012 Rev 1. The requirements listed for verification in 24590-WTP-ES-ENG-14-012 Rev 1 (July 20, 2016 Draft), see Section 3.0, mixing to support transfer and mixing to support sampling are briefly discussed for Newtonian conditions. The performance metric for mixing to support transfer in 24590-WTP-ES-ENG-14-012 Rev 1 (July 20, 2016 Draft) is a transfer pipeline velocity range when the transfer pump is at a constant operating speed (.i.e., constant variable frequency drive setting). In that case, the largest pipeline velocity changes can be incurred by solids loading changes and/or deposition of solids in the pipeline, which impact pump performance and pipeline head

loss. Thus, neglecting deposition, an adverse condition would have a maximum solids concentration change at the transfer line inlet over the test duration. For example, a process stream with a large fraction of solids that are elevated to the transfer line inlet by the PJM drive but settle below the transfer line inlet during refill. An evaluation of this behavior was not included when determining that Batch 108 was adverse.

For mixing to support sampling, 24590-WTP-ES-ENG-14-012 Rev 1 (July 20, 2016 Draft) provides the performance metrics of vessel blending. As described in Reynolds et al. (DRAFT), if the incoming liquid transfer into a Hanford waste storage tank is lower density than the existing supernatant liquid, limited mixing between the existing supernatant and the incoming liquid occurs. Stratification is often observed in double-shell tanks with little change over years and the liquid layers have to be mechanically mixed. Rassat et al. (2000) analyzed waste tank conditions with a mixer pump, and concluded that a liquid layer of 1.43 g/mL would be stable over a layer of 1.52 g/mL during the operation of a rotary jet centrifugal mixer pump. For a less dense supernatant liquid layer over a more dense layer, one adverse condition would therefore have the solids homogenously distributed over the initial vessel fill independent of the PJM cycle. However, as demonstrated for example in Meyer et al. (2012), increased solids loading at equivalent PJM nozzle velocity results in the solids being lofted to a lower height. Thus, the velocity at higher elevations in a vessel is reduced by the higher solids loading. An adverse condition for blending a less dense supernatant liquid layer over a more dense layer thus may be an optimization of the fraction of solids suspended for density difference effect and the fraction of solids at the vessel bottom between pulses to impact the fluid velocity at the layer interface. The effect of altered liquid head pressure depending on vessel fill level for PJM nozzle velocity may also impact blending performance. These conditions were not included in the evaluation determining Batch 108 as adverse.

For the performance metric for mixing to support transfer of the transfer pipeline velocity range, the fraction of the representative Newtonian MADC that are large dense particles would likely provide a fluctuating solids concentration at the transfer inlet. For blending, these particles, anticipated to be near the vessel bottom, may also be anticipated to impact the fluid velocity at the layer interface, while the lower density and smaller particles would likely contribute to the layer density difference. Therefore, the representative Newtonian MADC may be of interest for an adverse condition relative to the requirements listed for verification in 24590-WTP-ES-ENG-14-012 Rev 1 (July 20, 2016 Draft).

3.1.3 Newtonian Liquid Simulants

Newtonian liquids are needed for combining with the particles selected by the method discussed in Section 3.1.1. As indicated above, the average density for the solid phase will be 2.9 +/- 0.1 g/mL and will have a d95 of 210 microns. Further, the target solids concentration for the Newtonian simulant is 10 wt% (Slaathaug 2016). Based on these input data, WTP project staff have calculated that the carrier liquid must have a density of 1.137 +/- 0.1 g/mL to meet the design requirements for pipeline transfer. This calculation also provides a lower limit of 1.53 +/- 0.1 cP for the fluid viscosity. These parameters are defined at 20 °C, which is a representative design temperature.

3.2 Non-Newtonian Simulants

Pulse-jet mixer (PJM) performance depends on a slurry's physical and rheological properties and the size, density, and shape of the individual particles. Many of the slurries exhibit non-Newtonian rheology

while also having particles that may be large and/or dense enough to settle within the non-Newtonian fluids. A previous WTP evaluation has identified the slurry yield stress and consistency as important parameters for non-Newtonian slurries (Poirier and Martino 2015). Slaathaug (2016) defined the MADC for non-Newtonian slurries as the highest Bingham yield stress and highest Bingham consistency (viscosity) that are consistent with the design limit of for 30 Pa and 30 cP. Slaathaug also stated simulant target values and uncertainties of 33.0 +3/-0 Pa and 32.0 +3/-0 cP to account for measurement uncertainty. These target values are from an analysis by Josephson[1] that gave 33 Pa/32 cP as the mean (of three samples) Bingham yield stress and consistency that will provide 95% confidence that a simulant meeting or exceeding these values would exceed the 30 Pa/30 cP design limit. The uncertainties in Slaathaug show that simulant properties should exceed the targets. The slurry density of this simulant should fall between 1.0 and 1.3 g/mL, as practical, and both the rheology and density of the non-Newtonian simulants should be measured at 25° C (Slaathaug 2016). Note that the slurry solids content will be defined by the conditions required to achieve the desired rheology and are not bound by expected operations (that is, the total solids content is likely to be above 27 wt%). Further, the rheology and density targets in Slaathaug (2016) include added large-diameter particles that are described in the following section.

3.2.1 Settling Particles for Non-Newtonian Simulants

One or more challenging particles will be added to the non-Newtonian simulants to allow evaluation of PJM performance for suspending large and/or dense particles in non-Newtonian fluids. These added particles will be selected from the larger particles from the Newtonian simulant (Slaathaug 2016). Slaathaug further specifies the particle size range and concentration.

A settling particle will need to be compatible with the non-Newtonian slurries, most likely clay-based slurries. The following compatibility characteristics will need to be evaluated for potential settling particles:

- No corrosion or dissolution (note that the non-Newtonian simulant may include salts, however the low temperature and short contact time likely preclude any significant corrosion from occurring).
- Compatible (no formation of hard settled layers or agglomeration) with non-Newtonian simulant particles (such as clays).

The settling particles will also need the following characteristic:

- Physically separable from the non-Newtonian simulant.

3.2.2 Most Adverse Design Condition, Non-Newtonian

The requirements listed for verification in 24590-WTP-ES-ENG-14-012 Rev 1 (July 20, 2016 Draft, Section 3.0), mixing to support transfer and mixing to support sampling are briefly discussed with respect to non-Newtonian conditions. As for the Newtonian MADC, the largest pipeline velocity changes can be caused by solids loading changes and/or deposition of solids in the pipeline, and blending may be most adversely impacted by density gradients and jet velocity.

[1] G. Josephson , “non-Newtonian Rheology Uncertainty”, CALC NO. 24590-PTF-MVC-M59T-00001 Rev.0, Dated 06-10-2016.

With respect to vessel performance, solids loading changes may be incurred via slurry mobilization effects and ingestion into the transfer line. Data for both PJM mixed and waste feed delivery (WFD) vessels are available for the related metrics of bottom motion growth rate and transfer of solids out of vessel. The PJM vessel data include 24590-WTP-ES-PET-10-001, Rev. 0, 24590-WTP-RPT-ENG-11-164, Rev. 0, Gauglitz et al. (2009), Kuhn et al. 2013, and Meyer et al. (2012). Pertinent WFD delivery testing data include Adamson and Gauglitz (2011), Kelly et al. (2013), and Wells et al. (2012). The results presented in those references are supported by literature for jet applied stress (e.g., Poreh et al. 1967, Beltaos and Rajaratnam 1977), sediment mobilization (e.g. Torfs et al. 2001), and solid settling in a Bingham slurry (e.g., Ansley and Smith 1967). In general, bottom motion growth rate is suggested to be reduced by increasing Bingham yield stress, and the ingestion of solids into the transfer line is suggested to be reduced by decreasing Bingham yield stress. Both bottom motion growth rate and transfer of solids out of vessel are suggested to be decreased by decreased Bingham viscosity and slurry density. Settling solids that concentrate at the vessel bottom and have characteristics that maximize the depth and critical stress for erosion of the resultant composite are indicated as adverse in each case. Data are also available (e.g. Poloski et al. 2009) that suggest there are rheological conditions of interest throughout the range of yields stress and viscosity combinations that may increase the likelihood of particle deposition and impacts to the minimum operating requirements of the transfer pump. Testing specified in 24590-WTP-ES-ENG-14-012 Rev 1 (July 20, 2016 Draft) will address non-Newtonian test conditions other than the high Bingham yield stress with high Bingham viscosity during the pump out of the 10 and 20 % diluted non-Newtonian simulant test conditions.

3.3 De-Inventory Testing Liquid

Johnson (2016) (24590-WTP-ES-ENG-16-021, *De-Inventory Testing for the Standard High Solids Vessel*)) describes a proposed de-inventory test for evaluating the capability of the PJM mixing subsystem in conjunction with rinse and transfer functions to empty the SHSVD vessel over multiple pump downs. The recommendation for the de-inventory test is to measure the removal of bismuth oxide particles, with a median diameter of 150 μm and a density of 8.9 g/mL, in a suspending Newtonian liquid with a density and viscosity that are similar to 10 M NaOH[1]. The targets for this de-inventory Newtonian liquid simulant are a density of 1.325 +/- 0.1 g/mL and a viscosity
10.5 +/- 0.7 cP based on 10 M NaOH at 25 °C (Sipos et al. 2000), where equivalent uncertainties as for the Newtonian liquid given in Section 3.1.3 are assumed[2].

[1] In an e-mail from Paul Johnson of BNI dated July 26, 2016, the properties for 10 M NaOH should be at 25 °C.
[2] For density, the uncertainty is ± 0.1 g/mL for a target of 1.13 g/mL and this uncertainty seems appropriate for the higher density of 1.32 g/mL for the de-inventory simulant. For viscosity, the uncertainty is ± 0.1 cP for a target of 1.53 cP; an equal percentage uncertainty for a 10.5 cP target is ± 0.7 cP.

4.0 Summary

This section summarizes the Newtonian and non-Newtonian simulant bases described in the preceding sections. Slaathaug 2016 provides the basis for development of simulants that will be required for Standard High Solids Vessel Design (SHSVD) testing and provides most adverse properties within the design basis with respect from mixing perspective in a Newtonian slurry. Although not formally assessed by PNNL against the transfer and blending mixing requirements this has been considered by the WTP test planners. Their SHSVD Test Specification, section 4.6.4.4 states "that it is overall quantity of fast-settling particles that is expected to drive adversity with respect to both 3.5.1.1 Transfer (impact to flow in the transfer line) and 3.5.1.4 Sampling (impact on blend time)" (24590-WTP-ES-ENG-14-012).
This document provides the basis for simulant design and development and a comparison of the Slaathaug 2016 requirements against adverse Hanford waste slurry mixing and transfer metrics. Table 4.1 provides a summary of the Slaathaug simulant requirements. Subsequent documents will provide the actual simulant recipes that meet these requirements and provide the evidence that these formulations satisfy the requirements provided in this document.

Table 4.1. Summary of simulant property requirements.

	Particle Size Range	Average Particle Density (g/mL)	Liquid Density (g/mL)	Liquid Viscosity (cP)	Slurry Density (g/mL)	Bingham Yield Stress (Pa)	Bingham Consistency Viscosity (cP)	Solids Concentration (wt% or mass added)
Newtonian	RPP-9805 95% UL +700 µm max	2.9+/-0.1	1.137+/-0.1	1.53+/-0.1	1.03 – 1.7	NA	NA	10 +/- 1.0
Non-Newtonian	*	*	NA	NA	1.0 – 1.3	33+ 3/-0	32.0+ 3/-0	*
De-Inventory	150 µm median	8.9	1.325 +/-0.1	10.5 +/-0.7	NA	NA	NA	~ 3 kg in SHSV

* Spike simulant with two times the quantity of particles (total grams of particles per liter of simulant) in the 100 to 700 µm range as used in Newtonian simulant. Particles will have the same density as specified for the Newtonian simulant (Slaathaug 2016).

5.0 References

24590-QL-HC4-M00Z-00003-09-00176. 2015. *Pulse Jet Mixer (PJM) Test Platform Test Vessel V401 SHSVD Pilot-Scale Testing Test Sequence#: 8' SHSVD-Tests-32* Rev 00. Energy Solutions, Richland, Washington.

24590-WTP-ES-PET-10-001. 2010. *WSU Radial Flume Test Data Study*. Rev. 0. Bechtel National, Inc., Richland, Washington.

24590-WTP-RPT-ENG-11-164. 2012. *Non-Newtonian Proof of Concept Scoping Test Report*. Rev. 0. Bechtel National, Inc., Richland, Washington.

Adamson DJ, and PA Gauglitz. 2011. *Demonstration of Mixing and Transferring Settling Cohesive Slurry Simulants in the AY-102 Tank*. SRNL-STI-2011-00278, Rev. 0. Savannah River National Laboratory, Aiken SC.

Ansley RW, and TN Smith. 1967. "Motion of Spherical Particle sin a Bingham Plastic." *AIChE Journal*. Vol. 13, No. 6: 1193 – 1196.

ASME NQA-1-2000. *Quality Assurance Requirements for Nuclear Facility Applications.* American Society of Mechanical Engineers, New York, New York.

Beltaos S, and Rajaratnam N. 1977. "Impingement of axisymmetric Developing Jets." *Journal of Hydraulic Research* 15 (1977) no. 4: 311 – 326.

BNI. 2016 July 20, 2016 draft. Standard High Solids Vessel Design (SHSVD) Test Specification. 24590-WTP-ES-ENG-14-012 Rev 1 Bechtel National, Inc., Richland, Washington.

BNI. 2014. *ICD-19 – Interface Control Document for Waste Feed*. 24590-WTP-ICD-MG-01-019, Rev. 7, Bechtel National, Inc., Richland, Washington.

Gauglitz PA, BE Wells, JA Fort, PA Meyer. 2009. *An Approach to Understanding Cohesive Slurry Settling, Mobilization, and Hydrogen Gas Retention in Pulsed Jet Mixed Vessels*. PNNL-17707, WTP-RPT-177, Rev. 0. Pacific Northwest National Laboratory, Richland, WA.

Herting DL. 2012. *Simulant Qualification for Computational Fluid Dynamics Testing*. 24590-WTP-RPT-RT-12-002, Rev. 0, Bechtel National, Inc., Richland, Washington.

Jenkins, K, Y Deng, and S Orcutt. 2013. *2012 WTP Tank Utilization Assessment*. 24590-WTP-RPT-PE-12-001, Bechtel National, Inc., Richland, Washington.

Jewett, JR, SD Estey, L Jensen, NW Kirch, DA Reynolds, and Y Onishi. 2002. *Values of Particle Size, Particle Density, and Slurry Viscosity to Use in Waste Feed Delivery Transfer System Analysis*. RPP-9805, Rev 1, Numatec Hanford Corporation, Richland, Washington.

Johnson. 2016 . *De-Inventory Testing for the Standard High Solids Vessel*24590-WTP-ES-ENG-16-021. Bechtel National, Inc., Richland, Washington.

Kelly SE, RX Milleret, TA Wooley, and KP Lee. 2013. *One System Waste Feed Delivery Mixing Performance and Solids Accumulation Test Report*. RPP-RPT-53931, Rev. 0. Washington River Protection Solutions LLC, Richland WA.

Kuhn WL, DR Rector, SD Rassat, CW Enderlin, MJ Minette, JA Bamberger, GB Josephson, BE Wells, and EJ Berglin. 2013. *Scaling Theory for Pulsed Jet Mixed Vessels, Sparging, and Cyclic Feed Transport Systems for Slurries*. PNNL-22816. Pacific Northwest National Laboratory, Richland, WA.

Meyer PA, JA Bamberger, CW Enderlin, JA Fort, BE Wells, SK Sundaram, PA Scott, MJ Minette, GL Smith, CA Burns, MS Greenwood, GP Morgen, EBK Baer, SF Snyder, M White, GF Piepel, BG Amidan, A Heredia-Langner. 2012. *Pulse Jet Mixing tests with Noncohesive Solids*. PNNL-18098 Rev. 1, WTP-RPT-182, Rev. 1. Pacific Northwest National Laboratory, Richland, WA.

Poirier, MR and CJ Martino. 2015. *Properties Important to Mixing and Simulant Recommendations for WTP Full-Scale Vessel Testing*. Pre-Decisional, Deliberative Process Information SRNL-STI-2015-00301 Rev. I, Savannah River National Laboratory, Savannah River Nuclear Solutions, LLC, Aiken, South Carolina.

Poloski AP, HE Adkins, ML Bonebrake, J Chun, AM Casella, KM Denslow, MD Johnson, ML Luna, PJ MacFarlan, JM Tingey, and JJ Toth. 2009. Deposition Velocities of Non-Newtonian Slurries in Pipelines: Complex Simulant Testing. PNNL-18316, WTP-RPT-189, Rev. 0. Pacific Northwest National Laboratory, Richland, WA.

Poreh M, YG Tsuei, and JE Cermak. 1967. "Investigation of a Turbulent Radial Wall Jet." *Journal of Applied Mechanics*. June 1967:457-463.

Reynolds JG, C Groves, D Herting, JE Meacham, and L Cree. DRAFT. *Evaluation of Risks to the DFLAW Mission from Solids in East Area Double-Shell Tanks*. RPP-RPT-59586 DRAFT. Washington River Protection Solutions LLC, Richland WA.

Sipos, PM, G Hefter, and PM May. 2000. "Viscosities and Densities of Highly Concentrated Aqueous MOH Solutions (M+) Na+, K+, Li+, Cs+, (CH3)4N+) at 25.0 °C.", *J. of Chem. and Eng. Data,* 45(4):613-617.

Slaathaug, E. 2016. *Basis for Simulant Properties for Standard High Solids Vessel Mixing Testing*. 24590-PTF-RPT-PE-16-001 Rev 0, Bechtel National, Inc., Richland, Washington.

Torfs H, J Jiang, and AJ Mehta. 2001. "Assessment of Erodibility of Fine/Coarse Sediment Mixtures." *Coastal and Estuarine Fine Sediment Processes*. Elsevier Science B.V., WH McAnally and AJ Mehta, editors.

Wells BE, PA Gauglitz, and DR Rector. 2012. *Comparison of Waste Feed Delivery Small Scale Mixing Demonstration Simulant to Hanford Waste*. PNNL-20637, Rev. 2. Pacific Northwest National Laboratory, Richland, WA.

Appendix A

Assessment of Expected Feeds to WTP

Appendix A

Assessment of Expected Feeds to WTP

Previous studies characterizing Hanford waste solids (Jewett et al. 2002; Wells et al. 2007, 2011) provide a basis for the combined range of particle sizes and densities that are appropriate for Hanford tank waste, and Wells et al. (2012) provide a performance-based technical basis for determining if any given blend of simulant material density and particle size is representatively adverse relative to those tanks' wastes. Much of this information was generated outside of the WTPSP and as such is not part of the NQA1 pedigree of the WTPSP and has been included here as FIO. This basis was used by Lee et al. (2012) to develop adverse Newtonian[1] simulants of varying degrees for the Tank Operations Contractor (TOC) Waste Feed Delivery (WFD) Mixing and Sampling Program. For these performance-based simulant designs, the sizes and densities of simulant components are selected to provide comparable performance to the waste targets for a specific set of performance metrics for particle mobilization, suspension, settling, and transfer.

Hanford waste contains a broad spectrum of mineral oxides and hydroxides, with predominant insoluble solids phases being iron- and aluminum-bearing hydroxides and with trace contamination by actinide metal oxides and hydroxides. Likewise, extensive testing of high-level waste (HLW) finds a broad distribution of insoluble solid particle size that ranges from sub-micrometer colloids to greater than 1000 μm. One of the key challenges in supporting the River Protection Project mission includes the incidental and intentional blending between the tanks (West et al. 2012), which can alter the wastes' solid property characterizations, thereby affecting treatment process performance. Incidental blending may occur throughout retrieval, staging, and delivery of the wastes, while intentional blending occurs based on available space within the feed tanks and a need to improve waste processability and to meet the requirements of the Waste Acceptance Criteria (WAC). There are about 600 HLW feed batches planned during the WFD mission. Further, the caustic-leaching process within the Hanford Waste Treatment and Immobilization Plant (WTP) can also alter the waste properties. Therefore, representative Standard High Solids Vessel Design (SHSVD) Newtonian simulant solid properties were developed from actual waste characterization data that is informed by the anticipated feeds and treated wastes to and within the WTP.

The first step in this process is to assess the anticipated feeds to the WTP and the expected product from the Pretreatment Facility. These feed and treated batches were evaluated to determine the dominant chemical components. BNI (2011) states that HLW transfers to WTP Pretreatment are received between 10 and 200 grams of unwashed solids per liter. It may be inferred from Meacham et al. (2012) that these solids limits may result in feed that exceeds the BNI (2014) rheology limit of 1 Pa were other steps such as separation or dilution not undertaken. Regardless, the BNI (2014) rheology requirement indicates the feed is essentially Newtonian, and the feed and treated batch solids are treasured as such for the purpose of the analysis described herein.

[1] As defined by BNI (2011) Newtonian describes a waste's rheology characterized by a single viscosity, whereas non-Newtonian describes a waste whose rheology is characterized by both a Bingham yield stress and consistency, so the apparent viscosity is a function of the strain rate.

Hanford tank waste data are then reviewed to (1) identify major mineral phase and (2) isolate one or more actual tank waste samples in which those mineral phases dominate (to the greatest extent possible) the overall chemical fraction and which have accompanying particle size distribution (PSD) measurements. The latter part of this effort allows the predominant mineral phase to be associated with a measured size distribution, and this association allows a size distribution to be assigned to a given mineral phase. This is not to say that the assignment is exact. Some sources of uncertainty are as follows:

- It is difficult to determine PSD for minor mineral phases.
- The PSDs measured are assumed to be for crystals.
- The distributions are for mixes of materials, but are assigned to the primary phases without separation.

However, the exercise provides a basis to define the adverse waste batch for the SHSVD Newtonian simulant basis. Further, the selection of the PSDs was validated through comparison to full-scale tank settling data. Thus, SHSVD simulant performance metrics relative to vessel mixing are based on a density and size distribution that is grounded in actual waste measurements.

This appendix develops a basis for recommending simulant particle size and density distributions (PSDDs) to represent specific Hanford waste components. A four-step process is used:

1. The target waste components (e.g., aluminum) are identified.
2. One or more mineral phases are assigned to a given component (e.g., aluminum is associated with boehmite and gibbsite).
3. A particle size is associated with each mineral phase.
4. These results are integrated into a PSDD.

This evaluation resulted in a set of mineral phases and associated size distributions. Inputs to the evaluation include examination of the feed batches expected in the WTP (in terms of as-received solids and leached solids) as well as actual tank sludge compositions from a variety of characterization activities and the particle size of the selected primary waste components.

A.1 Identification of Target Waste Components from Feed Batches

The primary sludge components were derived from projected as-received and caustic-leached solids data. The as-received feed batch was delineated in 631 projected slurry deliveries to the WTP as defined in the WTP simulant model for the Tank Utilization Assessment (Jenkins et al. 2013). The input data were based on sludge expected to be received in HLP-VSL-00022, as estimated from the as-received feed batch and the Hanford Tank Waste Operations Simulator. Input data for the caustic-leached solids were derived from expected HLP-VSL-00027A/B and HLP-VSL-00028 sludge in 203 batches from the leached sludge feed batch.[2] In each case, the input feed batch data included masses of radionuclides (such as ^{99}Tc and ^{137}Cs), metals and metalloids (as cations, such as $Fe^{+3}$and Si^{+4}), non-metals (such as water and organic compounds), anions (both inorganic and organic, such as F^- and $C_2O_4^{-2}$), and the mineral gibbsite.

[2] The as-received and leached sludge input data were provided to RA Peterson (PNNL) by Kevin Jenkins (WTP) via email on October 30, 2014.

The feed batch did not include any other metal speciation, particle size, or particle density data. It should be noted that the feed batch evaluated was not derived from the final WTP flowsheet, as that information is not currently available. Therefore, flowsheet changes may alter the leached solids composition. However, as will be seen, the as-received feed batch provides the limiting case for the properties of interest, and thus this limitation will be of minimal impact. The following steps were implemented to reduce the element/component list to a realistic number for consideration in the SHSVD simulant.

1. Only the solids phases were selected; data inputs associated with liquid phases were removed from consideration.
2. The solids input data were screened based on component mass; all components that had a maximum batch value of less than 100 kg were deleted. The 100-kg threshold accounted for 99.5 wt% of the as-received solids mass (solids mass input ranged from 19,000 to 90,000 kg) and 99.2 wt% of the leached solids mass (solids mass input ranged from 34,000 to 72,000 kg).
3. Anions such as fluoride, oxide, and nitrate as well as bound water were eliminated from consideration. It was assumed that the appropriate anions and water would be accounted for in the mineral phase associated with the metal/metalloid. Oxalate and phosphate, however, were retained in the anticipated tank farm feed batches. Since they have low sodium salt solubilities, they could still be present in the anticipated feed under certain process conditions.
4. Gibbsite content, delineated in the as-received sludge feed batch, was incorporated at face value.

The average, maximum, and standard deviation of component mass fractions were determined, and the batch components that equaled or exceeded a maximum of 5 wt% were selected for further examination. These components are listed in Table A.1.

Table A.1. Components selected for evaluation in the SHSVD simulant.

As-Received Sludge from Tank Farms				Caustic-Leached Sludge			
Component	Average Wt%	Max. Wt%	Std. Dev.	Component	Average Wt%	Max. Wt%	Std. Dev.
$Al(OH)_3$	47%	68%	10%	Al	27%	58%	11%
Fe	5%	29%	4%	Fe	15%	46%	9%
PO_4^{3-}	7%	28%	7%	Zr	5%	38%	9%
Na	16%	26%	5%	Na	17%	31%	7%
Al	8%	24%	5%	Mn (prec)[(a)]	3%	22%	4%
$C_2O_4^{2-}$	3%	20%	4%	Ca	3%	19%	2%
Zr	1%	12%	3%	^{238}U	8%	18%	3%
Si	3%	11%	2%	Bi	5%	16%	4%
Bi	2%	6%	2%	Si	7%	15%	3%
^{238}U	2%	5%	1%	Ni	1%	10%	1%
Ca	1%	5%	1%	Sr	1%	8%	1%
				^{232}Th	1%	8%	1%
				K	1%	8%	1%
				Mn	2%	7%	1%

(a) Mn (prec) indicates precipitated Mn (as MnO_2) from the oxidative leach process.

The sodium, potassium, and phosphate were assumed to be incorporated into mineral phases such as clarkeite, zeolite, and cancrinite. Further evaluation of the oxalate was omitted from the feed batch analysis. Oxalate will likely be present as sodium oxalate, dissolving and reprecipitating throughout the treatment process. Therefore, since oxalate has a relatively low density and is easy to suspend, and because it will be difficult to assign a particle size for oxalate, it was omitted from the analysis.

A.2 Tank Sludge Mineral Phase Identification

The next step in the process is to identify the phases associated with each of these cations.

Results from actual tank waste characterization were reviewed to determine the most prevalent mineral phases for the primary waste elements identified in Table A.1. These primary waste elements included aluminum, bismuth, calcium, iron, manganese, nickel, potassium, silicon, sodium, strontium, thorium, uranium, and zirconium. Best estimates of component morphology, crystalline density, and size were obtained from the actual waste samples that contained high concentrations of that component. Characterization samples were linked to M12 waste groupings (Fiskum et al. 2008) to better tie into previous extensive characterization work.[3] Where the M12 groupings are not applicable, the indicated waste origins are related to the Best Basis Inventory (BBI) or groupings defined by Hill and Simpson (1994). Results of these examinations are discussed in this appendix.

A.2.1 Aluminum

Table A.2 shows the relative Al content in tank waste groups identified using the M12 categories (Fiskum et al. 2008). Approximately 83 wt% of the Al in the tank waste inventory can be accounted for in the identified groups. REDOX sludge contained the highest Al inventory (primarily boehmite), followed by cladding waste sludge (primarily gibbsite), and then bismuth phosphate saltcake. To the extent possible, Al phase characteristics were selected from the available analyses of both the washed and the caustic-leached sludge for these high-Al-bearing waste sludge sources.

Table A.2. Projected distribution of water-insoluble aluminum in M12-grouped tank waste.

M12 Group ID	Type	Al inventory, wt%
1	Bismuth phosphate sludge	4
2	Bismuth phosphate saltcake (BY, T)	13
3	CWP, PUREX cladding waste sludge	17
4	CWR, REDOX cladding waste sludge	10
5	REDOX sludge	29
6	S - saltcake (S)	8
7	TBP waste sludge	1
8	FeCN waste sludge	1

[3] The M12 designation applies to the characterization, parametric leach testing, and parametric filtration testing conducted for Bechtel National, Inc. (Fiskum et al. 2008, Edwards et al. 2009, Lumetta e al. 2009, Snow et al. 2009, and Fiskum et al. 2009a).

N/A	Other groups and balance	17

Table A.3 provides the identified Al mineral phase, chemical formula, related M12 group, tank sludge source, estimated weight percent of the identified phase in the sludge (M12 samples), and the reference source from which the data were obtained from the various washed sludge samples. Note that the M12 group sludges are generally a combination of several tank waste sludge sources within the categories defined in Table A.2. The weight percent values of the phases in the sludge were derived from the analytical data (chemical and X-ray diffraction [XRD]), as provided in the various M12-related reports; they should be considered approximations. As a point of reference, the phase contents reported separately for the whole tank are given in parenthetical values (Wells et al. 2011). As Table A.3 shows, the crystalline aluminum phases in washed sludge were dominated by boehmite and gibbsite.

Table A.4 provides the identified Al phases from the various wastes types in caustic-leached sludge and Table A.5 provides the identified Al phases from the oxidatively leached sludge. The data sets were primarily from M12-related reports, due in part to the limitation in reported data from other studies (e.g., XRD analysis was either not performed or results had limited value for Al species identification). The weight percent values of the phases in the M12 sludges were derived from the analytical data (chemical diffraction and XRD) and again should be considered approximations. Crystalline aluminum phases in the caustic-leached and oxidatively leached solids were dominated by boehmite and/or cancrinite; as expected, gibbsite was virtually eliminated by the caustic leach processing.

Table A.3. Identified aluminum phases in washed sludge.

Mineral Phase	Formula	M12 Group or Sludge Type	Sludge Source	Wt% Al	Estimated Wt% of Phase	Reference Report
Boehmite	AlOOH	5	M12	32.7	67[(a)]	Fiskum et al. 2008
		5	S-107	20.5	(46)	Lumetta et al. 1996a
		6	S-104	16.7	(60)	Temer and Villarreal 1995
		5	U-110	22-25	Major (51)	Jones et al. 1992
Gibbsite	$Al(OH)_3$	4	M12	34.4	Major/92	Snow et al. 2009
		6	M12	18.7	39	Fiskum et al. 2008
		Other	AP-104	31.3	Major (88)	Baldwin et al. 2003
		3	M12	33	Major/88	Snow et al. 2009
		3	C-105	27.2	Major (72)	Temer and Villarreal 1997
		CWP/TBP	BX-105	30.5	Major (N/A)	Temer and Villarreal 1995
		3	BX-103	21	Major (45)	Temer and Villarreal 1997
		5	S-112	8.4	Major (0.04)	Cantrell et al. 2008
		P3AZ1	AZ-101	22.6	Major (56)	Buck et al. 2003; Urie et al. 2004
		NA	C-108	16.4	Major (32)	Cantrell et al. 2010
		NA/Z	SY-102	17.1	Major (57)	Rapko et al. 2004; Onishi et al. 1996
		5	U-110	22-25	Major (N/A)	Jones et al. 1992
		2	M12	15	Major	Lumetta et al. 2009
Hydroxy-cancrinite	$(Na_2O)_{1.06}(Al_2O_3)(SiO_2)_{1.60}(H_2O)_{1.60}$	6	U-108	12.6	Major (N/A)	Rapko and Vienna 2002
Cancrinite	$Na_{7.92}(AlSiO_4)_6(NO_3)_{1.7}(H_2O)_{2.34}$	6	M12	18.7	Minor/7	Fiskum et al. 2008
		2	M12	15	Major	Lumetta et al. 2009

(a) Additionally, 5.1 wt% gibbsite was reported.

Notes:

Weight percent phases were estimated from the chemistry analysis constraints and XRD analysis of the reported specific sample analyzed and are approximations. The parenthetical values are provided on a whole-tank basis of washed sludge (Wells et al. 2011) and do not necessarily apply to the specific sample analyzed.

N/A = Phase was less than reportable (Wells et al. 2011).

Table A.4. Identified aluminum phases in caustic-leached and washed sludge.

Mineral Phase	Formula	M12 Group	Sludge	Wt% Al	Estimated Wt% of Phase	Reference Report
Boehmite	AlOOH	6	S-104	32.9	N/A	Temer and Villarreal 1995
		5	S-107	27.2	N/A	Lumetta et al. 1996a
		5	M12	11.6	Major	Shimskey et al. 2009
Cancrinite	$Na_{7.6}(Al_6Si_6O_{24})(HCO_3)_{1.2}(CO_3)_{0.2}(H_2O)_{2.28}$	5	M12	11.6	Minor	Shimskey et al. 2009
Hydroxy-cancrinite	$(Na_2O)_{1.06}(Al_2O_3)(SiO_2)_{1.60}(H_2O)_{1.60}$	6	M12	11.4	Indeterminate	Fiskum et al. 2008
		8	M12	5.0	Minor	Fiskum et al. 2009a
Cancrinite	$Na_{7.92}(AlSiO_4)_6(NO_3)_{1.7}(H_2O)_{2.34}$	6	M12	11.4	Indeterminate	Fiskum et al. 2008

Table A.5. Identified aluminum phases in oxidatively leached and washed sludge.

Mineral Phase	Formula	M12 Group	Sludge	Wt% Al	Estimated Wt% of Phase	Reference Report
Cancrinite	$Na_{7.92}(AlSiO_4)_6(NO_3)_{1.74}(H_2O)_{2.34}$	1-2	M12	8.3	Major	Lumetta et al. 2009
Sodium aluminum carbonate silicate	$3NaAlSiO_4$-Na_2CO_3	1-2	M12	8.3	Major	Lumetta et al. 2009

Images of typical boehmite and gibbsite phases are provided in Figure A.1 through Figure A.3; a probable cancrinite phase is shown in Figure A.4.

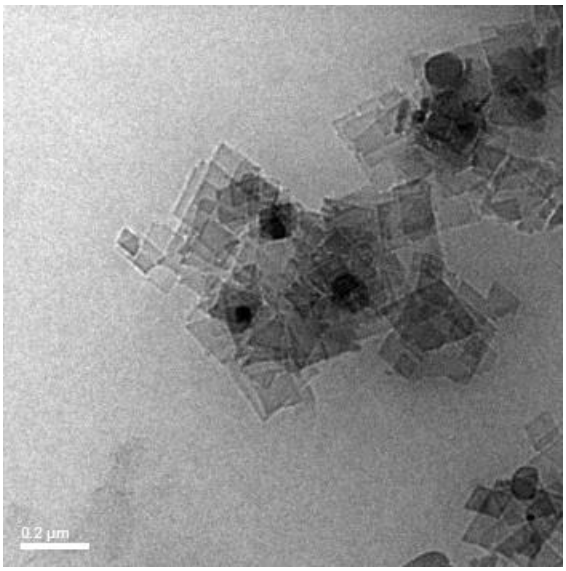

Figure A.1. Transmission electron microscopy (TEM) images of the washed M12 Group 5 sludge; boehmite is represented by the rectangular particles (Fiskum et al. 2008).

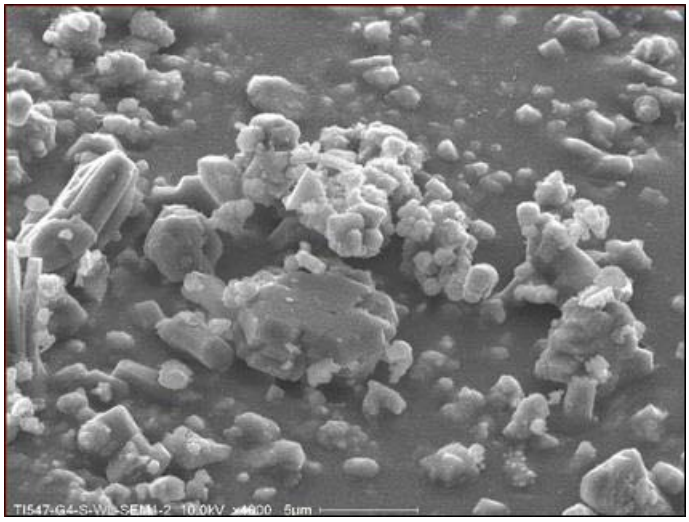

Figure A.2. Scanning electron microscopy (SEM) image of washed Group 4 sludge showing typical morphology and size (Snow et al. 2009).

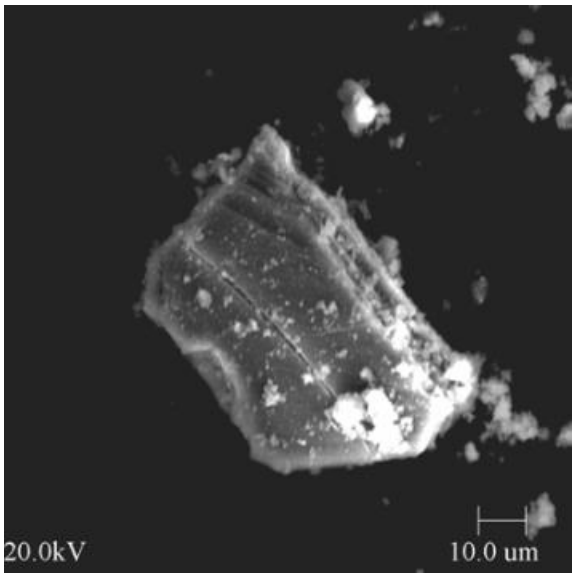

Figure A.3. Aluminum-rich particle in washed SY-102 sludge (Rapko et al. 2004).

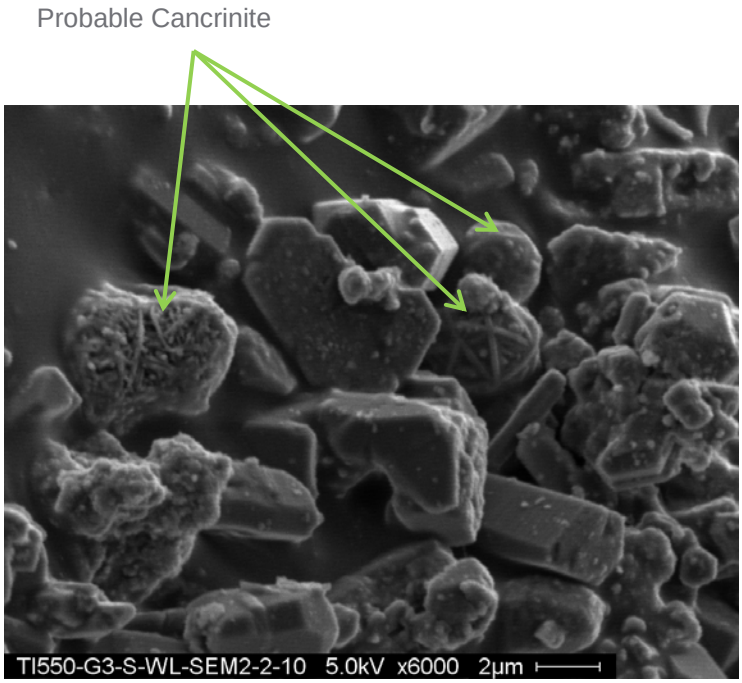

Figure A.4. Group 3 washed solids showing probable cancrinite (Snow et al. 2009).

The Al phase evaluation was simple and straightforward; gibbsite, boehmite, and cancrinite dominated the Al phases. Based on these evaluations, Al phases were assigned to gibbsite, boehmite, and aluminosilicates (cancrinite and zeolite) in the anticipated as-received feed batches. Except for the omission of gibbsite, the same phases were assigned to the anticipated leached feed batches. Densities of these phases are well-defined in the literature; see Table A.6.

Table A.6. Selected aluminum mineral phases and densities.

Mineral Phase	Density, g/mL	Reference
Boehmite	3.01	Kirk *Othmer Encyclopedia of Chemical Technology*, Misra 2000
Gibbsite	2.42	Kirk *Othmer Encyclopedia of Chemical Technology*, Misra 2000
Cancrinite $Na_6Ca_2{\cdot}(CO_3)_2Al_6Si_6O_{24}$	2.4 to 2.5	*CRC Handbook of Chemistry and Physics*, 92nd Edition and Webmineral.com
Zeolite $Na_2Al_2Si_{14}O_{32}{\cdot}3H_2O$	2.0 to 2.7	*Handbook of Hydrothermal Technology* 2nd Edition, K Byrappa, M Yoshimura, Elsevier, 2013. Waltham MA (p. 270).

A.2.2 Bismuth

Bismuth morphology and size were best estimated from the wastes that contain high concentrations of Bi. The Bi distribution in the tank waste, according to the BBI (TWINS 2013), is shown in Table A.7. Bismuth is predominantly associated with the first- and second-cycle bismuth phosphate precipitation process (1C and 2C), i.e., M12 Group 1.

Table A.7. Projected distribution of water-insoluble bismuth in tank waste.

M12 Group ID	Type	Bi, wt%
1	Bismuth Phosphate Sludge (first- and second-cycle decontamination [1C and 2C])	50
N/A	Lanthanum Fluoride Process (224-1 and 224-2)	18
	Balance	32

Tank waste analysis reports were reviewed for samples high in Bi; only Group 1-related samples/analyses were found. The weight percent Bi measured in these samples before and after caustic leaching is shown in Table A.8. Because the Bi was often found with Fe in specific mole ratios, the Fe content is also shown in Table A.8. Samples that contained >10 wt% Bi were targeted for identifying Bi phase characteristics. However, either (1) phase identification was confounded by the amorphous nature of the Bi phase or (2) no phase identification was attempted. The highest Bi concentrations were found in the caustic-leached samples. In the case where Bi concentration was highest (B-202 with 24 wt% Bi in the unleached sludge and 52 wt% Bi in the leached sludge), the Bi phase was amorphous.

Table A.8. Analyzed tank waste samples containing >10 wt% bismuth.

	Washed Solids		Leached Solids			
Sludge Source	Bi, wt%	Fe, wt%	Bi, wt%	Fe, wt%	Phase ID[(c)]	Reference Report
B-201	18	3.0	23	3.8	No	Lumetta and Rapko 1994
B-111	4.1	4.0	18	18	Yes	Rapko et al. 1995, 1996
BX-07	7.6	1.6	35	7.2	Yes	Rapko et al. 1995, 1996
T-104	4.1	2.8	20	12	Yes	Temer and Villarreal 1995
T-104[(a)]	5.5	2.9	11	5.9	Yes	Rapko et al. 1995, 1996
B-202	24	2.1	52	4.1	Amorphous	Temer and Villarreal 1995
Group 1, M12[(b)]	12	11	31	30	Yes/mostly amorphous	Lumetta et al. 2009

(a) The T-104 result was <20 wt% Bi, but the analysis was included because it did have specific Bi phase identification data.
(b) The Group 1 composite created for M12 testing consisted of 93 wt% B-104 solids.
(c) Phase identifications are provided in Table A.9 and Table A.10.

Table A.9 provides the identified crystalline Bi phases from the various washed sludge samples. The terms "major," "minor," and "trace" refer to the spectroscopist's assessment of the amount of crystalline material present; amorphous phases would not be included in this assessment.

Table A.9. Identified bismuth crystalline phases in washed sludge.

Mineral Phase	Formula	M12 Group	Sludge Source	Reference
Iron bismuth silicate hydroxide	Not provided	1	BX-107	Rapko et al. 1996
		1	B-111	Rapko et al. 1996
		1	T-104	Rapko et al. 1996
Bismuth oxide	Bi_2O_3	1	BX-107	Rapko et al. 1996
		1	B-111	Rapko et al. 1996
		1	T-104	Rapko et al. 1996
Bismuth iron phosphate	Not provided	1	BX-107	Rapko et al. 1996
Bismuth phosphate[(a)]	$BiPO_4$	1	Group 1	Lumetta et al. 2009
Bismuth chromium oxide	$Bi_{38}CrO_{60}$	1	B-111	Rapko et al. 1996
Aluminum bismuth oxide	$Bi_{24}Al_2O_{39}$	1	T-104	Temer and Villarreal 1995

(a) Bismuth was present at 12 wt%, but apparently existed mostly in an amorphous form.

It is noteworthy that bismuth phosphate was not clearly identified as a major component in any of the analytical samples in the suite. Wells et al. (2011) defined two Bi phases in the tank wastes: Bi_2O_3 and $BiFeO_3$. The pure form Bi_2O_3 was identified as a minor component in three samples; impure forms of this compound (containing Al or Cr) were also reported. None of the characterization reports specifically identified the $BiFeO_3$ phase.

Table A.10 shows the phase identifications for Bi compounds in the leached tank waste sludge. The only difference between the Table A.9 and Table A.10 results is the elimination of the bismuth phosphate. It is possible that the caustic-leached Bi phase differed from the washed Bi phase through a metathesis reaction with hydroxide, as was previously attributed to iron phosphate (Lumetta et al. 2009).

Table A.10. Identified bismuth crystalline phases in leached sludge.

Mineral Phase	Formula	M12 Group	Sludge Source	Reference Report
Iron bismuth silicate hydroxide	Not provided	1	BX-107	Rapko et al. 1996
		1	B-111	Rapko et al. 1996
		1	T-104	Rapko et al. 1996
Bismuth oxide	Bi_2O_3	1	BX-107	Rapko et al. 1996
		1	B-111	Rapko et al. 1996
		1	T-104	Rapko et al. 1996
Bismuth iron phosphate	Not provided	1	BX-107	Rapko et al. 1996
Amorphous	NA	1	Group 1	Lumetta et al. 2009
Bismuth chromium oxide	$Bi_{38}CrO_{60}$	1	B-111	Rapko et al. 1996
		1	T-104	Temer and Villarreal 1995
Bismuth iron oxide	$Bi_{36}Fe_2O_{57}$	1	T-104	Temer and Villarreal 1995
Aluminum bismuth oxide	$Bi_{24}Al_2O_{39}$	1	T-104	Temer and Villarreal 1995

The iron bismuth silicate hydroxide phase (structure not determined or not reported) was not further investigated. The three leached samples in which this phase was identified had an upper particle size of ~30 microns. In contrast, the amorphous leached Fe-Bi phase represented by Group 1 had an upper particle size of ~300 microns and was considered more challenging for mixing operations.

Although crystalline phases were identified in some samples, examination of available XRD spectra indicated a large amorphous component was present. Thus, for the bulk of the bismuth in the tank waste sludge, the phase was assigned as amorphous and chemistry interpretations were used to elucidate the nature of this component, as previously reported.[1]

The Fe-to-Bi mole ratio was found in generally three populations for leached solids: 0.6, 2.2, and 3.7. The Bi phase containing 3.7:1 mole ratio of Fe:Bi was selected as the primary Bi form for the feed batch analysis as $Fe_{3.7}Bi(OH)_{14.1}$, consistent with the approach previously taken; a density of ~3.3 g/mL was measured on co-precipitated material targeting this formulation.[1] Note that both the Bi:Fe ratio and the assigned density contain significant uncertainty. However, it is anticipated that the use of this mineral phase represents a significant improvement over prior efforts that assigned all Bi to a Bi-O phase with significantly higher density. The actual waste characterization for the bulk of the Bi-bearing wastes does not support a Bi-O phase assignment, but rather supports an amorphous mix of Bi and Fe. Note also that the density of 3.3 g/mL has a fairly large uncertainty, as the method of preparation of the material was

[1] King, W, R Eibling, M Hay, R Peterson, B Wells, S Fiskum, R Russell, C Burns, G Brown, C Carlson, D Rector W Kuhn, and J Fort. 2014. *FSVT Vessel Group 5 Simulant Supporting RLD-08T (90% Review Draft)*. GD-FSVT-017; SRNL-TR-2014-00032 DRAFT. Feb. 2014. Savannah River National Laboratory, Pacific Northwest National Laboratory.

still under development. The phosphate form using this Fe-Bi mole ratio was allowed in the unleached solids; the hydroxide form was applied exclusively to the leached solids.

A.2.3 Calcium

Finding a Ca-predominant phase in tank waste was difficult; eight samples from tank waste could be found where the Ca concentration exceeded 4 wt%. Table A.11 summarizes the identified samples with respect to tank origin, sludge type, related M12 grouping, weight percent Ca, leach condition, phase identification, and reference report. Table A.12 and Table A.13 provide the identified Ca phases from the various wastes types in washed and leached sludge, respectively.

Table A.11. Identified samples with >4 wt% calcium.

Sludge Source	Sludge Type	M12 Group	Ca, wt%	Leached?	Ca Phase ID?	Reference Report
BY-110	BY Saltcake, FeCN	--	9.0	Yes	Yes[(a)]	Lumetta et al. 1996a
AN-104	Other	--	4.6	Yes	No	Lumetta et al. 1997
BY-108	BY Saltcake, FeCN	--	5.1	Yes	Yes[(a)]	Lumetta et al. 1997
C-112	1C, 2C, FeCN	1, 8	4.7	No	No	Scheele et al. 1994
C-108	TBP, 1C, CW, OWW	--	12.2	Yes	Yes	Temer and Villarreal 1995
M12	CWR	4	[5][(b,c)]	Yes	No	Snow et al. 2009
M12	FeCN	8	6.4[(b)]	No	Yes	Fiskum et al. 2009a
M12	FeCN	8	7.9[(b)]	Yes	Yes	Fiskum et al. 2009a

CW = cladding waste
1C = first-cycle decontamination waste
TBP = tributyl phosphate
OWW = organic wash waste
FeCN = ferrocyanide scavenged waste
PCW = PUREX cladding waste

(a) TEM analysis
(b) Calcium was measured as an opportunistic analyte; results were not fully evaluated for quality control.
(c) Bracketed result indicates that the concentration was less than the estimated quantitation limit.

Table A.12. Identified calcium phases in washed sludge.

Mineral Phase	Formula	M12 Group	Sludge Source	Estimated wt%	Comments
Calcium phosphate	CaP_4O_{11}	8	M12	6.4	Possible fit
Bassanite	$Ca(SO_4)(H_2O)_{0.5}$				Possible contaminant

Table A.13. Identified calcium phases in caustic leached sludge.

Mineral Phase	Formula	M12 Group	Sludge Source	Estimated wt%	Comments
Hydroxyapatite	$Ca_5(PO_4)_3(OH)$	--	BY-110	9.0	TEM analysis
Not reported	$Ca_xSr_{10-x}(PO_4)_6(OH)_2$ where x = 8 or 9	--	BY-108	5.1	TEM analysis
Calcium sulfide phosphate Hydroxylapatite	$Ca_{10}(PO_4)_6S$ $Ca_5(PO_4)_3(OH)$	--	C-108	12.2	XRD analysis
Calcium phosphate Bassanite	CaP_4O_{11} $Ca(SO_4)(H_2O)_{0.5}$	8	M12	7.9	Possible fit Possible contaminant

Calcium was assigned to the cancrinite phase $Na_6Ca_2(CO_3)_2Al_6Si_6O_{24}$ (see Section A.2.3, Table A.22), density 2.42 g/mL, and $Ca(OH)_2$, density of 2.24 g/mL, in the feed batch for as-received and leached sludge. As noted above, more-complex calcium phases were present, mostly apatite phases. However, since calcium is a minor phase, the system was simplified to use only cancrinite and calcium hydroxide. This simplification will have minimal impact on the resultant calculations since the calcium hydroxide phase represents less than 1% of the total material present and since the other potential calcium phases would have densities similar to calcium hydroxide.

A.2.4 Iron

Table A.14 shows the groupings accounting for 59 wt% of the Fe in tank waste sludge. The highest Fe-containing group identified using this categorization was in bismuth phosphate sludge (Group 1). Note that 41 wt% Fe is not accounted for in these groupings. Note also that iron is distributed across all of the waste types. The largest identified groupings that are not captured are SRR, PFeCN, P2, and AR.

Table A.14. Projected distribution of water-insoluble iron in M12-grouped tank waste.

M12 Group ID	Type	Fe, wt%
1	Bismuth phosphate sludge	22
2	Bi phosphate saltcake (BY, T)	8
3	PUREX cladding waste sludge	5
4	REDOX cladding waste sludge	1
5	REDOX sludge	4
6	S - saltcake (S)	4
7	TBP waste sludge	7
8	FeCN waste sludge	7
	Balance	41

The predominant Fe morphology and size were best estimated from the wastes that contained high concentrations of Fe (e.g., Group 1) as well as Fe-rich subsamples, typically from caustic leached and washed sludge. Table A.15 summarizes reported Fe concentrations specific to tank analytical samples that resulted in >15 wt% Fe; the M12 identified sludge is generally a combination of several tank sludge samples fitting the categories defined in Table A.14. The Bi content is also reported for information only (Bi and Fe have often been identified together in a 1:1 wt% ratio, and therefore were evaluated as a common mixed Bi-Fe phase, see Section A.2.2). Useful Fe-phase identifications with XRD were made on a small fraction of this sample set; limited TEM phase analysis was conducted on three samples.

Table A.16 provides the identified Fe phases from the various waste types in washed sludge. Table A.17 provides the identified Fe phases from the various waste types in caustic-leached sludge. The nominal content of the identified phases (e.g., major, minor, or trace) was not provided in the cited reports. Selected samples containing <15 wt% Fe are shown (Table A.16) because the leached solids associated with the report were >15 wt% Fe; the phase comparison between unleached and leached solids was considered instructive. Wells et al. (2011) identified three Fe-containing phases as present in the tank waste: $BiFeO_3$, $FePO_4 \cdot 2H_2O$, and FeOOH. Similar phases are shown in Table A.16 and Table A.17 with the addition of many more. The Fe phase, $Fe_{3.7}Bi(OH)_{14.1}$, was selected as the primary Fe form for use in the feed batch analysis (as-received and leached sludge), followed by the most dense alternative form of Fe that was positively identified in the tank waste: hematite, Fe_2O_3. The $Fe_{3.7}Bi(OH)_{14.1}$ density was measured at 3.3 g/mL[1] and hematite density is 5.25 g/mL (Cramer and Covino 2003).

[1] King, W, R Eibling, M Hay, R Peterson, B Wells, S Fiskum, R Russell, C Burns, G Brown, C Carlson, D Rector W Kuhn, and J Fort. 2014. *FSVT Vessel Group 5 Simulant Supporting RLD-08T (90% Review Draft)*. GD-FSVT-017; SRNL-TR-2014-00032 DRAFT. Feb. 2014. Savannah River National Laboratory, Pacific Northwest National Laboratory.

Table A.15. Identified samples with >15 wt% iron.

Sludge Source	Sludge Type	M12 Group	Fe, wt%	Bi, wt%	Leached?	Fe Phase ID?	Reference Report
M12	Bi phosphate sludge	1	30.4	31.5	Yes	No	Lumetta et al. 2009
M12	TBP waste sludge	7	16.5	0.71	No	Yes	Edwards et al. 2009
M12	TBP waste sludge	7	33.1	1.4	Yes	No	Edwards et al. 2009
AZ-101/AZ-102	P3AZ1 /P3AZ2	--	29.1	<0.2	Yes	No	Rapko and Wagner 1997
AZ-102	P3AZ2	--	22.1	<0.06	Yes	No	Brooks et al. 2000a
AZ-101	P3AZ1	--	24.2	<	No	No	Bell 2001
M12	CWR	4	23.2	3.3	Yes	No[(a)]	Snow et al. 2009
BX-109	TBP	7	24.5	0.56	Yes	No	Temer and Villarreal 1996
B-111	2C, B	1	18.0	18.0	Yes	Yes	Rapko et al. 1995, 1996
C-103	NA	--	20.0	<0.07	No	No	Rapko et al. 1995
C-103	NA	--	21.0	0	Yes	No	Rapko et al. 1995
C-107	1C	1	17.9	0.03	No	Yes[(b)]	Lumetta et al. 1996a
C-107	1C	1	31.8	0.04	Yes	Yes[(b)]	Lumetta et al. 1996a
AZ-101	P3AZ1	--	20.2	N/A	Yes	No	Geeting et al. 2003
C-106	NA	--	18.7	0.03	Yes	Yes[(b)]	Lumetta et al. 1996a
T-107	1C, TBP, CWP	1, others	19.6	10.1	Yes	No	Temer and Villarreal 1995
BX-105	CWP, TBP	3, 7	20.6	0.21	Yes	No	Temer and Villarreal 1995
AY-102/C-106	NA	--	16.0	0.004	No	No	Coleman et al. 2004
M12	CWP	3	16.6	1.04	Yes	Yes	Snow et al. 2009

TBP = tributyl phosphate
CWP = PUREX cladding waste
CWR = REDOX cladding waste
N/A = unknown
1C = first-cycle decontamination waste
2C = second-cycle decontamination waste
P3AZ1 and P3AZ2 = PUREX high-level waste
B = high-level acid waste from PUREX processed at B Plant for Sr recovery

(a) Insufficient caustic-leached sample material available for analysis.
(b) TEM analysis only; phases consisting of Fe-O were identified.

Table A.16. Identified iron phases in washed sludge.

Mineral Phase	Formula	M12 Group	Sludge Source	Wt% Total Fe	Reference Report
Sodium iron phosphate	$Na_7(FeP_2O_7)_4(PO_4)$	7	M12	16.5	Edwards et al. 2009
Iron (III) phosphate oxide	Fe_2PO_5				
Humboldtine	$FeC_2O_4 \cdot 2H_2O$				
Lepidocrocite	FeOOH				
Hematite	Fe_2O_3	1	C-107	17.9	Lumetta et al. 1996a, b
Unknown	Fe-O (TEM)	--	C-106	7.6	Lumetta et al. 1996b
Vauxite	$FeAl_2(PO_4)_2(OH)_2 \cdot 6H_2O$	1	M12	11	Lumetta et al. 2009
Unknown	Fe-Bi-O/OH/ amorphous				
Iron bismuth silicate hydroxide	Not provided[(a)]	1	B-111	4	Rapko et al. 1996
Amorphous	Fe-O[(a)]				
Hematite	$Fe_{1.67}H_{0.99}O_3$	3	M12	1.8	Snow et al. 2009

Nominal content of phase (e.g., major, minor, or trace) generally was not provided.
Selected samples containing <15 wt% Fe are shown because the leached solids associated with the report were >15 wt% Fe; the phase comparison could be instructive.
(a) Reported as major phase.

Table A.17. Identified iron phases in leached sludge.

Mineral Phase	Formula	M12 Group	Sludge Source	Wt% Total Fe	Reference Report
Unknown Hematite	Amorphous Fe_2O_3 by TEM	7	M12	33	Edwards et al. 2009
Goethite or lepidocrocite	Fe(III)-O-OH (TEM)	1	C-107	32	Lumetta et al. 1996a, b
Goethite or lepidocrocite	FeOOH (TEM)	--	C-106	19	Lumetta et al. 1996b
Unknown	Amorphous Fe-Bi by SEM and TEM	1	M12	30	Lumetta et al. 2009
Iron bismuth silicate hydroxide Amorphous	Not provided[(a)] Fe-O[(a)]	1	B-111	18	Rapko et al. 1996
Hematite	Fe_2O_3	3	M12	17	Snow et al. 2009

Nominal content of phase (e.g., major, minor, or trace) generally was not provided.
Selected samples containing <15 wt% Fe are shown because the leached solids associated with the report were >15 wt% Fe; the phase comparison could be instructive.
(a) Reported as a major phase.

A.2.5 Manganese

Finding a predominant phase for Mn in tank waste was difficult; only three samples from tank waste could be found where the Mn concentration exceeded 7 wt%. In the case of precipitated Mn, only four samples could be found that exceeded 3 wt%. Table A.18 summarizes the identified samples with respect to tank origin, sludge type, related M12 grouping, weight percent Mn, and whether results were from post-caustic-leached solids or whether the Mn was from precipitation associated with the permanganate strike to solubilize Cr. Only one report for each condition identified one or more Mn phases, shown in Table A.19.

Table A.18. Screened high-manganese-bearing samples.

Sludge Source	Sludge Type	M12 Group	Mn, wt%	Leached?	Precipitated Mn?	Mn Phase ID?	Reference Report
T-111	224, 2C	224, 1	9.6	Yes	No	Yes	Rapko et al. 1995
M12	CWR	4	9.7	Yes	No	No	Snow et al. 2009
B-202	224	1	10.1	Yes	No	Amorphous	Temer and Villarreal 1995
M12	S saltcake	6	21.4	NA	Yes	Yes	Fiskum et al. 2008
AN-102/ C-104	NA	NA	6.7	NA	Yes		Hallen et al. 2003
M12	REDOX sludge and S saltcake	6/5	3.4	NA	Yes	No	Shimskey et al. 2009
M12	REDOX sludge and S saltcake	5/6	5.2	NA	Yes	No	Fiskum et al. 2009b

224 = lanthanum fluoride process "224 Building" waste
2C = second-cycle decontamination waste
CWR = REDOX cladding waste

Table A.19. Identified manganese phases in leached sludge.

Mineral Phase	Formula	M12 Group	Sludge Source	Wt% Total Mn	Comments
Not reported	Mn_2MnO_4[(a)]	224, 1	T-111	9.6	Caustic Leached
Not reported	Fe_2MnO_4[(a)]				
Not reported	MnO_2 (TEM)	6	M12	21.4	Precipitated Mn

(a) Component reported as a minor phase.

The precipitated form of Mn, MnO_2, was selected as the Mn form for evaluating the feed batch. Pyrolusite, a MnO_2 mineral, has a reported density of 4.4 to 5.06 g/mL (Webmineral.com) and 5.026 g/mL (*CRC Handbook of Chemistry and Physics*, 60th Edition). The average of this range, 4.73 g/mL, was selected for the MnO_2 density basis.

It is noted that the commercially available MnO_2 product, Carulite 400 E, was measured with a particle density of 3.5 g/mL.[1] Carulite 400 E may be less crystalline, or have some other production-induced differences from the pure materials relative to density. It is known to have very high surface area (329 m^2/g), which indicates high material porosity, and to contain some impurity (stoichiometrically low in Mn).

A.2.6 Nickel

Finding a Ni-predominant phase in tank waste was difficult; only six samples from tank waste could be found where the Ni concentration exceeded 4 wt%. Table A.20 summarizes the identified samples with respect to tank origin, sludge type, related M12 grouping, weight percent Ni, leach condition, phase identification, and reference report. A Ni phase, $Ni_3O_2(OH)_4$, was identified on only one sample (BY-110, which had undergone caustic leaching) using TEM; XRD analysis was not applied to this sample.

Table A.20. Identified samples with >4 wt% nickel.

Sludge Source	Sludge Type	M12 Group	Ni, wt%	Leached?	Ni Phase ID?	Reference Report
BY-110	BY saltcake, FeCN	--	4.4	Yes	Yes (TEM)	Lumetta et al. 1996a
C-105	TBP/SR-Wash/ CW/P	7	5.0	Yes	No	Temer and Villarreal 1997
C-109	1C, FeCN, CWP	1, 8	4.2	No	No	Scheele et al. 1994
C-112	1C, 2C, FeCN	1, 8	4.8	No	No	Scheele et al. 1994
C-108	TBP, 1C, CW, OWW	--	12.5	Yes	No	Temer and Villarreal 1995
M12	FeCN	8	4.6	Yes	No	Fiskum et al. 2009a

CW = cladding waste
CWP = PUREX cladding waste
1C and 2C = first and second cycle decontamination waste
TBP = tributyl phosphate
OWW = organic wash waste
FeCN = ferrocyanide scavenged waste
P = neutralized acid waste
PCW = PUREX cladding waste
Sr-Wash = particulates from wash of PUREX wastes containing high Sr

Nickel was not included in the as-received feed batch analysis. The Ni phase in the caustic-leached solids was assigned as $Ni(OH)_2$ with a density of 4.15 g/mL (Gangolli 2005).

[1] King W, R Eibling, M Hay, R Peterson, B Wells, S Fiskum, R Russell, C Burns, G Brown, C Carlson, D Rector W Kuhn, and J Fort. 2014. *FSVT Vessel Group 5 Simulant Supporting RLD-08T (90% Review Draft).* GD-FSVT-017; SRNL-TR-2014-00032 DRAFT. Feb. 2014. Savannah River National Laboratory, Pacific Northwest National Laboratory.

A.2.7 Silicon

Silicon was identified in actual tank waste at >5 wt% in nine samples. Table A.21 summarizes the identified samples with respect to tank origin, sludge type, related M12 grouping, weight percent Si, leach condition, phase identification, and reference report.

Table A.21. Identified samples with >5 wt% silicon.

Sludge Source	Sludge Type	M12 Group	Si, wt%	Leached?	Si Phase ID?	Reference Report
B-111	2C, B	1	6.5	Yes	Yes	Rapko et al. 1996
AW-101	--	--	6.3	No	No	Brooks et al. 1999
C-106	NA sludge	--	8.7	Yes	Yes (TEM)	Lumetta et al. 1996a
M12	Bismuth Phosphate Sludge	1	6.0	No	Yes	Lumetta et al. 2009
M12	Bismuth Phosphate Saltcake	2	9.2	Yes	Yes	Lumetta et al. 2009
M12	Bismuth Phosphate Sludge and Saltcake	1, 2	10.2	Yes	No	Lumetta et al. 2009
M12	Bismuth Phosphate Sludge and Saltcake	1, 2	8.5	Yes	Yes	Lumetta et al. 2009
M12	CWR	4	5.6	Yes	No	Snow et al. 2009
M12	TBP	7	5.3	Yes	Yes	Edwards et al. 2009

CWR = REDOX cladding waste
TBP = tributyl phosphate
2C = second-cycle decontamination process
B = high-level acid waste from PUREX processed at B Plant for Sr recovery

The Si phase analyses are provided in Table A.22. Aluminosilicates were identified in all evaluated waste types. The aluminosilicates can take on forms such as cancrinite (many different types) and zeolite. It is noted that zeolite, $NaAlSiO_4(H_2O)_{1.1}$, was identified in Group 7 unleached solids as a major phase where Si only comprised 0.7 wt% (Lumetta et al. 2009).

Table A.22. Identified silicon phases washed and leached in sludge.

Mineral Phase	Formula	M12 Group	Sludge Source	Wt% Total Si	Comments
		Washed Sludge			
Silicon oxide	SiO2	1	M12	6.0	Possible phase identification
		Leached Sludge			
Iron bismuth silicate hydroxide	Not provided	1	B-111	6.5	Major phase
Crystalline aluminosilicates	Not provided				Minor phase
Amorphous aluminosilicates	Not provided	--	C-106	8.7	TEM analysis
Cancrinite	$Na_{7.14}Al_6Si_{7.08}O_{26.73}(H_2O)_{4.87}$	2	M12	9.2	Caustic leached solids, excellent match/major
Sodium aluminum silicate nitrate hydrate	$Na_{7.92}(AlSiO_4)_6(NO_3)_{1.74}(H_2O)_{2.34}$	1, 2	M12	8.5	Caustic and oxidatively leached solids, predominant phase
Sodium aluminum carbonate silicate	$3NaAlSiO_4 \cdot Na_2CO_3$				
Cancrinite	$Na_6Ca_2Al_6Si_6O_{24}(CO_3)_2 \cdot 2H_2O$	7	M12	5.3	Caustic leached solids, minor phase

The silicon was assigned to the generic forms of cancrinite, $Na_6Ca_2(CO_3)2Al_6Si_6O_{24}$, and zeolite, $Na_2Al_2Si_{14}O_{32} \cdot 3H_2O$, in the feed batch analyses (as-received and leached solids). Quartz, SiO_2, was included in the as-received feed batch analysis. In the cases of zeolite and cancrinite, the particle densities were assigned 2.42 g/mL (webmineral.com and *CRC Handbook of Chemistry and Physics*, 92nd Edition). The quartz density was assigned 2.65 g/mL (*CRC Handbook of Chemistry and Physics*, 92nd Edition).

A.2.8 Strontium

Finding a Sr-predominant phase in tank waste was difficult; only four samples from tank waste could be found where the Sr concentration exceeded 3 wt%. Table A.23 summarizes the identified samples with respect to tank origin, sludge type, related M12 grouping, weight percent Sr, leach condition, phase identification, and reference report. The Sr appeared to be associated with the hydroxyapatite, $Ca_5(PO_4)_3(OH)$ in a sample from BY-110 and $Ca_xSr_{10-x}(PO_4)_6(OH)_2$ where x = 8 or 9 in a sample from BY-108 that had undergone caustic leaching (using TEM). The Sr phase identified in M12 Group 8, both before and after caustic leaching, was strontium hydrogen phosphite, $Sr(H_2PO_3)_2$, with a crystal density of 2.7 g/mL (Boldt et al. 2000).

Table A.23. Identified samples with >3 wt% strontium.

Sludge Source	Sludge Type	M12 Group	Sr, wt%	Leached?	Sr Phase ID?	Reference Report
BY-110	BY saltcake, FeCN	--	3.6	Yes	No	Lumetta et al. 1996a
BY-108	BY saltcake, FeCN		3.6	Yes	No	Lumetta et al. 1997
M12	FeCN	8	4.2	No	Yes	Fiskum et al. 2009a
M12	FeCN	8	5.4	Yes	Yes	Fiskum et al. 2009a

FeCN = ferrocyanide scavenged waste

Strontium was not included in the as-received feed batch analysis, but was included in the leached solids feed batch analysis. Vendors could not be found that provide $Sr(H_2PO_3)_2$.

The Sr phase was assigned to $SrCO_3$, which is the expected precipitation product following the Sr/TRU separation process (Wilmarth et al. 2011). The $SrCO_3$ density at 3.7 g/mL (*CRC Handbook of Chemistry and Physics*, 60th Edition) provides a more conservative basis relative to the $Sr(H_2PO_3)_2$ density.

A.2.9 Thorium

Only four tank waste samples were identified where the Th concentration exceeded 3 wt%—these specifically came from C-104. Table A.24 summarizes the identified samples with respect to tank origin, sludge type, related M12 grouping, weight percent Th, leach condition, and reference report. No Th phases were identified in any of the tank wastes.

Table A.24. Samples identified with >3 wt% thorium.

Sludge Source	Sludge Type	M12 Group	Th, wt%	Leached?	Reference Report
C-104	N/A	--	5.5	No	Brooks et al. 2000b
C-104	N/A	--	11	Yes	Brooks et al. 2000b
C-104	N/A	--	3.8	No	Lumetta et al. 2000
C-104	N/A	--	12	Yes	Lumetta et al. 2000

Thorium was assigned the phase ThO_2 for evaluating the feed batch of the leached solids and assigned the density of 9.86 g/mL (*CRC Handbook of Chemistry and Physics*, 60th Edition).

A.2.10 Uranium

The uranium morphology was best estimated from the wastes that contain high concentrations of U. Selected washed and caustic-leached wastes resulted in high U concentrations (>10 wt%), as shown in Table A.25. The U morphological characteristics were selected from the available dataset of caustic-leached sludge where the U concentration exceeded 20 wt%. This approach assumes that U chemical and morphological changes were minimal after caustic leach and wash and that one U phase surrogate will apply equally to both as-received and leached sludge.

Table A.25. Samples identified with >10 wt% uranium.

Sludge Source	Sludge Type	M12 Group	U, wt%	Leached?	U Phase ID?	Reference Report
M12	REDOX sludge	5	28.7	Yes	Yes	Fiskum et al. 2008
S-104	REDOX sludge	5	25.4	Yes	No[(a)]	Lumetta et al. 1997
BX-109	TBP/CW/1C	7	22.4	Yes	Yes	Temer and Villarreal 1996
C-105	TBP/SR-wash/ CW/P	7	31.5	Yes	Yes	Temer and Villarreal 1997
M12	TBP waste sludge	7	12.6	No	Yes	Edwards et al. 2009
M12	TBP waste sludge	7	21.8	Yes	Yes	Edwards et al. 2009
M12	CWP	3	21.3	Yes	Yes	Snow et al. 2009
BY-108	BY saltcake (solid)	--	19.6	Yes	No[(a)]	Lumetta et al. 1997
C-112	FeCN	8	19.0	No	No	Scheele et al. 1994
S-101	NA sludge with S1 and S2 saltcake	5	16.8[(a)]	Yes	No	Lumetta et al. 1997
M12	CWR	4	15.1	Yes	No	Snow et al. 2009
M12	FeCN	8	12.1	No	Yes	Fiskum et al. 2009a
M12	FeCN	8	15	Yes	Yes	Fiskum et al. 2009a

1C = first-cycle decontamination waste
2C = second-cycle decontamination waste
B = high-level acid waste from PUREX processed at B Plant for Sr recovery
CW = cladding waste
CWP = PUREX cladding waste
CWR = REDOX cladding waste
NA = unknown
FeCN = ferrocyanide scavenged waste
P3AZ1 and P3AZ2 = PUREX high-level waste
S1 and S2 saltcake = high salt concentrated waste from first and second 242-S evaporator campaigns
Sr-Wash = particulates from Sr wash of wastes TBP = tributyl phosphate
(a) TEM analysis conducted with limited phase identification.

Table A.26 summarizes the identified U phases in washed sludge; Table A.27 identifies the phases identified in leached sludge. Phase identification and assessment of major or minor phase contribution was largely determined by XRD. Sodium uranium oxide and clarkeite appeared as the best fits using XRD and most abundant U phases.

Table A.26. Identified uranium phases in washed sludge.

Mineral Phase	Formula	M12 Group	Sludge Source	Wt% Total U	Comments
Sodium uranium oxide	$Na_2U_2O_7$	8	M12	12.1	Excellent XRD fit
Sodium uranyl carbonate	$Na_4(UO_2)(CO_3)_3$				Good XRD fit as minor phase
Threadgoldite	$Al(UO_2)_2(PO_4)_2(OH)(H_2O)_8$	7	M12	12.6	Phases were not good matches to the XRD patterns
Dioxouranium(VI) bis(diydrogenphosphate(I)) hydrate	$(UO_2)(H_2PO_2)_2(H_2O)$				
Sodium uranyl phosphate	$Na_6(UO_2)_2(PO_4)_4$				

Table A.27. Identified uranium phases in caustic-leached sludge.

Mineral Phase	Formula	M12 Group	Sludge Source	Wt% Total U	Comments
Clarkeite	$Na(UO_2)O(OH)$	5	M12	28.7	Major phase
Sodium uranium oxide	$Na_2U_2O_7$				Possible phase
Not provided	$UO_3 \cdot 2H_2O$[(a)]	5	S-104	25.4	TEM ID
Not provided	β-U_3O_8[(a)]	--	BY-108	19.6	TEM ID
Sodium uranium oxide	$Na_2U_2O_7$	7	BX-109	22.4	Major—only phase identified
Sodium uranium oxide	$Na_2U_2O_7$		C-105	31.5	Major—only phase identified
Sodium uranium oxide hydrate	$Na_2U_2O_7 \cdot 6H_2O$	7	M12	21.8	Good fit-major phase
Becquerelite	$Ca(UO_2)_6O_4(OH)_6(H_2O)_8$				Good fit-major phase
Clarkeite	$Na(UO_2)O(OH)$				Good fit-major phase
Not provided	Na-U-PO_4[(a,b)]				TEM ID
Sodium uranium oxide hydrate	$Na_2U_2O_7 \cdot 6H_2O$	3	M12	21.3	Major phase
Sodium uranium oxide	$Na_2U_2O_7$				Major phase
Clarkeite	$Na(UO_2)O(OH)$				Major phase
Uranium oxide	α-U_3O_8[(a)]				TEM ID
Sodium uranium oxide	$Na_2U_2O_7$	8	M12	15	Excellent fit
Sodium uranyl carbonate	$Na_4(UO_2)(CO_3)_3$				Good fit as minor phase

(a) Determined from individual particle TEM analysis with electron diffraction.
(b) No structure identified; phase and density cannot be assessed.

The clarkeite ($Na(UO_2)O(OH)$) XRD pattern is very similar to the sodium uranium oxide ($Na_2U_2O_7$) XRD pattern; therefore, these phases cannot generally be definitively distinguished by XRD analysis.

TEM micrographs of the U-bearing phases were obtained in several cases. Caustic-leached Group 5 samples showed thin, elongated structures (lengths approaching 0.2 μm and widths closer to 0.02 μm) and circular structures, both of which were U-rich structures (see Figure A.5).

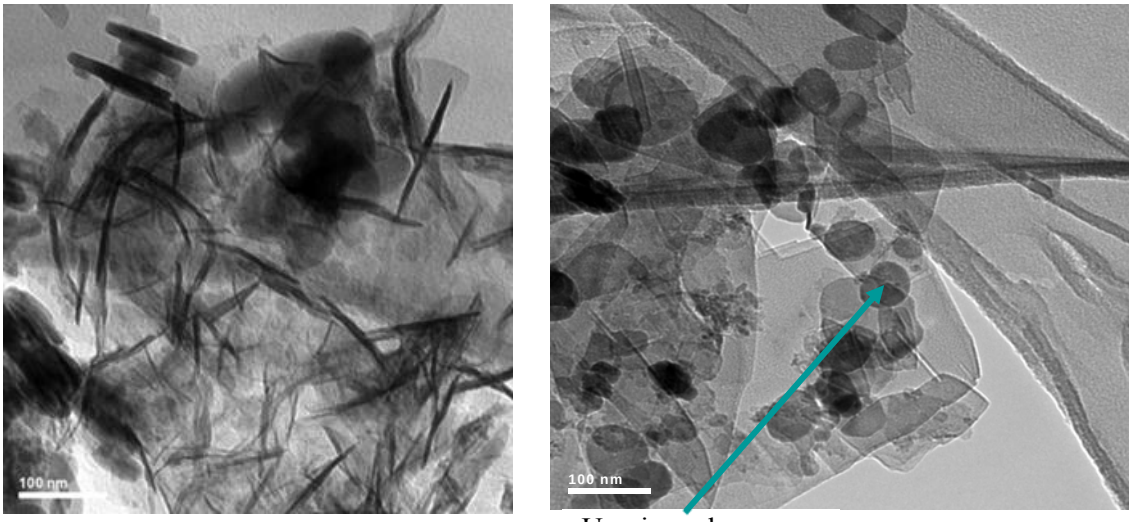

Figure A.5. Group 5 leached sludge U acicular and circular phases (Fiskum et al. 2008).

Characterization of leached S-104 sludge particle phase was limited to TEM and selected area diffraction. Acicular U particles attributed to $UO_3 \cdot 2H_2O$ were identified in the leached solids. This result was contrasted with the circular U phase attributed to U_3O_8 phase found before caustic leaching. TEM images of these phases are available in Lumetta et al. 1997 and are reproduced here in Figure A.6.

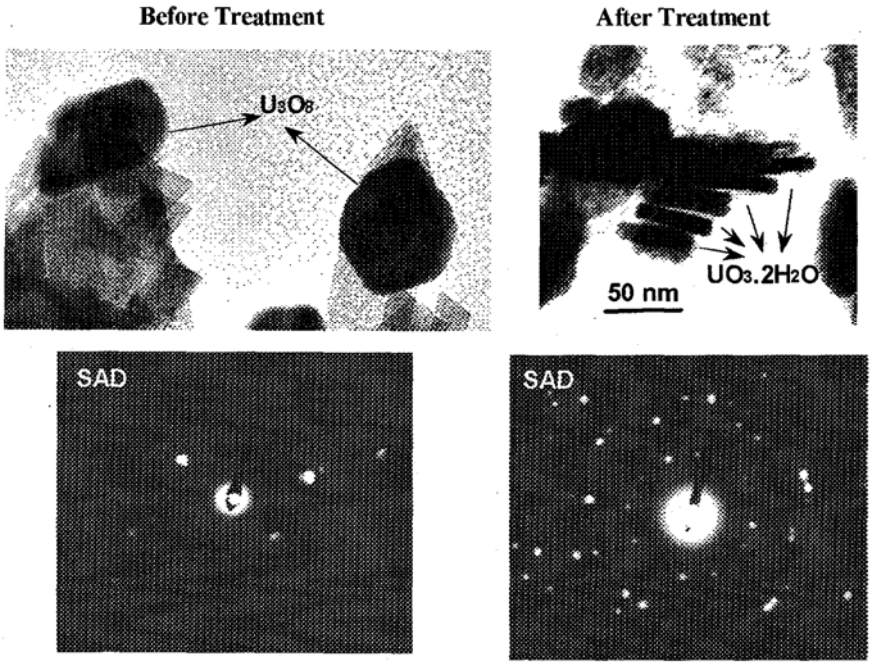

Figure A.6. Uranium oxide species before and after leaching S-104 sludge (Lumetta et al. 1997).

The Group 3 caustic-leached cladding waste samples showed thin, elongated structures (lengths approaching 0.2 μm and widths closer to 0.02 μm) and thin, wispy structures; both were U-rich structures (see Figure A.7).

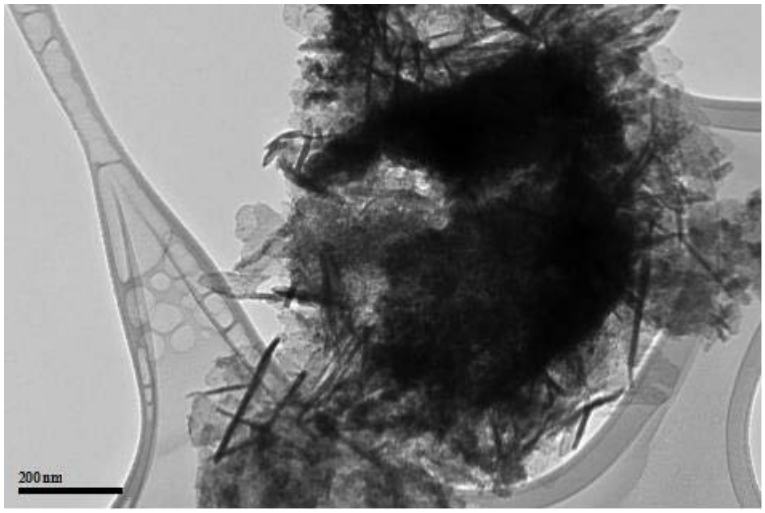

Figure A.7. TEM analysis of a typical particle agglomerate found in caustic-leached Group 3 sludge (Snow et al. 2009).

The TEM analysis showed large (several microns long and 1 to 2 microns across), rod-like U-P bearing crystalline structures (see Figure A.8) in the unleached sludge.

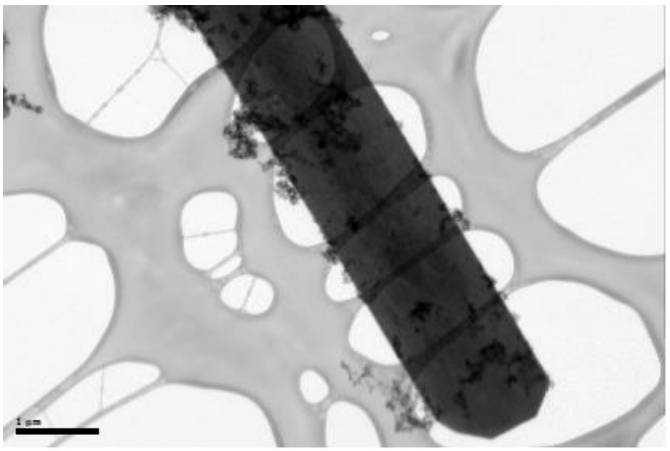

Figure A.8. Group 7 washed sludge uranyl phosphate phase (Edwards et al. 2009).

Discussion of the TEM analysis of the leached Group 7 sludge sample inferred that the U re-precipitated as a phosphate following the sodium hydroxide leach. The unleached uranium phosphate phase was highly crystalline and large (several microns long and up to 2 microns across). Crystalline uranyl phosphate phases in leached Group 7 sludge were not identified by XRD; however, TEM analysis identified submicron U-PO_4 structures and it thus appeared to be present as part of the amorphous components. Thus, in the case of TEM analysis, there was essentially no commonality between the U phases identified from pre-caustic leached samples and those found after caustic leaching.

The samples that were tested for the desired properties and containing high U were obtained from the caustic-leached and washed Group 5 REDOX waste, Group 3 cladding waste, and the Group 7 TBP waste. The densities of the identified U phases from these test groups are summarized in Table A.28. Based on these data, U is likely to exist in a form with a density ranging from 3.3 to 8.4 g/mL.

Clarkeite represents a good phase to simulate. Both clarkeite and sodium uranium oxide were the most often identified U phases in the various leached sludge samples and were present at a high enough concentration to be definitively identified by XRD, unlike U_3O_8. Clarkeite density at 6.7 g/mL is slightly higher than that of sodium uranium oxide. Thus, clarkeite uranium phase was selected for evaluating the feed batch of the as-received and leached solids.

Table A.28. Uranium phase densities.

Mineral Phase	Formula	Found in	Density, g/mL	Density Reference
Clarkeite	$Na(UO_2)O(OH)$	Group 5 M12, Group 3 M12, Group 7 M12	6.744 6.79	JADE, Ver. 8.0 Finch and Ewing 1997; ICSD# 83456
Sodium uranium oxide	$Na_2U_2O_7$	Group 5 M12, Group 3 M12, C-105, BX-103, Group 7 M12	6.554 6.648 6.69	JADE, Ver. 8.0 Kovba et al. 1958 PDF# 01-072-2295 Gasperin 1986
Sodium uranium oxide hydrate	$Na_2U_2O_7 \cdot 6H_2O$	Group 3 M12	[a]	
Uranium oxide[b]	α-U_3O_8	Group 3 M12	8.39 8.43 8.41	Loopstra 1977; ICSD# 28138 Andresen 1958; ICSD# 16756 Momin et al. 1974; ICSD# 647584
Threadgoldite	$Al(UO_2)_2(PO_4)_2(OH)(H_2O)_8$	Group 7 M12[f]	3.4 3.33 3.33	Webmineral.com Khosrawan-Sazedj 1982; ICSD# 31265; Piret et al. 1979; ICSD# 26347
Dioxouranium (VI) bis(dihydrogenphosphate(I)) hydrate	$(UO_2)(H_2PO_2)_2(H_2O)$	Group 7 M12[f]	3.53	Tanner and Mak 1999; ICSD# 88016
Sodium uranyl phosphate	$Na_6(UO_2)_2(PO_4)_4$	Group 7 M12	[c]	
Becquerelite (possible)	$Ca(UO_2)_6O_4(OH)_6(H_2O)_8$	Group 7 M12	5.14 5.12 5.1	Piret-Meunier and Piret 1982; ICSD# 201364 Pagoaga et al. 1987; ICSD# 202477 Burns and Li 2002; ICSD # 94620
Sodium uranium phosphate [d]	Na-U-PO4	Group 7 M12	[e]	
Uranium oxide	$UO_3 \cdot 2H_2O$[d]	S-104	7.29	*CRC Handbook of Chemistry and Physics* 61st Edition

ICSD = inorganic crystal structure database
PDF = powder diffraction file
(a) Density of anhydrous sodium uranium oxide may be similar to that of the hydrous compound.
(b) Determined from TEM analysis with electron diffraction.
(c) Structure and density not found; similar material, sodium tris(dioxouranium) hemihydrogentris (phosphate) with structure of $Na_{5.5}(UO_2)_3(H_{0.5}PO_4)(PO_4)_3$, has a density of 4.47 g/mL (Gorbunova et al. 1980).
(d) Determined from TEM analysis with energy dispersive spectroscopy and electron diffraction.
(e) No structure identified; phase and density cannot be assessed.
(f) Only found before caustic leaching and matched as possible phases.

The higher density U phase, clarkeite, was selected for evaluating the feed batch for both the as-received and leached condition, with a density of 6.74 g/mL.

A.2.11 Zirconium

Zirconium morphology and size were best estimated from the wastes that contain high concentrations of Zr. The Zr distribution in the tank waste solids, according to the BBI, is shown in Table A.29. Zirconium is predominantly found in the zirconium cladding waste (CWZr).

Table A.29. Projected distribution of water-insoluble zirconium in tank waste.

Sludge Source	Type	Zr, wt%
AN-101	CWP, CWZr,	17%
AW-103	CWZr	43%
AW-105	CWZr	26%
S-107	CWR, CWZr, R	8%
	Balance	14%

Finding a predominant Zr phase in tank waste was difficult; six samples from tank waste could be found where the Zr concentration exceeded 6 wt%. Only one sample, S-107, contained CWZr waste. Table A.30 summarizes the identified samples with respect to tank origin, sludge type, related M12 grouping, weight percent Zr, leach condition, and reference report. No phases were identified specifically as a crystalline Zr form; TEM examination proposed the Zr phase in S-107 caustic-leached sample to exist as ZrO_2.

Table A.30. Samples identified with >6 wt% zirconium.

Sludge Source	Sludge Type	M12 Group	Zr, wt%	Leached?	Zr Phase ID?	Reference Report
S-107	R1, CWR, CWZr	5	8.2	Yes	Yes[(a)]	Lumetta et al. 1996a
C-104	NA	--	11.2	Yes	No	Brooks et al. 2000b
C-104	NA	--	10.3	Yes	No	Lumetta et al. 2000
AZ-101	P3AZ	--	6.6	Yes	No	Geeting et al. 2003
AZ-101	P3AZ	--	8.5	No	No	Bell 2001
M12	CWP	3	14.4	Yes	No	Snow et al. 2009

CWP = PUREX cladding waste
CWR = REDOX cladding waste
CWZr = zirconium cladding waste
P3AZ = PUREX high-level waste
R1 = REDOX waste
(a) TEM phase identification.

Zirconium was assigned the phase ZrO_2 for evaluating the feed batch in both the as-received and leached conditions with a density of 5.68 g/mL (*CRC Handbook of Chemistry and Physics*, 92nd Edition).

A.3 Summary of Phase Identification

Results from this phase identification (of the most prevalent mineral phases for the primary waste elements identified in Table A.1) are provided in Table A.31. The as-received and leached solids waste feed batches are listed separately to highlight commonalities and differences. A significant fraction of the sodium and potassium was assumed to be associated with oxalate and phosphate (see Table A.1), as well as the relevant phases identified in Table A.31.

Table A.31. Minerals assigned to components.

As-received			Leached	
Component	Mineral Phase	Density, g/mL	Component	Mineral
Al^{3+} (a,f)	AlOOH $Na_6Ca_2\cdot(CO_3)_2Al_6Si_6O_{24}$ $Na_2Al_2Si_{14}O_{32}\cdot 3H_2O$ $Al(OH)_3$(a)	3.01 2.42 2.42 2.42	Al^{3+}	AlOOH $Na_6Ca_2\cdot(CO_3)_2Al_6Si_6O_{24}$ $Na_2Al_2Si_{14}O_{32}\cdot 3H_2O$
Fe^{3+} (c)	$Fe_{3.7}Bi(PO_4)_{4.7}$ $Fe_{3.7}Bi(OH)_{14.1}$ $Fe(PO_4)$ Fe_2O_3, hematite	3.3 3.3 3.06 5.25	Fe^{3+}	$Fe_{3.7}Bi(OH)_{14.1}$ Fe_2O_3, hematite
Zr^{4+}	ZrO_2	5.68	Zr^{4+}	ZrO_2
Ca^{2+} (e)	$Na_6Ca_2\cdot(CO_3)_2Al_6Si_6O_{24}$ $Ca(OH)_2$	2.42 2.24	Ca^{2+}	$Na_6Ca_2\cdot(CO_3)_2Al_6Si_6O_{24}$ $Ca(OH)_2$
Si^{4+} (d)	$Na_6Ca_2\cdot(CO_3)_2Al_6Si_6O_{24}$ $Na_2Al_2Si_{14}O_{32}\cdot 3H_2O$	2.42 2.42	Si^{4+}	$Na_6Ca_2\cdot(CO_3)_2Al_6Si_6O_{24}$ $Na_2Al_2Si_{14}O_{32}\cdot 3H_2O$
^{238}U	$NaUO_2OOH$	6.74	^{238}U	$NaUO_2OOH$
Bi^{3+} (b)	$Fe_{3.7}Bi(PO_4)_{4.7}$ $Fe_{3.7}Bi(OH)_{14.1}$	3.3 3.3	Bi^{3+}	 $Fe_{3.7}Bi(OH)_{14.1}$
PO_4^{3-}	$Fe_{3.7}Bi(PO_4)_{4.7}$	3.3		
		4.15	Ni^{2+}	$Ni(OH)_2$
		3.7	Sr^{2+}	$SrCO_3$
--	--	9.86	^{232}Th	ThO_2
--	--	4.73	Mn (prec) and Mn^{4+}	MnO_2

(a) Mass for $Al(OH)_3$ was defined in the anticipated feed batch.
(b) Bi assigned to $Fe_{3.7}Bi(PO_4)_{4.7}$ until phosphate limitation was reached, then $Fe_{3.7}Bi(OH)_{14.1}$ to complete the Bi phase assignment.
(c) Fe assigned first to $Fe_{3.7}Bi(PO_4)_{4.7}$, then $Fe(PO_4)$ until PO_4 was consumed, then remaining Fe was assigned to Fe_2O_3; if the Fe was phosphate limited, then Fe was assigned to $Fe_{3.7}Bi(PO_4)_{4.7}$, then to $Fe_{3.7}Bi(OH)_{14.1}$ until Bi was consumed, then the remainder was assigned to Fe_2O_3.
(d) Si first assigned to cancrinite (as limited by Ca or Al), then to zeolite (as limited by Al), then the remainder to SiO_2.
(e) Ca first assigned to cancrinite (as limited by Si or Al), remaining assigned to $Ca(OH)_2$.
(f) Al first assigned to cancrinite (as limited by Al or Ca), then to zeolite (as limited by Si), then remaining to boehmite.

Using the phases identified in Table A.31, the feed vector was analyzed to provide the mass fraction for each phase associated with the as-received and leached feed batches. This information is summarized in Table A.32. The gibbsite mass was provided directly in the as-received feed batch and was used as provided. In cases where only one phase was assigned, the entire phase was based on that component mass. However, many of the elements were assigned to several phases, and this increased the complexity of phase mass assignment. The as-received element distribution between the assigned phases was based on limiting conditions as indicated in Table A.31.

The leached sludge phases were assigned similarly to those of the as-received sludge except phosphate phases were omitted (phosphate was assumed to have been metathesized and removed during caustic leach and washing). The mass fractions of the phases in the as-received and leached feed batches were calculated. Table A.32 provides the average, minimum, and maximum mass fractions calculated for the various feed batches based on the phase assignments.

Table A.32. Calculated mineral phase weight percents in feed batches.

As-received				Leached			
Mineral Phase	Avg.	Min.	Max.	Mineral Phase	Avg.	Min.	Max.
$Al(OH)_3$	51.1%	27.9%	78.5%	--	--	--	--
AlOOH	15.3%	0.0%	45.5%	AlOOH	33.4%	5.2%	78.0%
Cancrinite	10.7%	2.5%	30.5%	Cancrinite	21.3%	7.4%	47.0%
$Fe_{3.7}Bi(OH)_{14.1}$	0.2%	0.0%	4.5%	$Fe_{3.7}Bi(OH)_{14.1}$	11.8%	0.10%	33.3%
$NaUO_2OOH$	3.4%	0.6%	7.7%	$NaUO_2OOH$	7.2%	0.85%	18.2%
Fe_2O_3	2.2%	0.0%	38.9%	Fe_2O_3	9.4%	0.00%	52.9%
$Fe_{3.7}Bi(PO4)_{4.7})$	7.6%	0.1%	26.6%	--	--	--	--
ZrO_2	2.1%	0.0%	18.7%	ZrO_2	4.8%	0.04%	39.0%
Zeolite	3.1%	0.0%	23.7%	Zeolite	3.2%	0.00%	16.9%
$Ca(OH)_2$	0.4%	0.0%	15.8%	$Ca(OH)_2$	0.71%	0.00%	21.3%
$FePO_4$	3.9%	0.0%	16.8%	MnO_2	2.1%	0.81%	9.7%
SiO_2	0.0%	0.0%	5.9%	MnO_2 Precip.	2.9%	0.00%	19.8%
--	--	--	--	$Ni(OH)_2$	1.6%	0.23%	11.5%
--	--	--	--	$SrCO_3$	0.93%	0.04%	12.2%
--	--	--	--	ThO_2	0.64%	0.03%	6.5%

The weighted average of the sludge density was determined for each of the projected slurry deliveries (see Section A.1) using the calculated specific phase mass fraction and associated phase particle density. The average particle density in the as-received sludge was 2.70 g/mL (range 2.50 to 3.17 g/mL for 631 projected as-received slurry deliveries). The average particle density for the leached sludge was 3.30 g/mL (range 2.85 to 4.23 g/mL for 203 projected leached slurry deliveries). Densities were assigned for each mineral using their mineral densities. It should be noted that this introduces some conservatism into the calculations, as many of the minerals have been shown to be present as agglomerates, which would have lower densities than pure mineral phases.

A.4 Particle Size Distribution of Identified Phases

The next step in developing simulant PSDDs is to assign a PSD to each component element. To develop a basis supporting selection of a given mineral phase's size distribution, historical Hanford tank waste composition and particle size characterization data were evaluated to identify wastes that (1) show the greatest contribution of a given element and (2) have corresponding PSD data against which a representative PSD for each element could be evaluated. When multiple PSDs were available, the larger PSD was generally selected to provide a conservative estimate of the mineral phase PSD with respect to particle sedimentation (settling), suspension, and re-suspension processes. More details regarding the PSD selection process are provided in Section A.7.

PSD analysis also considers waste as it will be transferred to the Pretreatment Facility. ICD-19 (BNI 2014) dictates that no waste solids larger than 310 μm be transferred to the plant; solids larger than this size "cut-off" will be separated from the waste or size-reduced. For this reason, each component has two PSDs associated with it: one representing the uncut "tank" PSD and another with this same PSD cut to 310 μm. The 310-μm cuts were created by clipping (zeroing) population contributions from size classes larger than 310 μm.[1]

PSDs for the uncut assumed phases for as-received and leached materials are presented in Figure A.9 and Figure A.10, respectively. It should be noted that the +310-μm "clipping" process significantly changed the PSDs for only two components: gibbsite and iron phosphate. Figure A.11 and Figure A.12 provide equivalent information using the 310-μm cut PSDs. The nature of the composition-based selection of PSDs, along with overlap of significant species in certain data sets, led to several elemental or base mineral phases having identical size distributions. Notable cases include cancrinite/zeolite and Ca/Sr pairs. Likewise, there were cases where there was insufficient information to distinguish PSDs for similar mineral phases, such that the same PSD was used for two different minerals. This is the case for $Fe_{3.7}Bi(PO_4)_{4.7}$ and $Fe_{3.7}Bi(OH)_{14.1}$, which both use the same Bi-elemental PSD. On the other hand, there were several cases where chemical information allowed differentiation between PSDs for mineral phases with the same parent element. This is the case for Al-bearing species (boehmite and gibbsite) and Fe-bearing species (hematite and iron-phosphate). In these cases, PSDs from separate PSD data sets were used to represent each component. Finally, although Cr is identified in "significant" fractions in waste samples, no significant Cr-bearing mineral phase was identified for use in the simulant basis. Thus, while it is possible to develop a PSD for Cr-bearing solids, no such PSD is included in the final set of PSDs reported below.

[1] In the analysis used to establish component PSDs, a uniform size classification, with 100 logarithmically spaced size bins spanning 0.02 to 2000 μm, was used for all distributions.

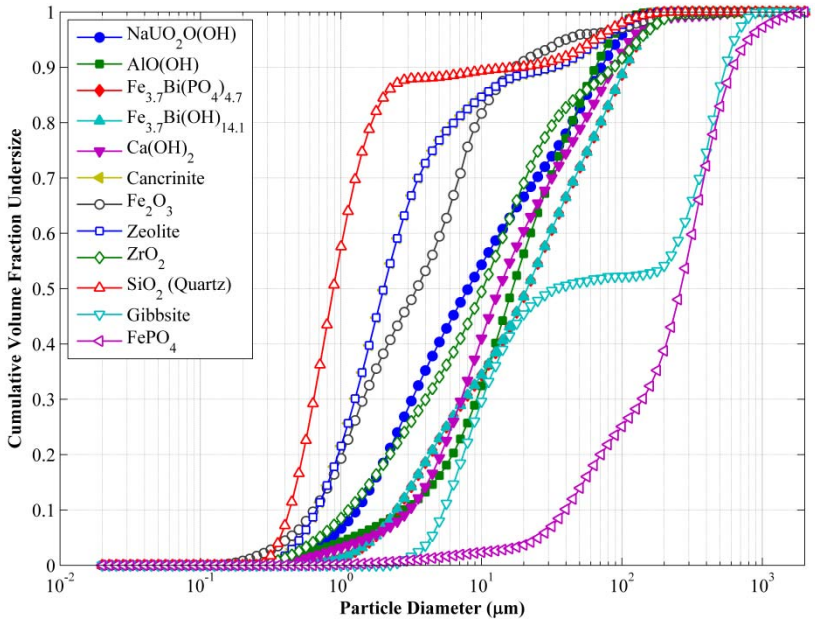

Figure A.9. Uncut particle size distributions (as cumulative volume fraction undersize as a function of particle diameter) for as-received phases in Table A.31. $Fe_{3.7}Bi(PO_4)_{4.7}$ and $Fe_{3.7}Bi(OH)_{14.1}$ have identical PSDs. Likewise, cancrinite and zeolite have identical PSDs.

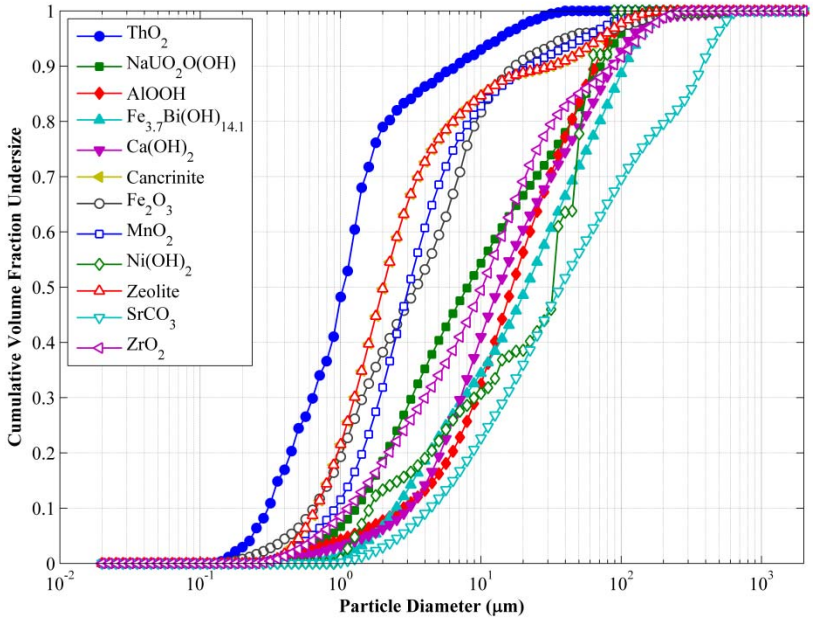

Figure A.10. Uncut particle size distributions (as cumulative volume fraction undersize as a function of particle diameter) for leached assumed phases in Table A.31. Cancrinite and zeolite have identical PSDs.

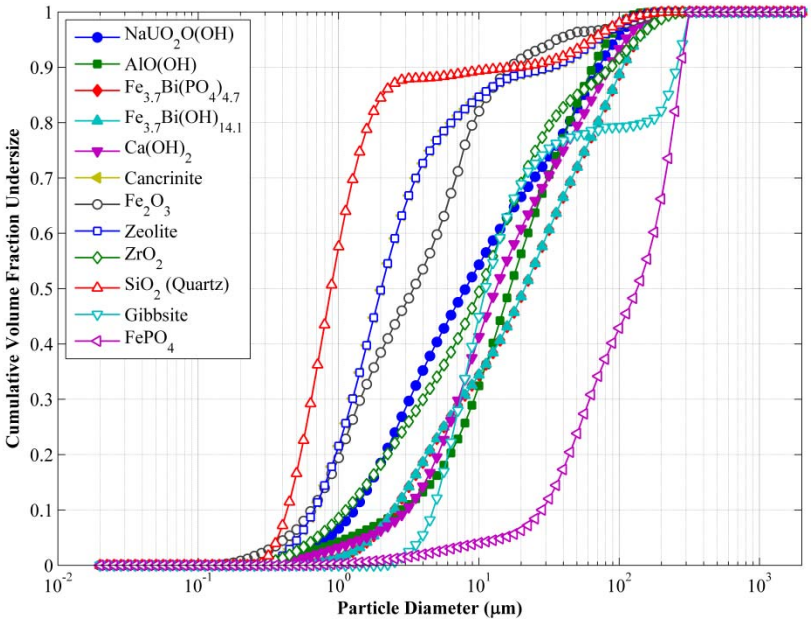

Figure A.11. 310-μm cut particle size distributions (as cumulative volume fraction undersize as a function of particle diameter) for as-received assumed phases in Table A.31. $Fe_{3.7}Bi(PO_4)_{4.7}$ and $Fe_{3.7}Bi(OH)_{14.1}$ have identical PSDs. Likewise, cancrinite and zeolite have identical PSDs.

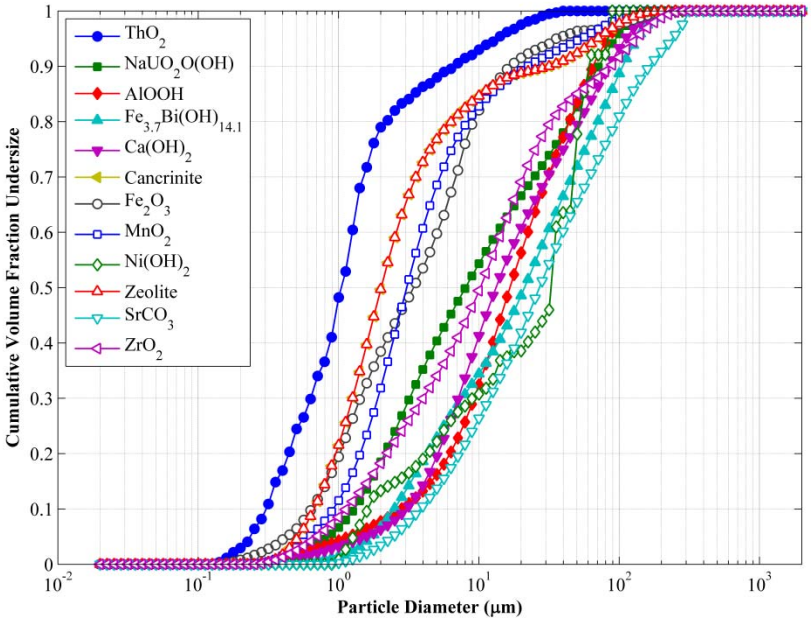

Figure A.12. 310-μm cut particle size distributions (as cumulative volume fraction undersize as a function of particle diameter) for leached assumed phases in in Table A.31. Cancrinite and zeolite have identical PSDs.

It should be noted that for some of the less common elements (e.g., Sr and Ni), these identified mineral phases are not present as a dominant phase in any of the characterized tank waste samples. For these components, the PSDs that result from the analysis above will be influenced by that of other, more dominant, mineral phases present in the wastes. As such, the accuracy of these minor component PSDs is low, but these are the "best" representations of these phases that can be arrived at from existing data. Since these phases are not present in large concentrations and are not characterized by high densities, minor component PSD uncertainty will have limited impact on the metrics that will be calculated from the resultant PSDs. It should also be noted that even for prevalent mineral phases such as gibbsite and boehmite, as one would expect, the tank waste samples are not pure mineral phases.

A.5 Validation of Selected Particle Characterizations

This section assesses the validity of the mineral phase density and size distributions that were defined in the previous sections. The validity of these assignments is determined through comparison with available actual HLW solids settling rate process data. Wells et al. (2011) evaluated and summarized Hanford solid settling rate data for 20 individual waste storage tanks and 7 waste-group composites. Two HLW storage tanks have in situ settling rate information as well as laboratory-scale data. The in situ settling rates provide actual waste process performance data against which the developed mineral phase density and size distributions can be compared. The AZ-101 interface settling rate data are from the WFD mixer pump operation tests (as described in Carlson et al. 2001), and the AY-102 data are from the sluicing retrieval of C-106 into AY-102 (Cuta et al. 2000). The AZ-101 data represent a much more direct interface settling rate measurement than the AY-102 data; see Wells et al. 2011.

Wells et al. (2012) compared the in situ settling rate process performance data to particle settling rate data for that waste to establish the basis for waste characterization. A similar comparison process is applied for this current work. The waste composition characteristics of the two individual HLW storage tanks (AZ-101 and AY-102) with in situ settling rate information are developed from the applicable components previously described.

The solid components listed in Table A.31 account for approximately 95% by mass of the solids in AZ-101 and approximately 82% by mass of the solids in AY-102. Individual particle settling rates can be computed for the resulting PSDD; see Section A.6.8. For individual particles in the unhindered settling regime, the settling velocity (U_T) relationship described by Camenen (2007) for spherical particles is used:

$$U_T = \frac{\mu}{\rho_L d}\left[\sqrt{15 + \sqrt{\frac{Ar}{0.3}}} - \sqrt{15}\right]^2 \tag{A.1}$$

where *Ar* is defined by

$$Ar = \frac{\left(\frac{\rho_S}{\rho_L} - 1\right) g d^3}{\left(\frac{\mu}{\rho_L}\right)^2} \tag{A.2}$$

where

μ = liquid fluid dynamic viscosity (Pa s)
d = particle size (m)
ρ_L = liquid density (kg/m^3)
ρ_S = solid particle density (kg/m^3)
g = gravitational acceleration (m/s^2).

and U_T is in m/s. The same calculation approach was used in Wells et al. 2011, 2012, and Lee et al. 2012.

The calculated particle settling rates for the AZ-101 and AY-102 wastes based on the particle characterizations of the uncut PSDs (Figure A.9) for as-received phases in Table A.31, denoted as "Recreate," are shown in Figure A.13 and Figure A.14, respectively. The figures are modified from Wells et al. 2011, where the new results added to the figures are only the Recreate data. The primary point of comparison for the new data is with the two red vertical lines shown in the Figure A.13. The red line/shaded area in the figures indicates the in situ determined unhindered solid-liquid interface settling rate. It should be noted that decreasing the AZ-101 settling rates from first principle assessments has been challenging. As seen in Figure A.13, the previous best efforts to predict this settling behavior indicated the settling rates as represented by approximately the 60th percentile. The new analysis gave the same approximation, indicating that the approach used in developing this assessment was as accurate as the previous analysis. Similarly, the assessment for AY-102 indicates that the revised PSDD provides an equivalent comparison to the in situ measured values as the PSDD used in the prior assessment.

The comparison of the process performance data (in situ determined unhindered solid-liquid interface settling rate) and TOC WFD simulant waste characterization basis (i.e., the unhindered settling velocity, no-flow unsonicated PSDDs) with the Recreate characterizations of the respective tank waste from the waste component characterizations described previously is favorable, as shown in Figure A.13 and Figure A.14 within the mass of solids represented. Therefore, the developed mineral phase density and size distributions are judged to have merit with respect to reproduction of the available HLW process performance data.

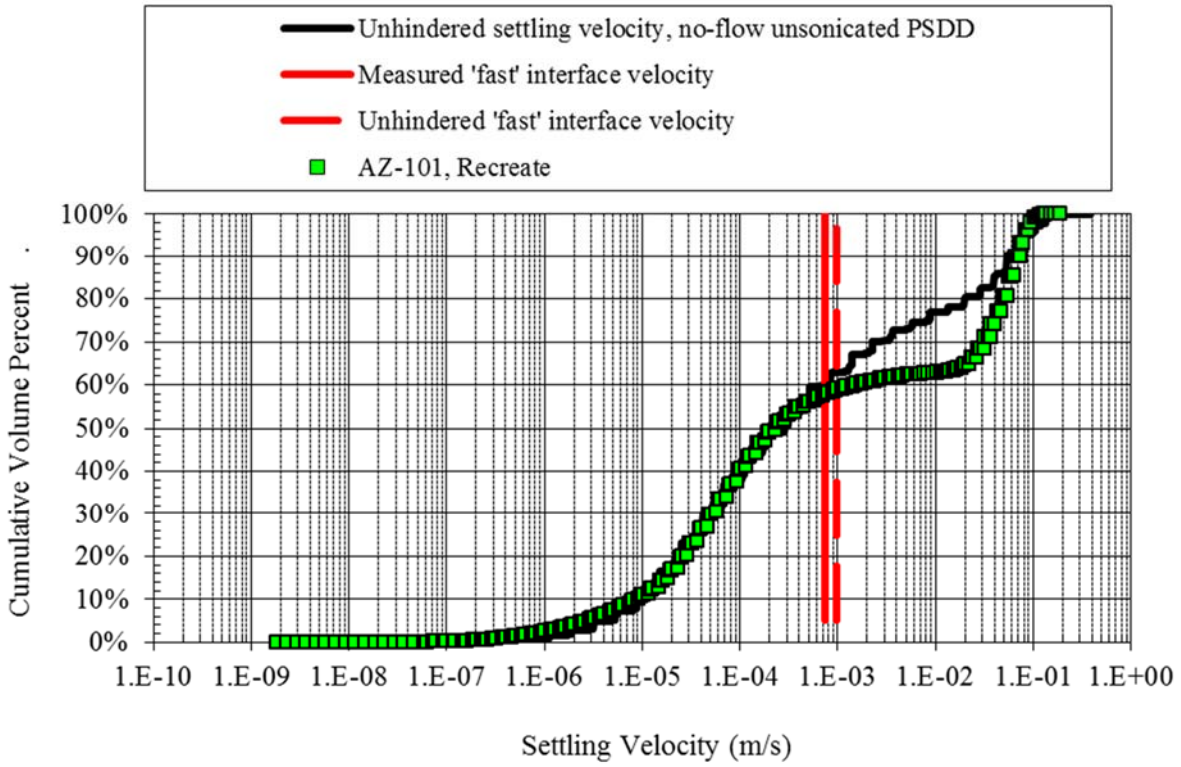

Figure A.13. Calculated settling velocity of recreated AZ-101 PSDD compared to specific waste particle characterization and process performance data. Modified from Wells et al. 2011.

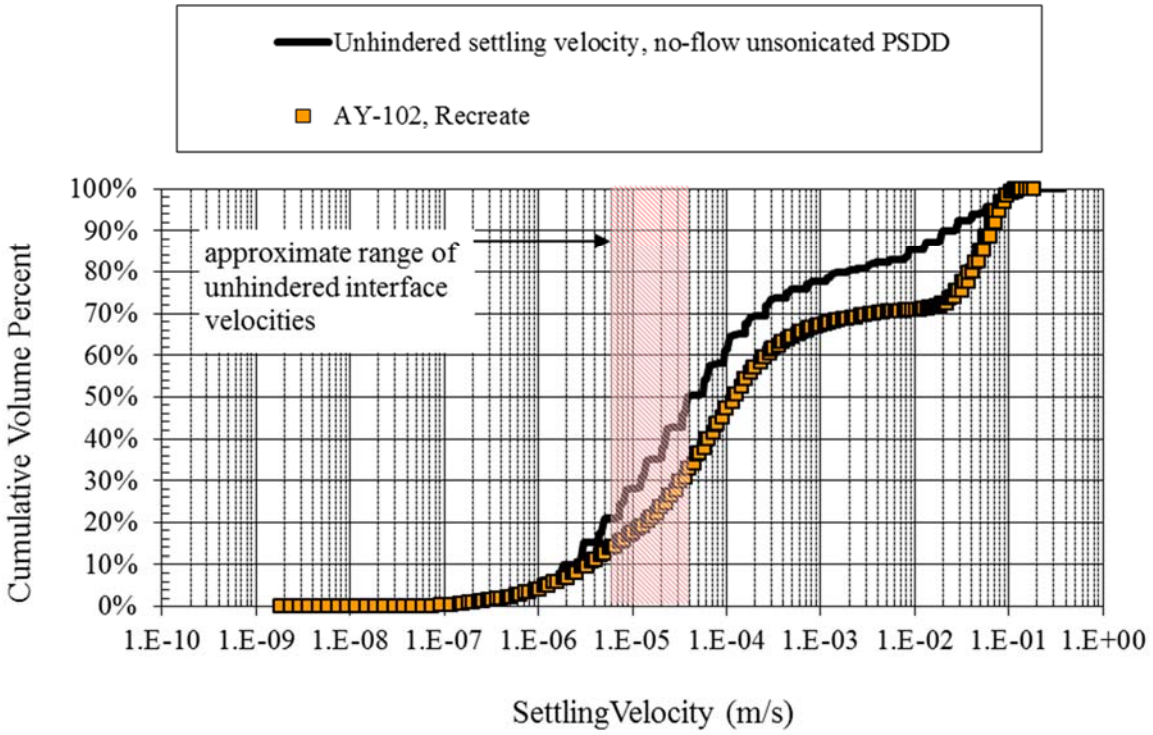

Figure A.14. Calculated settling velocity of recreated AY-102 PSDD compared to specific waste particle characterization and process performance data. Modified from Wells et al. 2011.

A.6 Process Performance Metrics

This section describes how the waste components and concentrations and waste component characteristics developed previously were combined to create the SHSVD Newtonian simulant performance target. The SHSVD Newtonian simulant performance target basis follows the process performance metric approach for the mobilization, suspension, and transfer of solids in a vessel and transfer line developed in Wells et al. 2012 and applied in Lee et al. 2012.[1]

A.6.1 Process Performance Metrics

The parameters that are most important to pulse-jet mixer (PJM) mixing of WTP tanks with Newtonian slurries are specified in Poirier and Martino 2015 as the particle size, particle density, and particle concentration. Likewise, previous studies of mixing and transfer in the tank farm WFD system with waste simulants have demonstrated that the system performance depends on the distribution of solid particle sizes and densities (e.g., Wells 2013). Thus, WTP process performance, as specified by the mixing requirements (Mauss 2010) for a specific particle depends on the overall size and density distribution of the particulate in the simulant.[2,3] Here, process performance is generally described as particle mobilization, suspension, settling, transfer-line intake, and pipeline transfer. Predicting actual process performance of polydisperse slurries is difficult with the unique waste feed processing systems (e.g., PJM-mixed vessels) and because performance models are typically applicable only for mono-disperse particle slurries (e.g., mobilization, pipeline transport). To compare slurries with variable particle sizes and densities, a method developed for WFD simulants (Wells et al. 2012) is to calculate a performance metric that combines the effect of size and density. However, different performance metrics can have different functionalities with particle size and density.

An example selection of performance metrics is listed in Table A.33, and the effect of a particle's size can be more or less significant than its density depending on the process being considered. Particle settling in the Stokes flow regime has a greater dependence on particle size, while particle mobilization, off-bottom suspension, and pipeline transport critical velocity are all shown to be more dependent on particle density than size. These performance metrics can represent an aspect of the Mauss (2010) mixing requirements, and a comparison using one metric may produce different results than a comparison based on another metric depending on the mixing requirement being evaluated, and a particle that is representative or challenging for one aspect of the system may not be for another aspect of that system. The simulant design approach therefore considers all the metrics representing or related to aspects of the system at the same time to demonstrate that the simulant is representative for all metrics (e.g., Wells et al. 2012; Lee et al. 2012; Wells 2013).

---

[1] The RLD-08T simulant development process followed the same approach: King, W, R Eibling, M Hay, R Peterson, B Wells, S Fiskum, R Russell, C Burns, G Brown, C Carlson, D Rector, W Kuhn, and J Fort. 2014. *FSVT Vessel Group 5 Simulant Supporting RLD-08T; (90% Review Draft)*. GD-FSVT-0017, SRNL-TR-2014-00032 DRAFT. The WTP Full Scale Vessel Testing Program National Laboratory Technical Authority Team, Richland, WA.

[2] The mixing requirements of Mauss (2010) are superseded by those of the Standard High Solids Vessel Design (SHSVD) Test Specification 24590-WTP-ES-ENG-14-012 Rev 1 (July 20, 2016 Draft) as addressed in Section 3.

[3] For this document, the waste solid particle characteristics for the Newtonian simulant performance target are evaluated with respect to process performance, not the specific performance of the prototypic system. Therefore, the effect of particle concentration is not evaluated herein.

Table A.33. Example performance metric functionality.

Metric	Reference	Functionality[(a)]
Archimedes number, Ar	Camenen 2007	$Ar \propto \left(\frac{\rho_S}{\rho_L} - 1\right) d^3$
Particle settling, U_T	McCabe and Smith 1976 (Ar << 15)	$U_T \propto \left(\frac{\rho_S}{\rho_L} - 1\right) d^2$
Radial jet velocity needed to achieve a certain degree of solid suspension, U_n	Kale and Patwardhan 2005	$U_n \propto \left(\frac{\rho_S}{\rho_L} - 1\right)^{0.38} d^{0.14}$
Radial jet velocity for off-bottom suspension, V_{js}	Paul et al. 2004	$V_{js} \propto \left(\frac{\rho_S}{\rho_L} - 1\right)^{0.28} d^{0.1}$
Just-suspended impeller speed, N_{js}	Paul et al. 2004	$N_{js} \propto \left(\frac{\rho_S}{\rho_L} - 1\right)^{0.45} d^{0.2}$
Critical shear stress for erosion of noncohesive particles, τ_c	Chien and Wan 1983 (for $1.5 \leq Ar^{1/3} < 10$)	$\tau_c \propto \rho_L{}^{0.183}(\rho_S - \rho_L)^{0.817} d^{0.45}$
Pipeline critical transport velocity, U_C	Oroskar and Turian 1980	$U_C \propto \left(\frac{\rho_S}{\rho_L} - 1\right)^{0.545} d^{0.167}$

(a) d = particle size, ρ_L= fluid density, ρ_S = solids density

In the absence of models specific to each mixing requirement, a suite of eight process-performance metrics from Lee et al. 2012 representing particle mobilization, suspension, settling, transfer-line intake, and pipeline transfer was used to calculate the SHSVD simulant performance target basis (Table A.34). Each particle size and density of the PSDDs is evaluated separately. Therefore, it is the comparison of the model results for the particulates that is of significance, not the specific model results themselves.

The waste particles, as described by their PSDDs developed as detailed in Section A.6.8, are compared via the performance models with all other inputs (as defined in the subsequent sections) held constant and with water (1.0 g/mL, 1.0 cP) used as the fluid in all cases. Model parameters such as vessel diameter and fluid jet operational conditions, among others, are set to constant values within the range of the model basis or application. Other parameters that could influence the comparison not encompassed in the model forms or without sufficient characterization (e.g., particle shape) were not addressed.

Hanford waste particles are denser than waste liquids and, therefore, will gravity settle. At low solids concentrations, individual particles can settle without interacting with other particles (unhindered settling). At higher solids concentrations, interactions between particles can reduce settling rates (hindered settling). For individual particles in the unhindered settling regime, the settling rate is computed as described in Section A.5. Sections A.6.2 through A.6.7 summarize the remaining metric calculations.

Table A.34. Process performance metrics.

Metric	Symbol	Process Performance	Reference
Archimedes number	Ar	All	Camenen 2007
Settling velocity (m/s)	U_T	Settling	Camenen 2007
PJM critical suspension velocity for noncohesive solids (m/s)	U_{CS}	Mobilization	Fort et al. 2010
PJM cloud height for noncohesive solids (m)	H_c	Suspension, Settling, Transfer-line intake	Fort et al. 2010
Radial jet velocity needed to achieve a certain degree of solid suspension (m/s)	U_n	Mobilization	Kale and Patwardhan 2005
Critical shear stress for erosion of noncohesive particles (Pa)	T_c	Mobilization	Paphitis 2001
Pipeline critical transport velocity (m/s)	U_c	Pipeline transfer	Oroskar and Turian 1980
Just-suspended impeller speed (rps)	N_{js}	Mobilization	Paul et al. 2004

A.6.2 PJM Critical Suspension Velocity for Noncohesive Solids

The WTP is applying PJM technology for tank mixing applications requiring solids mixing, solids suspension, and fluid blending. PJMs are non-steady jet mixing devices that use compressed air as the motive force. The WTP defines critical suspension velocity as the lowest jet nozzle velocity that can suspend all solids in a process vessel. The critical suspension velocity model of Fort et al. (2010) depends on waste and jet properties as well as vessel and mixing equipment configuration (i.e., vessel dimensions and the positions, orientations, and number of jets), and the bulk of the data used to develop the Fort et al. (2010) model was based on the WTP HLP-22 vessel. The critical suspension velocity is calculated from

$$U_{CS} = U_{TH}\, 2.302 \left(\frac{D^*}{Ar^{0.673}} \right)^{0.261} \tag{A.3}$$

where the hindered settling velocity is represented by

$$U_{TH} = U_T \left(1 - \frac{\phi_S}{0.6} \right)^6 \tag{A.4}$$

In Eq. (A.3), D* is defined by

$$D^* = \frac{D(S-1)g\phi_S}{DC\ U_{TH}{}^2 \phi_P{}^{0.898} \phi_J{}^{1.958}} \tag{A.5}$$

where

DC = PJM duty cycle
D = tank diameter
S = ρ_S/ρ_L

ϕ_J = jet density (= nd_j^2/D^2)
d_j = PJM nozzle diameter
n = number of operating jets/pulse tubes
ϕ_P = pulse volume fraction
ϕ_S = solids volume fraction (volume of undissolved solids per a reference tank volume defined as $\frac{\pi}{4}D^3$).

Calculations are conducted using configuration and operational parameters for WTP vessel HLP-22 as specified in Meyer et al. 2012, which are provided in Table A.35, and $\phi_S = 0.1$.

Table A.35. HLP-22 operational parameters (Meyer et al. 2012).

Parameter	Value (units)
D	38 (ft)
DC	0.22
ϕ_P	0.05
ϕ_J	0.00208

A.6.3 PJM Cloud Height for Noncohesive Solids

During PJM operation in a WTP waste process vessel, some eroded solids are lifted upward, often forming a distinct slurry layer above which a clear liquid exists. The cloud height, H_C, expresses the height of this slurry layer above the vessel bottom, and thus provides the maximum vertical distribution of the suspended solids. Fort et al. (2010) provide a model for cloud height as

$$\ln\left[H_C^* \, Re^{-0.143}\right] = 8.223\left(\frac{U}{U_{TH}}\right)^{0.1364} \tag{A.6}$$

where

$$H_C^* = \frac{H_C (S-1) g \phi_S N^{0.658}}{DC \; U_{TH}{}^2 \phi_P{}^{0.898} \phi_J{}^{1.662}} \tag{A.7}$$

where the Reynolds number $Re = Ud_j/\nu$, ν is the liquid kinematic viscosity (m^2/s), U is the jet nozzle velocity, and N is the number of PJMs. For HLP-22, U is set to 12 m/s and N = 12 (Meyer et al. 2012). All other parameters are as listed in Section A.6.2 for the PJM critical suspension velocity.

A.6.4 Radial Jet Velocity Needed to Achieve a Certain Degree of Solids Suspension

Kale and Patwardhan (2005) provide a correlation for the suspension of solids in 0.5- to 1-m-diameter tanks with radial wall jets. A semi-empirical model to predict the jet velocity needed to achieve a certain degree of solids suspension (e.g., 75% or 100% of the solids suspended) is expressed as a function of the Ar number by

$$U_n = \frac{\nu}{d}\left[0.13X^{0.22}Ar^{0.38}\left(\frac{D}{d_j}\right)^2\left(1+0.25\left(\frac{z}{d_j}\right)\right)^{-0.25}\left(1+0.75\left(\frac{z}{D}\right)\right)\right] \quad (A.8)$$

where d_j is the jet nozzle diameter and z is the nozzle clearance above the tank bottom. The evaluations are made with the solids loading ratio X and tank diameter D set to the maximum tested by Kale and Patwardhan (2005), 5 and 1 m, respectively. Likewise, the nozzle diameter and clearance are set to nominal testing values of 0.04 and 0.5 m, respectively.

A.6.5 Critical Shear Stress for Particle Erosion

The critical shear stress for erosion (τ_C) is the applied stress required to mobilize particles from the surface of a sediment bed. In Wells et al. 2012, the Paphitis (2001) critical shear stress relation is shown to be applicable to the particle characteristic basis for Hanford waste particles, and the expression is

$$\tau_* = \frac{0.273}{1+1.2D_*} + 0.046\left(1-0.576e^{-0.02D_*}\right) \quad (A.9)$$

where $D_* = Ar^{1/3}$ and

$$\tau_* = \frac{\tau_C}{(\rho_S - \rho_L)gd} \quad (A.10)$$

where τ_C is in units of Pa, density terms are kg/m^3, and particle size d is in meters.

A.6.6 Pipeline Critical Transport Velocity

Hanford waste slurry will be transferred through pipelines within tank farms, between tank farms, from tank farms to the WTP, and between process vessels within the WTP. The Oroskar and Turian (1980) model is used to estimate the pipeline critical velocity via

$$U_C = 1.85\sqrt{gd(S-1)}C_V^{0.1536}(1-C_V)^{0.3564}\left(\frac{d}{D_P}\right)^{-0.378}\left[\frac{D_P\rho_L\sqrt{gd(S-1)}}{\mu}\right]^{0.09}\chi^{0.30} \quad (A.11)$$

where

S = ρ_S/ρ_L
C_V = solid volume fraction
D_P = pipe diameter (m)
χ = fraction of eddies having velocities equal to or greater than the settling velocity.

For these evaluations, $C_V = 0.1$ and $D_P = 3$ in, and χ is set to 0.96 (Wells et al. 2007).

A.6.7 Just-Suspended Impeller Speed

A well-known correlation for the just-suspended impeller speed (N_{js}) is that of Zweitering, given in Paul et al. 2004 as

$$N_{js} = S_Z \nu^{0.1} \left[\frac{g(\rho_S - \rho_L)}{\rho_L} \right]^{0.45} X^{0.13} d^{0.2} D^{-0.85} \quad \text{(A.12)}$$

where S_Z is a dimensionless number that is a function of impeller type, X is the mass ratio of solids to liquid, and D is the impeller diameter. The inputs are set as S_Z to a nominally typical value of 5 (Paul et al. 2004), X to 10 (nominal solid-to-liquid mass ratio in AY-102 multiplied by 100; Wells and Ressler 2009), and a 1-m impeller diameter. Eq. (A.12) has been shown to reliably fit experimental data between solids loadings of 5 to 170 (Paul et al. 2004).

A.6.8 Performance Target

The waste components and concentration component characteristics developed previously are combined to identify the SHSVD simulant performance target. A volume-weighted PSDD was constructed from the "cut" component PSD and density in combination with each of the component mass fractions representing a range of process streams for both as-received and leached waste. As detailed the components and characteristics vary between the as-received and leached waste, but within those respective streams, the component characterization data are held constant over the evaluated range of compositions. Each resulting process stream PSDD was used to calculate the performance metrics presented in Section A.6.1. Resulting metric calculations, along with the corresponding volume fraction and cumulative distribution, are used to examine adverse conditions and identify an adverse process stream PSDD.

A.6.9 Composition

Representative compositions were developed for the 631 as-received waste streams and 203 leached waste stream batches (Section 2.0). These mass fraction data are used to calculate the volume fraction for each component based on the individual and composite component density. For each batch, the composite density, shown in Eq. (A.13), is calculated from the component density and mass fraction. Eq. (A.14) is used to determine component volume fraction.

$$\rho_{sb} = \sum_{i=1}^{15} \frac{1}{\left(\frac{w_i}{\rho_i}\right)} \quad \text{(A.13)}$$

$$\emptyset_i = w_i \left(\frac{\rho_{sb}}{\rho_i}\right) \quad \text{(A.14)}$$

where

ρ_{sb} = composite density (g/cm^3)
ρ_i = component density (g/cm^3)
w_i = component mass fraction
$\emptyset_i$ = component volume fraction.

A.6.10 PSDD and Process Metric Calculations

The waste stream batch PSDDs, three-dimensional matrices of the volume probability for each particle size and density pair, are created by multiplying the volume-based PSD probabilities by the component volume fractions (Section A.6.9), which yields the probability of that component particle size in the composite. This results in the volume-weighted simulant PSD, and is described by

$$\emptyset_{Si} = \emptyset_i(\emptyset_{PSDi}) \tag{A.15}$$

where

$\emptyset_{Si}$ = volume fraction for the simulant component PSD
$\emptyset_{PSDi}$ = volume fraction for the component PSD data point.

The combination of this probability with the component density generates the PSDDs for each batch.

The eight metrics listed in Table A.34 are calculated using each batch's PSDD as described in Section A.6.1, and represent a set of process-performance evaluation metrics. The resulting metric calculation results and the corresponding batch PSDD volume fraction are sorted in ascending order to create a cumulative distribution of each metric result for every batch. The percentile results for each metric of the as-received and leached waste stream batches can thus be determined.

A.6.11 Process Metric Results

The compiled percentile data can be used to identify and examine adverse conditions. One method is to consider a specific percentile, and the percentile range of the values at that percentile. A reasonable adverse condition of the metric distributions was selected as the 80th percentiles of each of the 631 as-received waste streams and 203 leached waste streams for the eight metrics. Further, by batch count, probability ranges of the results can be considered at this percentile. The 80th to 100th percentile values of the 80th percentile metric results were considered.

The basis for selecting the 80th percentile as the specific percentile is as follows. In addition to the 80th percentile being an indication of adverse conditions (80% of the calculated results are slower settling, have lower critical stress for erosion, etc.), it was observed that single process batches that were adverse at the 90th percentile were not typically adverse over the entire distribution. This observation is illustrated in Figure A.15 for the settling velocity of as-received waste batches. The abscissa is the calculated settling velocity, and the ordinate is the cumulative volume distribution of the PSDD-based calculated results. The green, blue, and red large symbol lines represent the minimum, median, and maximum metric result at the given percentile, respectively, over the 631 as-received waste stream batches. A selection of 20 different as-received batches representing the 80th to 100th percentile values of the 90th percentile metric results are shown, denoted by the batch number as well as the bulk average solid density. The batches represent more-adverse conditions (maximum metric results) at the 90th percentile

(the batches essentially coincide with the maximum result), but are more representative of the median metric results at the 70th and 80th percentiles (the batches essentially coincide with the median result). In contrast, a selection of 20 different as-received batches representing the 80th to 100th percentile values of the 80th percentile metric results is shown in Figure A.16. The batches are now shown to be more adverse over the entire distribution (the batches are close to the maximum result over the entire distribution).

Given that the suite of process-performance metrics represents various aspects of the system, it is most desirable to have the selected adverse condition be the most adverse for all or a majority of the metrics. Further, the SHSVD will process both as-received and leached waste streams. Therefore, a representative adverse batch is determined from the metric calculation results for both process streams for all eight metrics. Out of the 631 as-received and 203 leached evaluated batches, 20 batches each were selected that have at least five concurrent metric results (the batches had results in the 80th to 100th percentile values of the 80th percentile metric results for at least five of the eight metrics).

Figure A.17 through Figure A.24 show the cumulative percentile distributions of 20 batches in the 80th to 100th percentile values of the 80th percentile metric results with at least five concurrent metrics for each calculated metric. Also shown are the minimum, median, and maximum as-received and minimum and maximum leached results. At the 80th percentile, the as-received waste batches are generally more adverse or equal to the leached batches, so the 20 shown batches are as-received waste. Batch 108, the 108th of the 631 as-received waste stream batches (denoted by the large red symbols in Figure A.17 through Figure A.24), is selected for the representative adverse waste composition for both the as-received and leached waste streams based on the individual particle performance as calculated from the general performance metrics. Recall, as previously specified, it is the comparison of the model results for the particulates that is of significance, not the specific model results.

A.6.12 Process Metric Conclusion

The yellow symbol line shown in Figure A.17 through Figure A.24 denotes the calculated metric results for the HLW Feeds Basis of Design (Reid 2014). Batch 108, shown as comparable to the basis of design waste, meets the WAC specification for particle size and is therefore the selected representative SHSVD Newtonian waste solids simulant performance target based on the general metrics for particle mobilization, suspension, settling, and pipeline transfer.

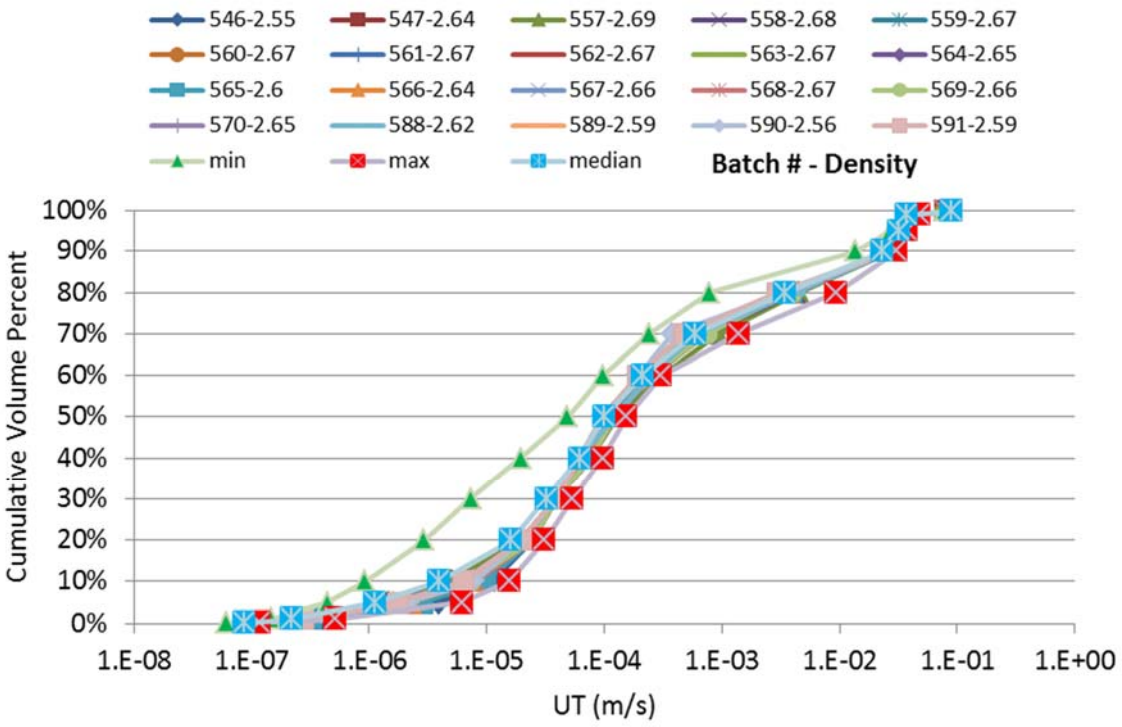

Figure A.15. Selected 80th to 100th percentile of the 90th percentile U_T batch results.

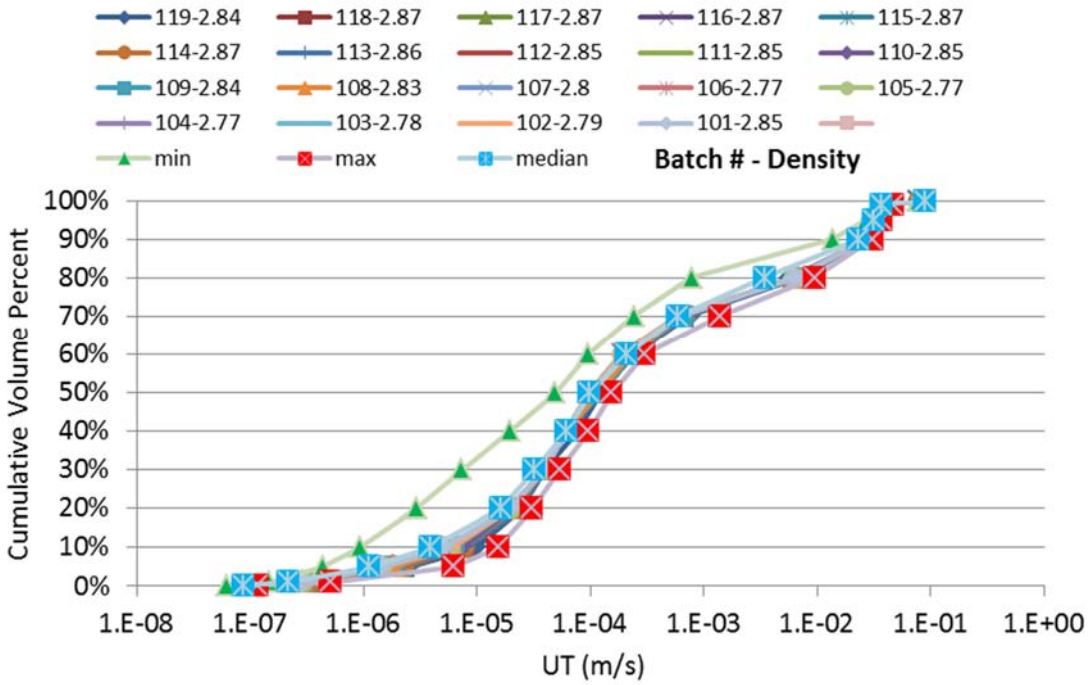

Figure A.16. Selected 80th to 100th percentile of the 80th percentile U_T batch results.

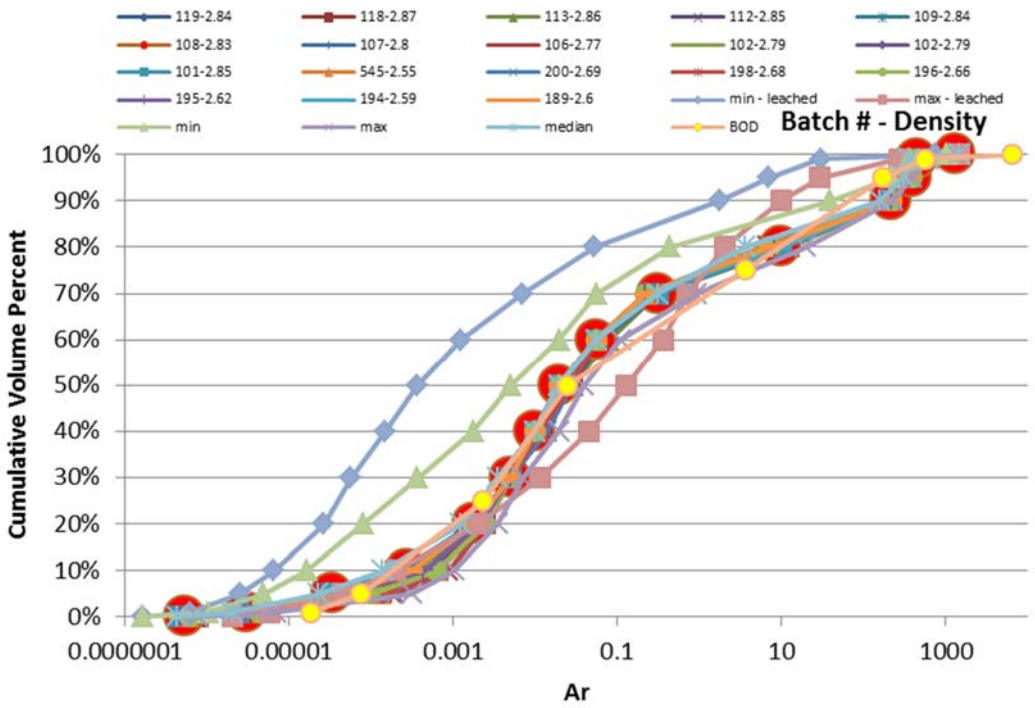

Figure A.17. Selected 80th to 100th percentile of the 80th percentile Ar batch results.

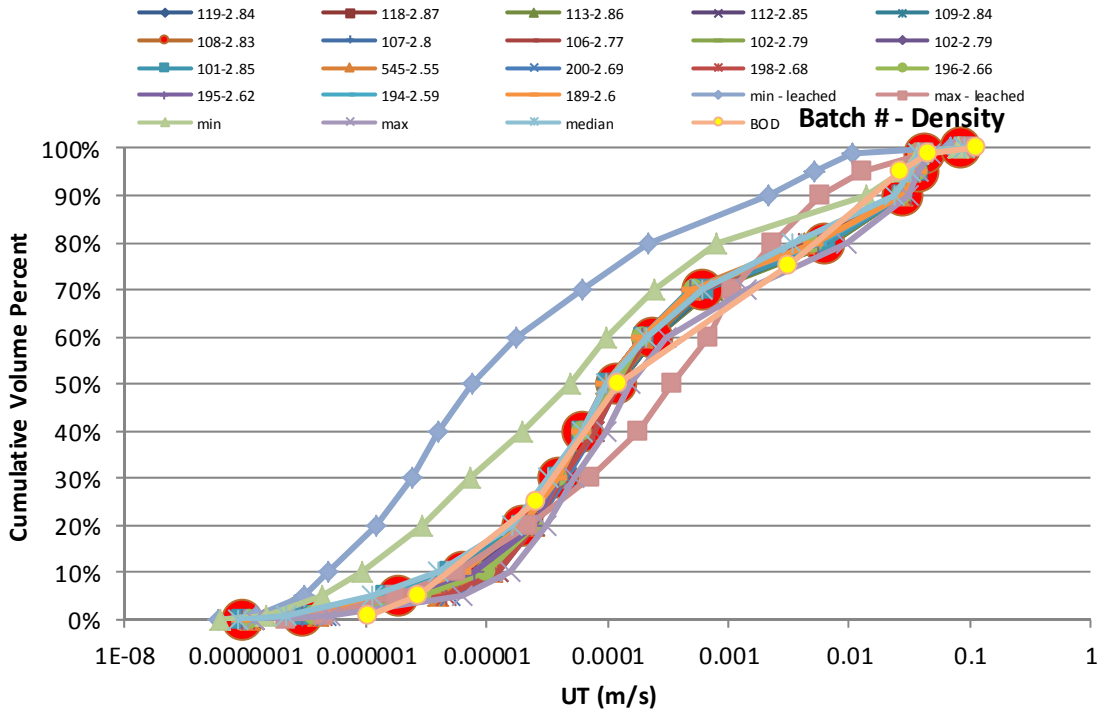

Figure A.18. Selected 80th to 100th percentile of the 80th percentile U_T batch results.

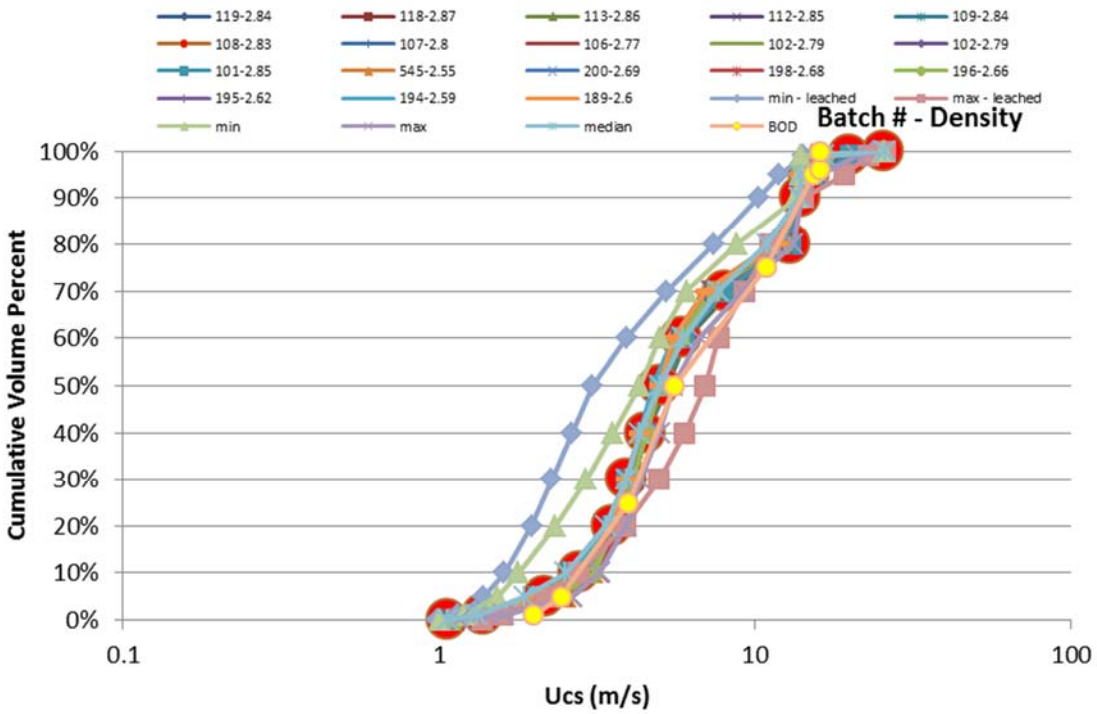

Figure A.19. Selected 80th to 100th percentile of the 80th percentile U_{CS} batch results.

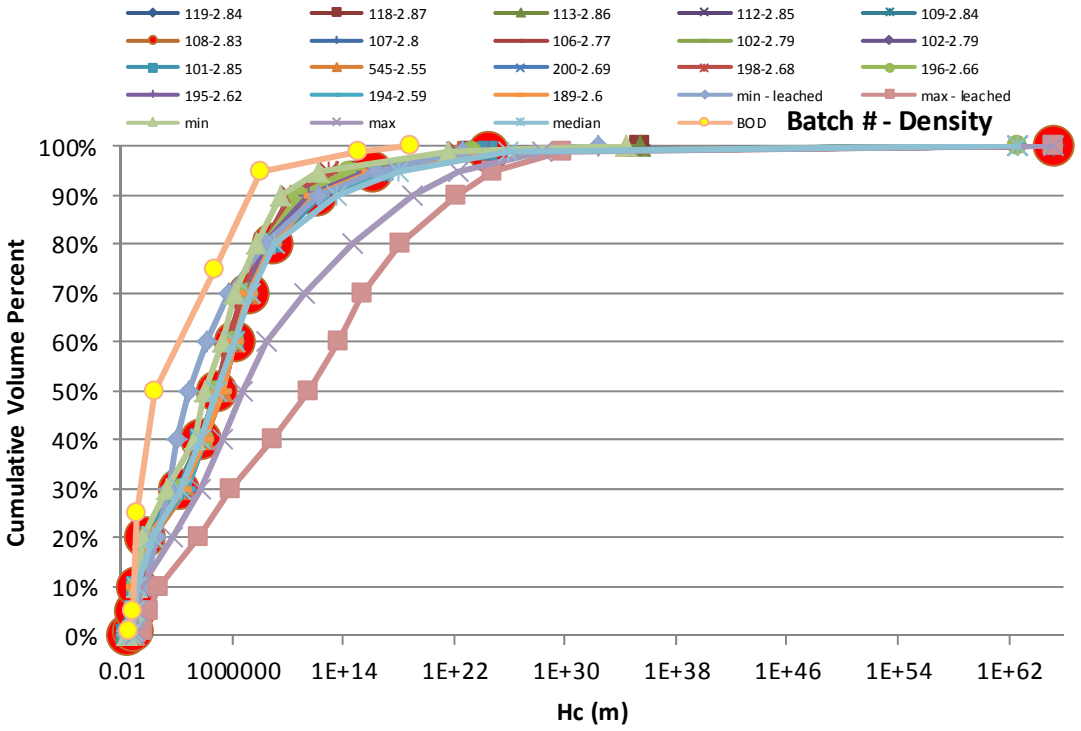

Figure A.20. Selected 80th to 100th percentile of the 80th percentile H_c batch results.

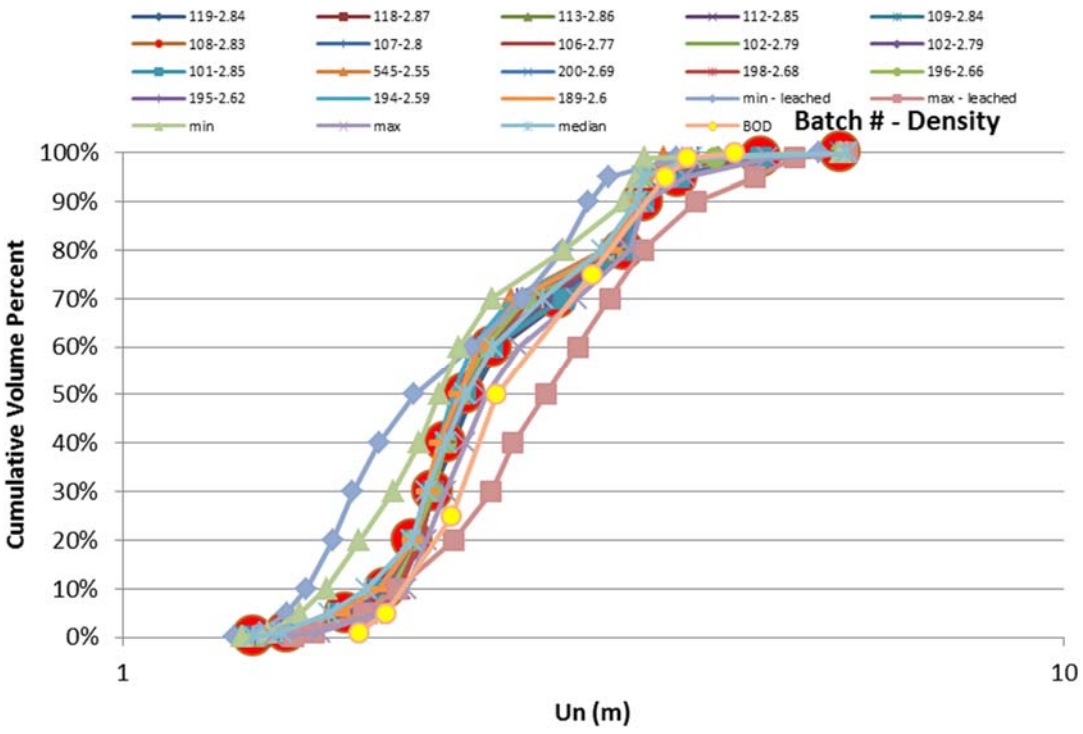

Figure A.21. Selected 80th to 100th percentile of the 80th percentile U_n batch results.

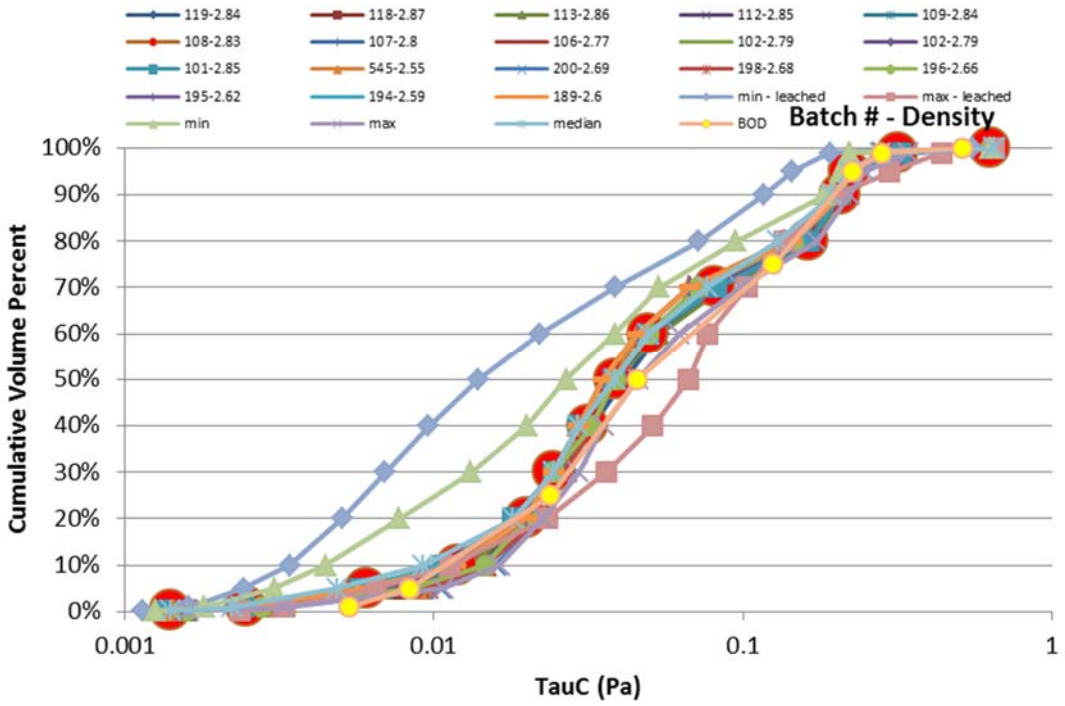

Figure A.22. Selected 80th to 100th percentile of the 80th percentile τ_c batch results.

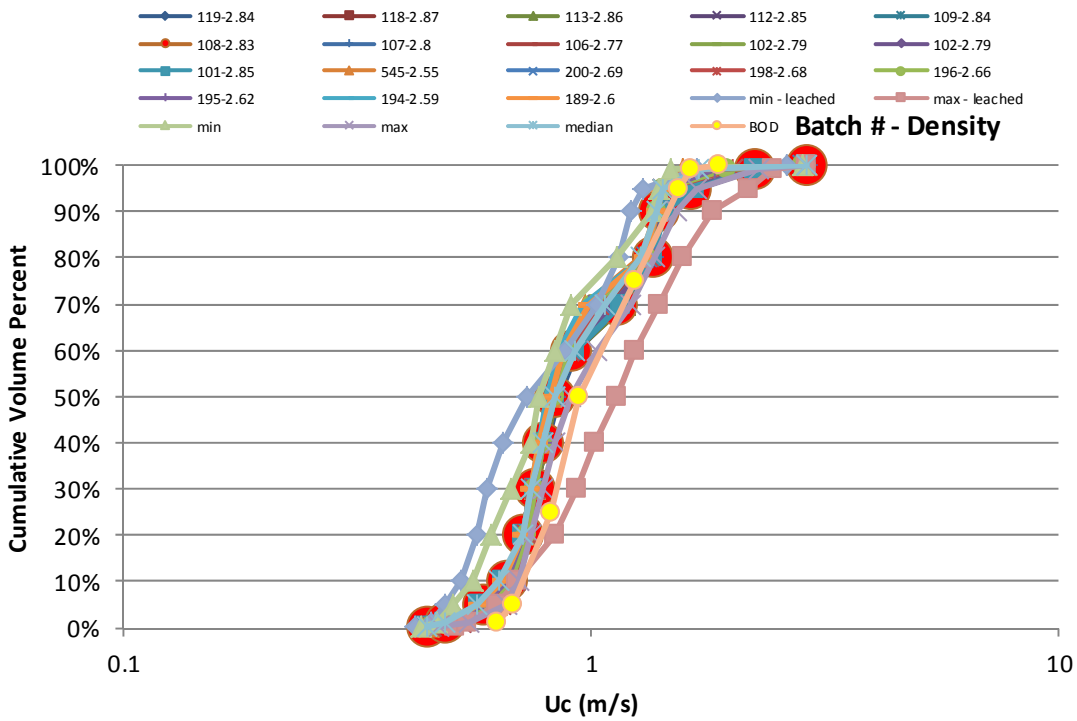

Figure A.23. Selected 80th to 100th percentile of the 80th percentile U_c batch results.

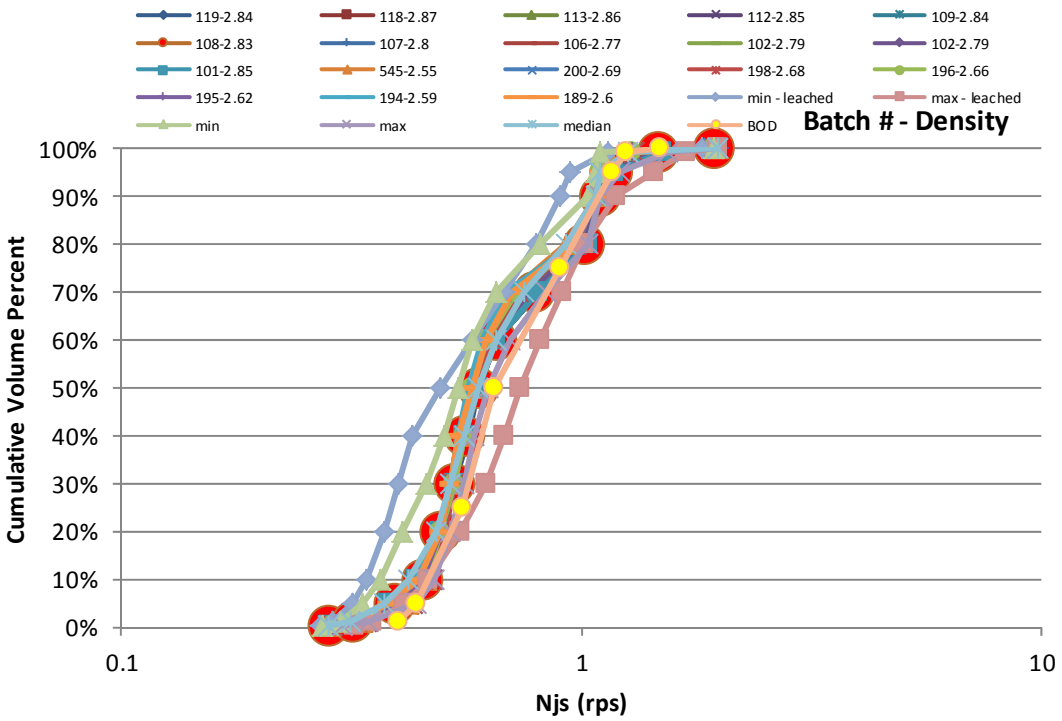

Figure A.24. Selected 80th to 100th percentile of the 80th percentile N_{js} batch results.

A.7 Selection of Particle Size Distributions; Details for Section A.4

This section provides the details of the PSD selection process as referenced in Section A.4. Table A.36 provides a high-level summary of source elemental data used to downselect PSDs for each component. Use of PSD data to represent a given element is only considered when the waste contains a significant fraction of that element. The threshold values for delineating which wastes contain a "significant" fraction of a given element are listed in Table A.37. The specific threshold for each element is selected to limit the number of input PSDs for each element to 10 or less.

Table A.36. High-level summary of historical particle size distributions and significant phases (expressed in terms of weight percent element). Summary indicates if PSDs are available (marked with an "X") for unleached (UL), caustic-leached (CL), and oxidatively leached (OL) wastes. Elements are listed when significant (see Table A.37).

		PSDs Available			
Source Report	Tank or Waste Type	UL	CL	OL	Significant Element(s) [max wt%]
Lumetta and Rapko 1994	B-201	X	X	--	Bi [23%]
	U-110	X	X	--	--
Rapko et al. 1995	B-111	X	X	--	--
	BX-107	X	X	--	Bi [35%]
	C-103	X	X	--	--
	S-104	X	X	--	Al [33%]
	SY-103	X	X	--	Cr [22%]
	T-104	X	X	--	--
	T-111	X	X	--	Mn [9.6%]
Lumetta et al. 1996a	S-107	X	X	--	Zr [8.2%]
	C-107	X	X	--	Fe [31.8%]
	BY-104	X	X	--	Cr [11.2%], Sr [2.6%]
	BY110	X	X	--	Ca [9%], Ni [4.4%], Sr [3.6%]
	SX-108	X	X	--	--
Lumetta et al. 1997	AN-104	X	X	--	Cr [10.3%]
	BY-108	X	X	--	Ca [5.1%], Sr [3.6%], U [19.6%]
	S-101	X	X	--	U [16.8%]
	S-104	--	--	--	Sr [1.6%], U [25.4%]
	S-111	--	X	--	--
PNNL-12010	S-107	X	X	--	Al [31.5%]
Brooks et al. 2000a	AZ-102	X	X	--	--
Brooks et al. 1999	AW-101	X	--	--	--
Brooks et al. 2000b	C-104	X	X	--	Th [11.3%], Zr [11.2%]
Rapko and Wagner 1997	AZ-101/102	X	X	--	Fe [29.1%]
Lumetta et al. 2000	C-104	--	--	--	Th [11.7%], Zr [10.3%]
Urie et al. 2004	AZ-101	X	--	--	--
Geeting et al. 2003	AZ-101	X	X	--	Zr [6.6%]

Source Report	Tank or Waste Type	PSDs Available			Significant Element(s) [max wt%]
		UL	CL	OL	
Bell 2001	AZ-101	X	--	--	Zr [8.8%]
Buck et al. 2003	AN-102	X	--	--	--
WTP-RPT-027	AN-102	--	--	--	--
PNL-10099	B-111	X	--	--	--
PNL-10101	T-102	X	--	--	--
Scheele et al. 1994	C-109	X	--	--	--
	C-112	X	--	--	U [17%]
Lumetta et al. 1996b	C-106	X	X	--	Si [8.7%]
PNL-7758	AZ-101	X	--	--	--
Temer and Villarreal 1995	T-104	X	X	--	Bi [20.4%]
	T-107	X	X	--	--
	B-202	X	X	--	Bi [52.4%], Mn [10.1%]
	S-104	X	X	--	Al [32.9%]
	BX-105	X	X	--	Al [30.5%]
	C-108	X	X	--	Ca [12.2%], Ni [12.5%]
Coleman et al. 2004	AY-102/C-106	X	--	--	--
Hallen et al. 2003	AN-102/ C-104	--	--	X	Mn (Pr.) [6.7%], Sr (Pr.) [9.7%]
Fiskum et al. 2008	REDOX Sludge	X	X	--	Al [38.8%], Sr (Pr.) [1.5%], U [28.7%]
	S-Saltcake	X	X	X	Cr [16.8%], Mn (Pr.) [21.4%]
Shimskey et al. 2009	REDOX Sludge	X	X	--	--
	REDOX/ S-Saltcake	--	--	X	Mn (Pr.) [3.4%]
Fiskum et al. 2009b	REDOX/ S-Saltcake	X	X	X	Al [31.3%], Mn (Pr.) [5.2%]
Lumetta et al. 2009	$BiPO_4$ Sludge	X	X	--	Bi [31.5%], Fe [30.4%]
	$BiPO_4$ Sludge	X	X	--	Si [9.2%], Sr [1.7%]
	$BiPO_4$ Sludge/Saltcake	X	X	X	Mn (Pr.) [1.5%], Si [10.2%]
Snow et al. 2009	PUREX Cladding	X	X	--	U [21.3%], Zr [14.4%]
	REDOX Cladding	X	--	--	Al [33%], Mn [9.7%], U [15.1%]
Edwards et al. 2009	TBP Wastes	X	X	--	Fe [33.1%], U [21.8%]
Fiskum et al. 2009a	FeCN Sludge	X	X	--	Ca [7.9%], Ni [4.6%], Sr [5.4%]

Table A.37. Element significance threshold and number of candidates identified during evaluation of reports listed in Table A.36.

Element	Threshold, wt%	Number of Candidates
Al	30	8
Bi	20	6
Ca	5	5
Cr	5	5
Fe	25	4
Mn	7	3
Ni	4	3
prec Mn	1	6
Si	8	6
Sr	1	8
prec Sr	1	2
Th	5	3
U	15	8
Zr	5	9

The downselection process limits the number of size distributions that will represent each component. However, the downselected data can still provide multiple size distribution measurements, including replicate measurements, measurements of materials with similar chemical treatments, and multiple wastes with similar component enrichment. The next step in selecting component PSDs was to further downselect and average size distributions measurements[1] to (1) provide component-specific PSDs that represent the size distribution of that component in the Hanford tank farms and (2) provide a solid that is challenging with respect to mobilization by planned WTP mixing systems (e.g., PJMs). With respect to the former, the source PSD data for each component and mineral are selected by considering only wastes enriched in that component (relative to other Hanford wastes). The latter (i.e., selection of PSDs that are challenging to mix) is accomplished by selecting size distribution measurements showing larger (in terms of size) particles over those indicating small particles.

Overall, the method for selecting PSDs for each mineral phase can be summarized as follows:

1. The first round of PSDs selected is based on the composition data in Table A.36. For the PSDs to be considered, the corresponding composition of the target component (e.g., Al) must be large relative to other tank waste samples. For major tank components (namely Al and Fe), the concentration of a given element in the selected PSD samples may be up to 50%. For minor components (e.g., Th), the concentration may be 5% or less. Selection is also subject to the availability of PSD and chemical speciation information.
2. For each target element (e.g., Al or Bi), criterion 1 provides a set of one or more component PSD measurements. In all cases, the source PSD is taken from existing raw measurement data files or measurement data (either graphical or tabular) reported in the Hanford tank waste physical properties literature. When only one PSD is available, it becomes the PSD for the target component. When there is more than one PSD, the PSDs are passed through a second downselection process to obtain

[1] As is described in the Section 3.0 of report, downselection can lead to multiple size distributions from the same target element. In many cases, the PSDs in the final set were averaged rather than simply selecting the most conservative (i.e., largest) PSD. Averaging serves to moderate some of the conservatism of the method and attempts to limit the impact of an anomalous size measurement on the simulant selection process. That said, averaging is done on a volume contribution basis, such that the final PSD will include anomalous particle populations, but at a reduced fractional contribution relative to the original anomalous measurement.

one or more conservatively large PSDs from that subset and further processed to produce one representative, but conservatively large, PSD for the target component. The PSD downselection process is discussed in criterion 3. The PSD analysis strategy is discussed in criterion 4.

3. Multiple samples could be considered for inclusion in the representative PSD. PSDs for replicate measurements on the same sample were typically included. Likewise, PSDs for samples derived from the same source material and subject to similar processing (e.g., two samples generated by splitting as-received waste and both subject to caustic leaching and washing) were also typically included. For individual sample measurements, non-flow PSDs were preferred, as these typically yield the largest PSDs (Wells et al. 2011). However, non-flow PSD measurements were not always available. Thus, PSD measurements selected for inclusion include both flow and non-flow conditions, with an emphasis on finding the largest available PSD. Likewise, PSD data for sonicated samples were excluded where both sonicated and non-sonicated measurements were made. For PSD data run under multiple measuring conditions (e.g., at different flow rates), the two PSDs exhibiting large populations of large particles are preferentially selected for inclusion in criterion 4 analysis. Individual PSD measurements may be excluded if evaluation of the result indicates significant impact from laser alignment, sticking of particles to the windows, solid dissolution, or agglomeration (in order of decreasing significance for exclusion).
4. When multiple PSDs are downselected for components, a single, representative PSD is created by averaging or resampling (both of which produce similar results).

A.8 References

Andresen, A. 1958. "The Structure of U3O8 Determined by Neutron Diffraction." *Acta Crystallographica* 11:612-14.

Baldwin, DL, JA Campbell, SK Fiskum, GM Mong, RD Scheele, MR Smith, RG Swoboda, MW Urie, PR Bredt, OT Farmer, LR Greenwood, AP Poloski, CZ Soderquist, LA Snow, MP Thomas, and JJ Wagner. 2003. *Chemical Analysis and Physical Property Testing of 241-AP-104 Tank Waste*. PNWD-3334; WTP-RPT-069, Battelle, Pacific Northwest Division, Richland, Washington.

Bell, KE. 2001. *Tank 241-AZ-101 Grab Samples from Mixer Pump Test Events 5, 7, 8, and 9 Analytical Results for the Final Results for the Report*. HNF-6062, Fluor Hanford, Richland, Washington.

BNI. 2011. *Basis of Design*. 24590-WTP-DB-ENG-01-001, Rev. 1Q, Bechtel National, Inc., Richland, Washington.

BNI. 2014. *ICD-19 – Interface Control Document for Waste Feed*. 24590-WTP-ICD-MG-01-019, Rev. 7, Bechtel National, Inc., Richland, Washington.

Boldt, K, B Engelen, M Panthöfer, and K Unterderweide. 2000. "Stereochemical Equivalence of PIII-Bonded Hydrogen Atoms and |SeIV Lone Electron Pairs in Sr(H2PO3)2 and Sr(HSeO3)2." *European Journal of Inorganic Chemistry* 2000(9):2071-75. doi:10.1002/1099-0682(200009)2000:9<2071::AID-EJIC2071>3.0.CO;2-O.

Brooks, KP, PR Bredt, GR Golcar, SA Hartley, LK Jagoda, KG Rappe, and MW Urie. 2000b. *Characterization, Washing, Leaching and Filtration of C-104 Sludge*. BNFL-RPT-030; PNWD-3024, Battelle, Pacific Northwest Division, Richland, Washington.

Brooks, KP, PR Bredt, GR Golcar, SA Hartley, MW Urie, JM Tingey, KG Rappe, and LK Jagoda. 1999. *Ultrafiltration and Characterization of AW-101 Supernatant and Entrained Solids*. PNWD-3000; BNFL-RPT-002, Battelle, Pacific Northwest Division, Richland, Washington.

Brooks, KP, PR Bredt, SK Cooley, GR Golcar, LK Jagoda, KG Rappe, and MW Urie. 2000a. *Characterization, Washing, Leaching, and Filtration of AZ-102 Sludge*. PNWD-3045 (BNFL-RPT-038 Rev. 0), Battelle, Pacific Northwest Division, Richland, Washington.

Buck, EC, BW Arey, SK Fiskum, JGH Geeting, ED Jenson, BK McNamara, and AP Poloski. 2003. *Identification of Washed Solids from Hanford Tanks 241-AN-102 and 241-AZ-101 with X-Ray Diffraction, Scanning Electron Microscopy, and Light-Scattering Partcle Analysis*. PNWD-3300; WTP-RPT-076, Battelle, Pacific Northwest Division, Richland, Washington.

Burns, PC, and Y-P Li. 2002. "The Structures of Becquerelite and Sr-Exchanged Becquerelite." *American Mineralogist* 87:550-57.

Camenen, B. 2007. "Simple and General Formula for the Settling Velocity of Particles." *Journal of Hydraulic Engineering* 133(2):229-233.

Cantrell, KJ, KM Krupka, KN Geiszler, BW Arey, and HT Schaef. 2010. *Hanford Site Tank 241-C-108 Residual Waste Contaminant Release Models and Supporting Data*. PNNL-19425, Pacific Northwest National Laboratory, Richland, Washington.

Cantrell, KJ, KM Krupka, KN Geiszler, MJ Lindberg, BW Arey, and HT Schaef. 2008. *Hanford Tank 241-S-112 Residual Waste Composition and Leach Test Data*. PNNL-17593, Pacific Northwest National Laboratory, Richland, Washington.

Carlson, AB, PJ Certa, TM Hohl, JR Bellomy III, TW Crawford, DC Hedengren, AM Templeton, HS Fisher, SJ Greenwood, DG Douglas, and WJ Ulbright Jr. 2001. *Test Report, 241-AZ-101 Mixer Pump Test*. RPP-6548, Rev. 1, Numatec Hanford Corporation, Richland, Washington.

Chien, N and ZH Wan. 1983. *Mechanics of Sediment Movement*. Science Publications, Beijing (in Chinese).

Coleman, C, MS Hay, and KB Martin. 2004. *Compositing and Characterization of Samples from Hanford Tank 241-AY-102/C-106*. WSRC-TR-2003-00205, SRT-RPP-2003-00086, Westinghouse Savannah River Company, Aiken, South Carolina.

Cramer SD and BS Covino, Jr. 2003. *ASM Handbook, Volume 13A - Corrosion: Fundamentals, Testing, and Protection*. ASM International, Materials Park, Ohio. Online version available at: http://app.knovel.com/hotlink/toc/id:kpASMHVAC8/asm-handbook-volume-13a/asm-handbook-volume-13a).

CRC Handbook of Chemistry and Physics, 61st Edition. 1980. CRC Press, Inc., Boca Raton, Florida.

CRC Handbook of Chemistry and Physics, 62nd Edition. 1979. CRC Press, Inc., Boca Raton, Florida.

CRC Handbook of Chemistry and Physics, 92nd Edition. 2011. CRC Press, Inc., Boca Raton, Florida.

Cuta, JM, KG Carothers, DW Damschen, WL Kuhn, JA Lechelt, K Sathyanarayana, and LA Stauffer. 2000. *Review of Waste Retrieval Sluicing System Operations and Data for Tanks 241-C-016 and 241-AY-102*. PNNL-13319, Pacific Northwest National Laboratory, Richland, Washington.

Edwards, MK, JM Billing, DL Blanchard, Jr, EC Buck, AJ Casella, AM Casella, JV Crum, RC Daniel, KE Draper, SK Fiskum, LK Jagoda, ED Jenson, AE Kozelisky, PJ MacFarlan, RA Peterson, RW Shimskey, LA Snow, and RG Swoboda. 2009. *Characterization, Leaching, and Filtration Testing for Tributyl Phosphate (TBP, Group 7) Actual Waste Sample Composites.* PNNL-18119, WTP-RPT-169 Rev. 0, Pacific Northwest National Laboratory, Richland, Washington.

Finch, R, and R Ewing. 1997. "Clarkeite: New Chemical and Structural Data." *American Mineralogist* 82:607-19.

Fiskum, SK, EC Buck, RC Daniel, KE Draper, MK Edwards, TL Hubler, LK Jagoda, ED Jenson, AE Kozelisky, GJ Lumetta, PJ MacFarlan, BK McNamara, RA Peterson, SI Sinkov, LA Snow, and RG Swoboda. 2008. *Characterization and Leach Testing for REDOX Sludge and S-Saltcake Actual Waste Sample Composite.* PNNL-17368, WTP-RPT-157 Rev. 0, Pacific Northwest National Laboratory, Richland, Washington.

Fiskum, SK, JM Billing, EC Buck, RC Daniel, KE Draper, MK Edwards, ED Jenson, AE Kozelisky, PJ MacFarlan, RA Peterson, RW Shimskey, and LA Snow. 2009b. *Laboratory Demonstration of the Pretreatment Process with Caustic and Oxidative Leaching Using Actual Hanford Tank Waste*. PNNL-18007; WTP-RPT-171, Pacific Northwest National Laboratory, Richland, Washington.

Fiskum, SK, JM Billing, JV Crum, RC Daniel, MK Edwards, RW Shimskey, RA Peterson, PJ MacFarlan, EC Buck, KE Draper, and AE Kozelisky. 2009a. *Characterization, Leaching, and Filtrations Testing of Ferrocyanide Tank Sludge (Group 8) Actual Waste Composite*. PNNL-18120, WTP-RPT-170, Pacific Northwest National Laboratory, Richland, Washington.

Fort, JA, PA Meyer, JA Bamberger, CW Enderlin, PA Scott, MJ Minette, and PA Gauglitz. 2010. *Scaled Testing to Evaluate Pulse Jet Mixer Performance in Waste Treatment Plant Mixing Vessels*. 10487, WM2010 Conference, March 7-10, 2010, Phoenix, Arizona.

Gangolli, S. 2005. *Dictionary of Substances and Their Effects* (DOSE, 3rd Electronic Edition). Royal Society of Chemistry. Online version available at: http://app.knovel.com/hotlink/toc/id:kpDSTEDOS3/dictionary-substances/dictionary-substances.

Gasperin. 1986. "Synthese et Structure d'un Monocristal." *Journal of the Less-Common Metals* 119:83-90.

Geeting, JGH, RT Hallen, LK Jagoda, AP Poloski, RD Scheele, and DR Weier. 2003. *Filtration, Washing, and Caustic Leaching of Hanford Tank AZ-101 Sludge*. PNWD-3206, Rev. 1, WTP-RPT-043, Rev. 1, Battelle, Pacific Northwest Division, Richland, Washington.

Gorbunova, YE, SA Linde, AV Lavrov, and AB Pobedina. 1980. "Synthesis and Structure of Na6-x(UO2)3(HxPO4)(PO4)3 (x=0.5)." *Doklady Akademii Nauk SSSR* 251:385-89.

Hallen, RT, JGH Geeting, DR Jackson, and DR Weier. 2003. *Combined Entrained Solids and Sr/TRU Removal from AN-102 Waste Blended with C-104 Sludge Pretreatment Solutions*. PNWD-3264, Rev. 1, WTP-RPT-044, Rev. 1, Battelle, Pacific Northwest Division, Richland, Washington.

Handbook of Hydrothermal Technology, 2nd Edition, K Byrappa, M Yoshimura, Elsevier, 2013. Waltham, Massachusetts (p. 270).

Hill, JG, and BC Simpson. 1994. *The Sort on Radioactive Waste Type model: A method to sort single-shell tanks into characteristic groups*. PNL-9814; Pacific Northwest Laboratory, Richland, Washington.

Jenkins, K, Y Deng, and S Orcutt. 2013. *2012 WTP Tank Utilization Assessment*. 24590-WTP-RPT-PE-12-001, Bechtel National, Inc., Richland, Washington.

Jewett, JR, SD Estey, L Jensen, NW Kirch, DA Reynolds, and Y Onishi. 2002. *Values of Particle Size, Particle Density, and Slurry Viscosity to Use in Waste Feed Delivery Transfer System Analysis*. RPP-9805, Numatec Hanford Corporation, Richland, Washington.

Jones, EO, NG Colton, GR Bloom, GS Barney, SA Colby, and RG Cowan. 1992. "Pretreatment Process Testing of Hanford Tank Waste for the US Department of Energy's Underground Storage Tank Integrated Demonstration." *Proceedings of the International Topical Meeting on Nuclear and Harzardous Waste Managemnt Spectrum '92*, American Nuclear Society, Inc., La Grange Park, Illinois.

Kale, RN and AW Patwardhan. 2005. "Solid Suspension in Jet Mixers." *The Canadian Journal of Chemical Engineering* 83(5):816-828.

Khosrawan-Sazedj, F. 1982. "On the Space Group of Threadgoldite." *Tschermarks Mineralogische und Petrographische Mitteilungen* 30(2):111-15.

Kovba, LM, EA Ippolitova, YP Simanov, and VI Spitsyn. 1958. "An X-ray Study of Alkali Metal Uranates." *Doklady Akademii Nauk SSSR* 120(5):1042-44.

Lee, KP, BE Wells, PA Gauglitz, and RA Sexton. 2012. *Waste Feed Delivery Mixing and Sampling Program Simulant Definition for Tank Farm Performance Testing*. RPP-PLAN-51625, Rev. 0, Washington River Protection Solutions, LLC, Richland, Washington.

Loopstra, B. 1977. "On the crystal structure of alpha-U3O8." *On the Crystal Structure of alpha-U3O8* 39:75-85.

Lumetta, GJ, and BM Rapko. 1994. *Washing and Alkaline Leaching of Hanford Tank Sludges: A Status Report*. PNL-10078, Pacific Northwest National Laboratory, Richland, Washington.

Lumetta, GJ, BM Rapko, MJ Wagner, J Liu, and YL Chen. 1996a. *Washing and Caustic Leaching of Hanford Tank Sludges: Results of FY 1996 Studies*. PNNL-11278 Rev. 1, Pacific Northwest National Laboratory, Richland, Washington.

Lumetta, GJ, DJ Bates, JP Bramson, LP Darnell, OTF III, SK Fiskum, LR Greenwood, FV Hoopes, CZ Soderquist, MJ Steele, RT Steele, MW Urie, and JJ Wagner. 2000. *C-104 High-Level Waste Solids: Washing/Leaching and Solubility versus Temperature Studies*. PNWD-3027; BNFL-RPT-021, Battelle, Pacific Northwest Division, Richland, Washington.

Lumetta, GJ, EC Buck, RC Daniel, K Draper, MK Edwards, SK Fiskum, RT Hallen, LK Jagoda, ED Jenson, AE Kozelisky, PJ MacFarlan, RA Peterson, RW Shimskey, SI Sinkov, and LA Snow. 2009. *Characterization, Leaching, and Filtration Testing for Bismuth Phosphate Sludge (Group 1) and Bismuth Phosphate Saltcake (Group 2) Actual Waste Sample Composites.* PNNL-17992, WTP-RPT-166 Rev. 0, Pacific Northwest National Laboratory, Richland, Washington.

Lumetta, GJ, IE Burgeson, MJ Wagner, J iu, and YL Chen. 1997. *Washing and Caustic Leaching of Hanford Tank Sludge: Results of FY 1997 Studies*. PNNL-11636, Pacific Northwest National Laboratory, Richland, Washington.

Lumetta, GJ, MJ Wagner, FV Hoopes, and RT Steele. 1996b. *Washing and Caustic Leaching of Hanford Tank C-106 Sludge*. PNNL-11381, Pacific Northwest National Laboratory, Richland, Washington.

Mauss, J. 2010. *Determination of Mixing Requirements for Pulse-Jet-Mixed Vessels in the Waste Treatment Plant*. 24590-WTP-ES-ENG-09-001, Rev. 2, Bechtel National, Inc., Richland, Washington.

McCabe, WL and JC Smith. 1976. *Unit Operations of Chemical Engineering*. ISBN 0-07-044825-6. McGraw-Hill, Inc., New York.

Meyer, PA, JA Bamberger, CW Enderlin, JA Fort, BE Wells, SK Sundaram, PA Scott, MJ Minette, GL Smith, CA Burns, MS Greenwood, GP Morgen, EBK Baer, SF Snyder, M White, GF Piepel, BG Amidan, A Heredia-Langner. 2012. *Pulse Jet Mixing tests with Noncohesive Solids*. PNNL-18098, Rev. 1, WTP-RPT-182, Rev. 1, Pacific Northwest National Laboratory, Richland, Washington.

Misra, C. 2000. "Aluminum Oxide (Alumina), Hydrated." In *Kirk-Othmer Encyclopedia of Chemical Technology*. John Wiley & Sons, Inc., Hoboken, New Jersey.

Momin, A, V Jakkal, and M Karkhanavala. 1974. "Low Temperature X-ray Diffraction Studies on U3O8." *Indian Journal of Chemistry* 12:752-53.

Onishi, Y, R Shekarriz, and KP Recknagle. 1996. *Tank SY-102 Waste Retrieval Assessment: Rheological Measurements and Pump Jet Mixing Simulations*. PNNL-11352, Pacific Northwest National Laboratory, Richland, Washington.

Oroskar, AR and RM Turian. 1980. "The Critical Velocity in Pipeline Flow of Slurries." *AIChE Journal* 26(4):550 - 558.

Pagoaga, MK, DE Appleman, and JM Stewart. 1987. "Crystal Structures and Crystal Chemistry of the Uranyl Oxide Hydrates Becquerelite, Billietite, and Protasite." *American Mineralogist* 72:1230-38.

Paphitis, D. 2001. "Sediment Movement Under Unidirectional Flows: An Assessment of Empirical Threshold Curves." *Coastal Engineering* 43:227 - 245.

Paul, EL, VA Atiemo-Obeng, and SM Kresta. 2004. *Handbook of Industrial Mixing Science and Practice*. John Wiley & Sons, Inc., Hoboken, New Jersey.

Piret, P, J Declecq, and D Wauters-Stoop. 1979. "Structure of Threadgoldite." *Acta Crystallographica B* 35:3017-20.

Piret-Meunier, J, and P Piret. 1982. "Nouvelle Determination de la Structure Cristalline del la Becquerelite." *Bulletin de Mineralogie* 105:606-10.

Poirier, MR and CJ Martino. 2015. *Properties Important to Mixing and Simulant Recommendations for WTP Full-Scale Vessel Testing*. Pre-Decisional, Deliberative Process Information SRNL-STI-2015-00301, Rev. I, Savannah River National Laboratory, Savannah River Nuclear Solutions, LLC, Aiken, South Carolina.

Poloski, AP, PA Meyer, LK Jagoda, and PR Hrma. 2004. *Non-Newtonian Slurry Simulant Development and Selection for Pulse Jet Mixer Testing.* PNWD-3495, WTP-RPT-111 Rev. 0, Battelle-Pacific Northwest National Division, Richland, Washington.

Rapko, BM, and JD Vienna. 2002. *Selective Leaching of Chromium from Hanford Tank Sludge 241-U-108*. PNNL-14019, Pacific Northwest National Laboratory, Richland, Washington.

Rapko, BM, and MJ Wagner. 1997. *Caustic Leaching of Composite AZ-101/AZ-102 Hanford Tank Sludge*. PNNL-11580, Pacific Northwest National Laboratory, Richland, Washington.

Rapko, BM, DL Blanchard, NG Colton, AR Felmy, J Liu, and GJ Lumetta. 1996. *The Chemistry of Sludge Washing and Caustic Leaching Processes for Selected Hanford Tank Wastes*. PNNL-11089, Pacific Northwest National Laboratory, Richland, Washington.

Rapko, BM, GJ Lumetta, and MJ Wagner. 1995. *Washing and Caustic Leaching of Hanford Tanks Sludges: Results of FY 1995 Studies*. PNL-10712, Battelle, Pacific Northwest Laboratory, Richland, Washington.

Rapko, BM, JGH Geeting, SI Sinkov, and JD Vienna. 2004. *Oxidative-Alkaline Leaching of Washed 241-SY-102 and 241-SX-101 Tank Sludges*. PNWD-3512, WTP-RPT-117, Battelle, Pacific Northwest Division, Richland, Washington.

Reid, D. 2014. *Basis of Design.* 24590-WTP-DB-ENG-01-001, Rev. 2, Bechtel National, Inc., Richland, Washington.

Scheele, RD, LL Burger, RL Sell, PR Bredt, and RJ Barrington. 1994. *Ferrocyanide Safety Project: Comparison of Actual and Simulated Ferrocyanide Waste Properties*. PNL-10175, Pacific Northwest Laboratory, Richland, Washington.

Shimskey, RW, JM Billing, EC Buck, RC Daniel, KE Draper, MK Edwards, JGH Geeting, RT Hallen, ED Jenson, AE Kozelisky, PJ MacFarlan, RA Peterson, LA Snow, and RG Swoboda. 2009. *Filtration and Leach Testing for REDOX Sludge and S-Saltcake Actual Waste Sample Composites.* PNNL-17965, WTP-RPT-172, Rev. 0, Pacific Northwest National Laboratory, Richland, Washington.

Snow, LA, EC Buck, AJ Casella, JV Crum, RC Daniel, KE Draper, MK Edwards, SK Fiskum, LK Jagoda, ED Jenson, AE Kozelisky, PJ MacFarlan, RA Peterson, and RG Swoboda. 2009. *Characterization and Leach Testing for PUREX Cladding Waste Sludge (Group 3) and REDOX Cladding Waste Sludge (Group 4) Actual Waste Sample Composite.* PNNL-18054; WTP-RPT-167, Rev. 0, Pacific Northwest National Laboratory, Richland, Washington.

Tanner, PA and TCW Mak. 1999. "Synthesis, structure and spectroscopy of rare earth hypophosphites. 2. Uranyl hypophosphite monohydrate and uranyl hyppophosphite-hypophosphorous acid (1/1)." *Inorganic Chemistry* 38:6024-6031.

Temer, DJ, and R Villarreal. 1995. *Sludge Washing and Alkaline Leaching Tests on Actual Hanford Tank Sludge: A Status Report*. LAUR-95-2070, Los Alamos National Laboratory, Los Alamos, New Mexico.

Temer, DJ, and R Villarreal. 1996. *Sludge Washing and Alkaline Leaching Tests on Actual Hanford Tank Sludge: FY 1996 Results*. LAUR-96-2839, Los Alamos National Laboratory, Los Alamos, New Mexico.

Temer, DJ, and R Villarreal. 1997. *Sludge Washing and Alkaline Leaching Tests on Actual Hanford Tank Sludge: FY 1997 Results*. LAUR-97-2889, Los Alamos National Laboratory, Los Alamos, New Mexico.

TWINS. 2013. *Tank Waste Information Network System*. Pacific Northwest National Laboratory, Richland, Washington. Accessed May 2015 at https://twinsweb.labworks.org/twinsdata/Forms/About.aspx (last updated January 2013).

Urie, MW, PR Bredt, JA Campbell, OT Farmer, SK Fiskum, LR Greenwood, EW Hoppe, LK Jagoda, GM Mong, AP Poloski, RD Scheele, CZ Soderquist, RG Swoboda, MP Thomas, and JJ Wagner. 2004. *Chemical Analysis and Physical Property Testing of 241-AZ-101 Tank Waste--Supernatant and Centrifuged Solids*. PNWD-3215, Rev. 1; WTP-RPT-048, Rev. 1, Battelle, Pacific Northwest Division, Richland, Washington.

Wells, BE and JJ Ressler. 2009. *Estimate of the Distribution of Solids within Mixed Hanford Double-Shell Tank AZ-101: Implications for AY-102*. PNNL-18327, Pacific Northwest National Laboratory, Richland, Washington.

Wells, BE, DE Kurath, LA Mahoney, Y Onishi, JL Huckaby, SK Cooley, CA Burns, EC Buck, JM Tingey, RC Daniel, and KK Anderson. 2011. *Hanford Waste Physical and Rheological Properties: Data and Gaps*. PNNL-20646, Pacific Northwest National Laboratory, Richland, Washington.

Wells, BE, MA Knight, EC Buck, SK Cooley, RC Daniel, LA Mahoney, PA Meyer, AP Poloski, JM Tingey, WS Callaway III, GA Cooke, ME Johnson, MG Thien, DJ Washenfelder, JJ Davis, MN Hall, GL Smith, SL Thomson, and Y Onishi. 2007. *Estimate of Hanford Waste Insoluble Solid Particle Size and Density Distribution*. PNWD-3824, WTP-RPT-153, Rev. 0, Battelle, Pacific Northwest Division, Richland, Washington.

Wells, BE, PA Gauglitz, and DR Rector. 2012. *Comparison of Waste Feed Delivery Small Scale Mixing Demonstration Simulant to Hanford Waste*. PNNL-20637, Rev. 2, Pacific Northwest National Laboratory, Richland, Washington.

Wells, BE. 2013. *Simulant Development for Hanford Tank Farms Double Valve Isolation (DVI) Valves Testing*. PNNL-22121, Pacific Northwest National Laboratory, Richland, Washington.

West, EB, PJ Certa, TM Hohl, JS Ritari, BR Thompson, and CC Haass. 2012. *Integrated Waste Feed Delivery Plan Volume 1 – Process Strategy*. RPP-40149-VOL1, Rev. 2, Washington River Protection Solutions, LLC, Richland, Washington.

Wilmarth, WR, GJ Lumetta, ME Johnson, MR Poirier, MC Thompson, PC Suggs, and NP Machara. 2011. "Review: Waste-Pretreatment Technologies for Remediation of Legacy Defense Nuclear Wastes." *Solvent Extraction and Ion Exchange* 29(1):1-48. doi:10.1080/07366299.2011.539134.

Distribution*

No. of Copies

#10 EXTERNAL DISTRIBUTION

7 Bechtel National Inc.

Steve Barnes	PDF
Wiliam Donigan	PDF
Jeff Monahan	PDF
Bob Voke	PDF
Eric Slauthaug	PDF
Fred Damerow	PDF
Paul Townson	PDF
Dan Herting	PDF

3 Savannah River National Laboratory

Sam Fink	PDF
Michael Poirier	PDF
Erich Hansen	PDF

No. of Copies

14 INTERNAL DISTRIBUTION

14 Pacific Northwest National Laboratory

John Geeting	PDF
Jagan Bontha	PDF
Loni Peurrung	PDF
Eugene Morrey	PDF
Dawn Wellman	PDF
Steve Schlahta	PDF
Carolyne Burns	PDF
Reid Peterson	PDF
Richard Daniel	PDF
Sandra Fiskum	PDF
Phil Gauglitz	PDF
Beric Wells	PDF
Diana Linn	PDF
SR Suffield	PDF
Information Release	PDF
Project File (1)	K6-28

*All distribution will be made electronically

Pacific Northwest
NATIONAL LABORATORY

Proudly Operated by **Battelle** *Since 1965*

U.S. DEPARTMENT OF
ENERGY

902 Battelle Boulevard
P.O. Box 999
Richland, WA 99352
1-888-375-PNNL (7665)

www.pnnl.gov